Magnetic Actuation of Smooth Muscle Cells Loaded with Superparamagnetic Iron Oxide Nanoparticles

Ioannis Angelopoulos

Submitted for the Degree of Doctor of Philosophy

December 2014

Supervisors

Dr Richard Day

Professor Quentin Pankhurst

Applied Biomedical Engineering Group

Division of Medicine

University College London

Declaration

I, Ioannis Angelopoulos confirm that the work presented in this thesis is my own work. This work is based on research that was undertaken by me at University College London (UCL), during the period 30th of September 2010 to 30th of September 2013.

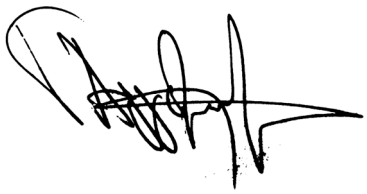

……

Ioannis Angelopoulos

20th June 2014

Abstract

Faecal incontinence (FI) is a debilitating disorder that affects a significant portion of the population. The research included in this thesis aimed to test the hypothesis that magnetic actuating of smooth muscle cells loaded with superparamagnetic iron oxide nanoparticles (SPION) can modify the cell phenotype, which could be used with as a future therapy. The research focused on exploring a novel method of magnetic actuation and assessing its effects on the phenotype and biocompatibility of human rectal smooth muscle cells (HRSMC). A 2D model was used to demonstrate the effects of SPION on HRSMC. Initially, the effect of incubating HRSMC with different concentrations of SPION (0, 31.25, 250 and 1000 μg/ml) for 24 hours was investigated. Transmission electron microscopy revealed that SPION were endocytosed by cells and became concentrated inside endosomes. Superconducting quantum interference device (SQUID) measurements showed that SPION loading was concentration dependent and also that saturation occurred for concentrations above 250 μg/ml. SPION loading of HRSMC led to inhibition of the gene expression of actin and calponin when incubated in differentiation medium, with or without magnetic actuation, suggesting SPION caused the cells to shift towards a more proliferative phenotype. Live cell imaging revealed actuation of SPION-loaded HRSMC with stronger magnets led to an observable movement of internalized SPION and the plasma membrane.

The findings from this research indicate SPION is biocompatible and may alter the phenotype of HRSMC. Therefore, SPION may offer novel benefits for regenerating damaged muscle in the treatment of FI. Further investigation is needed to assess the effects of magnetic actuation on SPION loaded cells.

Acknowledgements

I would like to thank my supervisors Dr Richard Day and Professor Quentin Pankhurst for their support and advice, Dr Daniel Ortega for his help with the transmission electron microscopy images and the dynamic light scattering data and Dr Paul Southern for his help with the superconducting quantum interference device data. Many thanks to George Frodsham for helping me with the magnetic field plots, Dr Andrew Mcquillin for his help with real time PCR data and Jamie Evans for his help with the flow cytometry data, also Dr Christopher Thrasivoulou for helping me with the confocal microscope and Mark Turmaine for his help with electron microscopy. Also I would like to thank Crucible center for the funding and support particularly Ms Roselle Thoreau and Professor Nick Tyler.

All my love and appreciation is to my wife Paulina. I would like to thank her for the help, the motivation, the understanding, and the endless hours we spent together talking about this work.

Last but no least, my total gratitude goes to my parents Kostas and Dina, my brother Andreas and my aunty Katerina for their love and support during this period. Without them this could have not been possible.

Publications and Presentations Arising from this Thesis

Publications

Angelopoulos Y, Frodsham G, Southern P, Pankhurst QA, Day R. Superparamagnetic Iron Oxide Nanoparticles Regulate Smooth Muscle Cell Phenotype Independently of Magnetic Actuation (Submitted).

Gonzalez-Molina J, Riegler J, Southern P, Ortega D, Frangos CC, **Angelopoulos Y**, Husain S, Lythgoe MF, Pankhurst QA, Day RM. Rapid magnetic cell delivery for large tubular bioengineered constrcuts. JR sOC Interface. 2012 Nov 7; 9 (76): 3008-16.

Presentations

Day R, Palmar N, Puri J, **Angelopoulos Y.** (2013). TIPS for Building Rings with Spheres: A Regenerative Medicine Perspective. Incontinence: The Engineering Challenge IX. London, UK.

Angelopoulos Y, Day R. (2013). Smooth Muscle Cells Loaded with Superparamagnetic Iron Oxide Nanoparticles for Use in the Treatment of Incontinence. The Innovating for Continence Conference, Chicago, USA.

Angelopoulos Y, Pankhurst QA, Day R. (2w012). "The Effect of Magnetic Materials on Smooth Muscle Cells Phenotype". PhD Seminar Series, Division of Medicine, UCL. London, UK.

Angelopoulos Y, Pankhurst QA, Day R. (2012). "The Effect of Magnetic Materials on Smooth Muscle Cells Phenotype". XCAR Early Career Researchers Conference, International Centre for Life, Newcastle, UK.

Angelopoulos Y, Pankhurst QA, Day R. (2011). "Sphincter regeneration: A Magnetic Actuation Approach". XCAR Early Career Researchers Conference, International Centre for Life, Newcastle, UK.

Table of Contents

Page

List of Figures

List of Tables

Page

Abbreviations

CO_2	Carbon dioxide
cm	Centimetre
°C	Degrees Celsius
dH2O	Distilled water
ECM	Extracellular matrix
EDTA	ethylenediaminetetraacetic acid
ELISA	Enzyme-linked immunosorbent assay
MEME	Minimum Essential Medium Eagle
FBS	Foetal bovine serum
FDA	Food and Drug Administration
FI	Faecal incontinence
g	Gravitational force
h	Hour/s
kDa	KiloDalton
L	Length
LDH	Lactate dehydrogenase
min	Minute/s
µl	Microlitre
µm	Micrometre
ml	Millilitre
mm	Millimetre
mM	Millimolar
MRI	Magnetic resonance imaging
MTS	3-(4,5-dimethylthiazol-2-yl)-5-(3-carboxymethoxyphenyl)-2-(4-sulfophenyl)-2H
MW	Molecular weight
NEAA	Non-essential amino acids
nm	Nanometre
PBS	Phosphate buffered saline
pg	Picogram
pN	PicoNewton
PMS	Phenazine methosulfate

rpm	Revolutions per minute
RT-PCR	Reverse transcription polymerase chain reaction
TEM	Transmission electron microscopy
TGF-β	Transforming growth factor-beta
U	Units
UV	Ultraviolet
v/v	Volume/volume

Chapter 1

Introduction and Thesis Overview

1. Introduction

1.1 Faecal Incontinence

Faecal incontinence has been defined as an alteration of the faecal passage where the patient experiences involuntary loss of flatus, liquid or solid faecal contents (1, 2). Consequently, the patient is unable to control the passage of faecal mass through the anus experiencing in some cases an urge of faecal incontinence (with a feeling before leaking) or a passive incontinence (without experiencing the urge before leaking) (3). This affliction is a consequence, sign or symptom of other alterations including mechanical, neurological and sensorial causes (1, 4). The multi-aetiology of faecal incontinence makes it difficult to effectively treat. Patients who suffer from faecal incontinence experience social isolation and stigma which can bring significant negative consequences to their quality of life (5). Patients who suffer from incontinence have to plan their lives around a quick access to the toilet. Therefore this have a consequence on their quality of life by avoiding activities such as shopping, go to the cinema, dinning with friends or family are some examples. In addition there are not very reluctant to share their problem with a healthcare professional due to the embarrassment that augments the difficulty of their situation. Epidemiological studies showed that men and women are equally affected (6-9). Therefore, there is a need to provide an effective and long-term solution to this problem. Before exploring the available treatments, it is important to understand the epidemiology, assessment and aetiology of faecal incontinence.

1.2 Epidemiology

The statistics of faecal incontinence are very inconsistent therefore is difficult to be very accurate with the severity of the condition. It has been estimated that the number

of patients suffering from faecal incontinence varies between 2.2 to 20.7%(6, 10).

Previous epidemiological studies were conducted in order to determine the number of people affected by faecal incontinence. In an American telephone survey of the population of Wisconsin (USA), 2570 households were randomly selected and telephoned (200 households per month) resulting in 6959 individuals. The survey showed only 153 individuals were affected by faecal incontinence, which accounts approximately 3% out of the total population. Specifically 36% were incontinent to solid feaces, 54% to liquid feaces and 60% to gas. In this study the number of women affected was more than men (63%) with 30% to be more than 65 years old (11).

Additionally, the results from a different study showed that 18.4% suffered from faecal incontinence out of 81 randomly selected individuals. The severity had increased with age and men were affected more than women. Finally that 1/3 of the individuals ever discussed their condition with a physician due to embarrassment and the fear of social exclusion (12).

There are several studies that have explored the prevalence of faecal incontinence in women. However women at all ages could be affected by faecal incontinence but the severity increases with age. In a community-dwelling woman in a health maintenance organization (HMO) in Washington State (USA) a total of 6000 women were examined (aged between 30-90 years old) for prevalence of faecal incontinence. The results showed only 7.2% of the total population was affected and the prevalence was more notable with age(13). Similar results were observed in a community study in Olmsted County, Minnesota (USA) where the results showed that severity of faecal incontinence increases with age out of a population of 2,800 women (14).

The prevalence of faecal incontinence has investigated not only by age or sex but also by race, geographical location or even if it is a hospital or a community home.

In a study, 6,099 individuals were interviewed door to door. The results showed that 585 individuals out of 6,099 resulting 9.6% suffered from faecal incontinence. Faecal incontinence is associated with age but is more prominent in the black population rather than the white. (15).

The geographical location or the place is also a contributing factor of faecal incontinence. In a study in a care facility in France, 234 patients out of 1,186 patient (aged 60 years old and older) suffered from faecal incontinence resulting in 20% (16). In a similar study with French population in a household community, a questionnaire was given to 7,196 patients (aged 15 years and older). The evaluation showed that 16.8% of the patients had experienced problems with faecal incontinence. (17).

However in a community study of western Syndney (Australia) different results were observed. A questionnaire was sent to 220 individuals with average age 53 years old (55% women). The results showed that 2-9% of the total population suffered from faecal incontinence (18). However, in a hospital outpatient clinic north Queensland (Australia), a notable increase in the number of people affected from faecal incontinence was observed. Out of 435 patients (n=261 with gynecological problems and n=174 with colorectal problems) with average age 53 years old 90 showed symptoms of faecal inconitence which account in 20.7% out of the total population. According to the authors that were the highest percentage reported in the literature of people affected from feacal incontinence on a hospital setting in north Queensland apart from nursing home studies. It was suggested that people who suffer from chronic constipation or urinary incontinence should be reported to their physicians to be checked for faecal incontinence as well. In this study the number of people affected by faecal incontinence was significantly increased compared to the previous study(19).

From the previous studies, the number of people affected from faecal incontinence

varies due to geographical location, race, sex and hospital setting or community home. Faecal inconitinece except from a debilitating condition that decreases the quality of life of individuals as described above but also is an economical burden as well. The average costs of 63 women who suffered from feacal incontinence due to obstretic damage injury were investigated. The results showed that the average cost per patient was $17,166 and evaluation and follow up charges reached to a total $65,412. Therefore the total charges for all the patients were totaled $559,341, and physician charges accounted for 18% of these charges (20). Similarly, the cost of 457 patients with mean age 73.6 years for men and 73.8 years for women were evaluated. The results showed that the total annual cost of frequency of urinary and faecal incontinent was $9771 (21).

According to a NHS report; 31% of primary care patients receive basline examination (relevant medical history, general examination, general examination and anorectal examination) as part of the assessment. The salary of a health care professional providing this care is approximately £38,923 and the cost per patient £43. Additionally the patients who receive the baseline examination will need a follow up assessment in 1 year costing about £22 (22).

As described faecal incontinence is a socio-economical problem for the community. New treatment modalities, should be assessed to determine their cost-effectiveness

1.3 Etiology

The anal sphincter is partly responsible for faecal continence. This sphincter consists of two layers (Figure 1.1). The internal anal sphincter (IAS) is a ring of circular smooth muscle (23, 24). The IAS surrounds the entire anal canal and it has a thickness of 2 to 3 mm (24). The Internal anal sphincter is innervated by the sympathetic (which

causes contraction) and parasympathetic nervous systems (responsible for its relaxation). The IAS is under autonomic control and produces 80% of the anal sphincter resting tone. The external sphincter contracts voluntarily and generates a constant baseline pressure(25). The IAS is supplied by rectal blood vessels (23). The external anal sphincter has an oval tube shape and consists of skeletal muscle fibres.

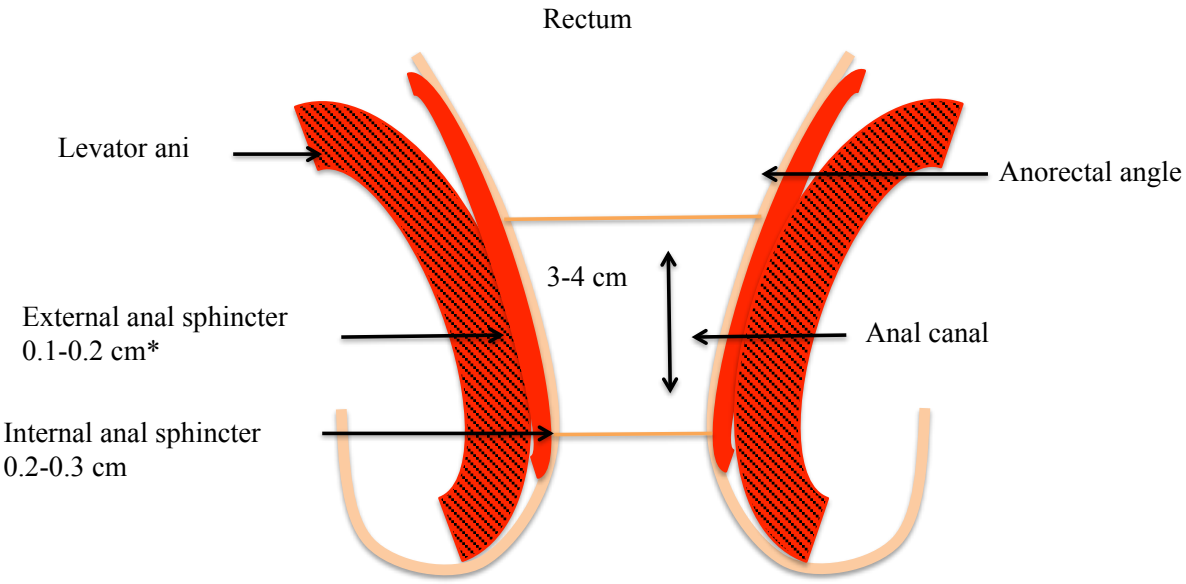

Figure 1.1 Anatomy of the Anal Sphincter.

The etiology of faecal incontinence could be multifactorial. The causes could be congenital neurological such as spina bifida, myelomeningocele, and meningocele or acquired such as stroke, multiple sclerosis and spinal cord injury. Also abnormal gastrointestinal function such as intestinal malabsorption, inflammatory bowel disease are amongst others. Finally the cause of faecal incontinence could be a combination of different factors. The possible causes of incontinence are summarized in table 1.1

Congenital	**Anatomical Obstetric injury**	**Neurological**	**Functional**
Imperforate anus	Vaginal delivery	Diabetes mellitus	Psychiatric disorder
Rectal agenesis	Anorectal surgery	Multiple sclerosis	Malabsorption
Cloacal defects	Sphincter-sparing bowel resection	Stroke	Inflammatory bowel disease
Myelomeningocele	Pelvic fracture	Dementia	Radiation proctitis
Meningocele	Anal impalement	Central nervous system tumour, infection, trauma	Hypersecretory tumours
		Spina bifida	Rectal intussusception, prolapse
		Pudendal neuropathy	Faecal impaction
			Physical disabilities

Table 1.1 Causes of Faecal incontinence (adapted from Madoff, R.D.)

People who suffer from 3rd degree haemorrhoids and decide to have a haemorrhoidectomy are prone of developing faecal incontinence (26).

Aging is an important factor of developing faecal incontinence. In a study, the resting anal canal pressure (RAP) and the squeeze pressure (MSP) was measured by comparing 143 patients suffering from faecal incontinence to a control population of 157 healthy individuals. The results showed that the RAP was significant lower in females 40 years of age and over as compared to males in the control population. MSP values were significantly lower in females at virtually all ages. The authors concluded that aging affects the RAP in both sexes but to a greater degree in women. (27).

Patients who suffer from rectal cancer and recently had a low anterior resection (LAR) are really prone to develop faecal incontinence at some stage. In a study, 17 patients

were investigated with anorectal manometry after LAR surgery the results showed that 14 patients out of 17 were incontinent with damage to sphincter muscle fibers or innervation (28). Similar results were observed in 99 patients with anorectal cancer after been subjected to surgery and radiochemotherapy. The results showed 36 (36.4%) patients experienced urgency to defecate with inability to delay defecation for more than 15 min, also Incontinence to flatus, liquid and solid stools was reported at least once a week in 24 (24.2%), 11 (11.1%) and 5 (5.1%) patients, respectively (29)

People who underwent lateral internal sphincteroplasty due to chronic anal fissures also are really prone of developing faecal incontinence in the future. In a study 585 patients were treated with lateral internal sphincteroplasty. The results showed that fissures were healed up to 96% but 45% of the patients developed faecal incontinence occurred in 53.4 percent of women and 33.3 percent of men (30). In another study, where a total of 298 patients (158 males; 53 % mean age, 46.9 years;) were subjected to sphincteroctomy due to chronic anal fissures. Reappearance of the fissure occurred in 17 patients (5.6 percent) of whom 9 (52 percent) were females. Temporary incontinence was reported in 31 percent of patients and persistent incontinence to gas occurred in 30 %(31).

Finally another factor of faecal incontinence is vaginal childbirth. There are lots of studies that have investigated the effects of vaginal delivery. In a study 184 women were investigated for faecal incontinence with anorectal manometry 6 weeks after delivery. The results showed that 42 of 168 (25%) after vaginal delivery had developed faecal incontinence and 76 out of 168 (45%) had abnormal anal physiology however 16 women (9%) who delivered by cesarean remain continent(32). Similarly in another study, the sphincter squeeze pressure was examined in 159 females after delivery with endoanal ultrasound and anal manometry. The manometric data provided confirmatory

evidence, with significantly reduced maximum squeeze pressures in patients with a disrupted anal sphincter (33).

Primiparous women are more prone to develop faecal incontince compare to multiparous women. In a study 38 primiparous women with average age 31 years old were evaluated with anal manometry, endoanalultrasonography and pudendal nerve terminal motor latency during pregnancy and after delivery. The results showed that 6 patients developed external anal sphincter disruptions as revealed with endoanal ultrasonography (1 patient had light scarring in the external anal sphincter). As control samples 3 patients were used who underwent cesarean section. (34). In another study, at the antenatal clinic at the University Hospitals of Geneva, Switzerland, 100 women with vaginal delivery of their first child were assessed for anal incontinence. The results showed 16 out of 92 women (17%) after 3 months of delivery had anal incontince and 11 out of 77 (14%) at 30 months(35).

1.4 Assessment

The way clinicians use to asses if the patient suffer from faecal incontinence is: 1) clinical history, 2) scoring system (36), 3) physical examination, 4) manometry (37). 5) MRI and 6) ultrasound. Clinicians need to record the type of incontinence (flatus, liquid, or solid stool), the frequency and changes in the stool consistency. Findings from the physical examination such as a breakdown perianeal skin, scars from previous operations also contribute towards the correct assessment. Except from the physical examination the grade scoring and the clinical history, the anorectal physiology is a useful diagnostic tool and a way to confirm the degree of the problem (6, 9).

1.5 Management

Depending on the severity of incontinence, several treatment options can be considered to enhance the quality of life of patients (4, 38). In general terms, treatments for faecal incontinence can be classified as non invasive, minimally invasive and invasive. Non invasive include 1) Pharmacological treatments (39), 2) Biofeedback (40-44) and 3) Diet (45), minimally invasive include 1) Bulking agents (minimally invasive) (46-48) and finally invasive techniques such as 1) sacral nerve stimulation (4, 49, 50), 2) Graciloplasty (4, 51, 52), Artificial anal sphincter (AAS) (50, 53) and Colostomy (54). The clinician always should start from a conservative treatment such as diet and biofeedback towards a more destructive treatment. Changes in the diet include the addition of supplementary fibre and avoid foods that cause diarrhea. Anti-diarrhea medications also are prescribed such as loperamide, diphenoxylate. Occasionally the anti-diarrhea medication could resolve the problem with no further action. If the patient remain incontinent after the conservative treatment further action need to be taken. Semi-invasive techniques such as bulking agents could be the solution for some individuals, if that treatment is not sufficient invasive surgery is the last option for someone who suffers from faecal incontinence. An algorithm for the treatment of faecal incontinence is summarized in Figure 1.2 (6, 8)

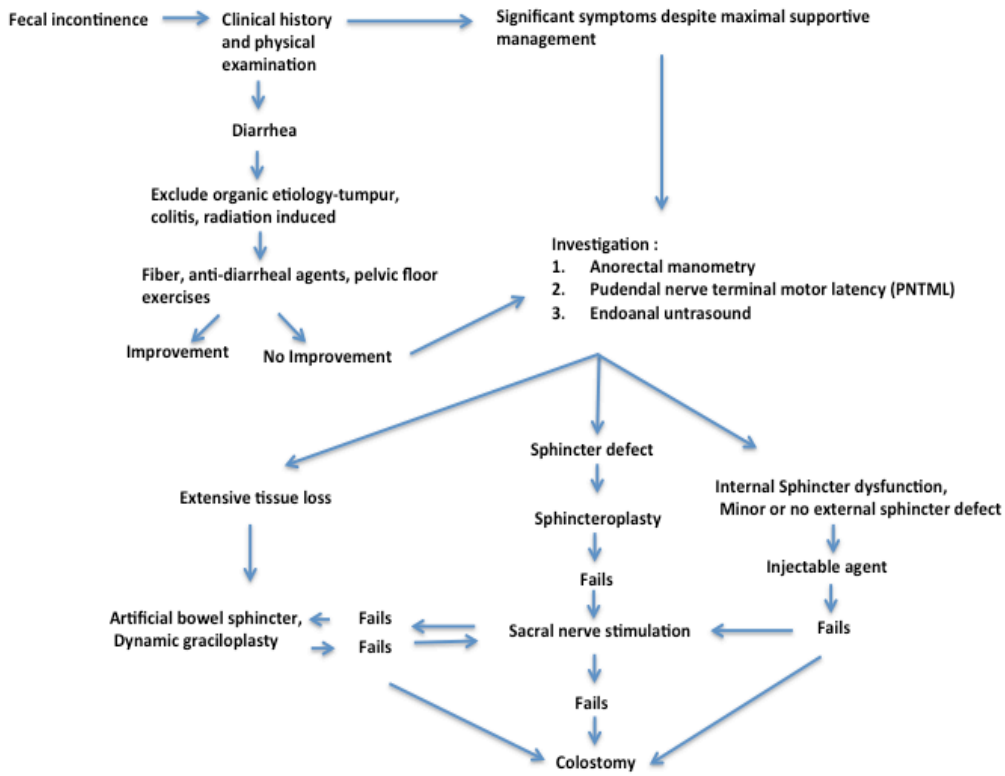

Figure 1.2 Algorithm for incontinence (adapted from Madoff, R.D.)

1.5.1 Conservative Treatment

1.5.1.1 Biofeedback

Biofeedback is used as a conservative treatment for patients who suffer from faecal incontinence. In a study the effects of augmented biofeedback with those of sensory biofeedback was investigated in a population of 40 women with dysfunctional sphincter after childbirth. All patients were assessed before and after twelve weeks of biofeedback training, using a fecal incontinence questionnaire and anorectal manometry. The results showed that patients were improved in both type of biofeedback but the patients who received augmented biofeedback had a better manometry results. Augmented biofeedback training is superior to sensory biofeedback alone in the treatment of impaired fecal continence after obstetric trauma (55). Biofeedback had also beneficiary results to an elderly population. In a different

study, 13 geriatric patients were allocated to sphincter exercises. Basically, they had to perform 50 sphincter exercises per day for a four weeks period. The results showed that biofeedback training had significantly augmented the sphincter strength and was associated with greater than 75% decreases in incontinence for 10 of the patients (77%). Improvements were maintained up to 60% six months later but then dropped to 42% after 1 year. (56). On the contrary in a different study, 171 patients who suffered from faecal incontinence divided in 4 groups: (1) standard care (advice); (2) advice plus instruction on sphincter exercises; (3) hospital-based computer-assisted sphincter pressure biofeedback; and (4) hospital biofeedback plus the use of a home electromyelogram biofeedback device. The results showed that biofeedback did not show any functional improvement than standard care with advice (53% improved in group 3 vs. 54% in group 1). These improvements were maintained for 1 year after finishing the treatment. (44).

Conservative treatment improves the quality of life of patients who suffer from faecal incontinence but only for a short period of time. More invasive procedures required tackling the problem.

1.5.2 Semi-Invasive Treatment

1.5.2.1 Bulking Agents

In patients with faecal incontinence in whom conservative treatment fails different options are incorporated such as bulking agent. Bulking agents have been used to narrow the anal canal and consequently to help retain stool (4, 48). The use of these agents is considered a minimally invasive treatment for incontinence (46). Bulking agents are placed in the submucosa above the dentate line to create a bulge.

Several injectable agents have been identified and are still under study including carbon-based, silicone particles, collagen agents, autologous fat and calcium particles (48). In a study the long-term effects of carbon beads (Durasphere) in 18 patients and found significant increase in continence 12 months after the delivery (46). In a different study a silicone-based agent (Bioplastique^{TM}) was used in 10 incontinent patients (6 females; median age, 64, range, 41-80 years). The patients were examined before and 6 weeks after their treatment with clinical assessment, anorectal manometry and ultrasound. Ultrasound confirmed the correct position of the silicon in all patients and the maximum resting and squeezing pressured did not change significantly before and after treatment. The results showed that after 6 weeks, 6 out of 10 patients showed an improvement, however, 3 patients did not improve and remain incontinent. Finally 5 out of 10 experiencing pain and ulceration at the injection site (47). Bioplastique^{TM} was also used in a different study. 6 patients (4 males, average age 53 years) were received the treatment. The injection was introduced circumferentially, trans-sphincterically. The findings were confirmed with anorectal manometry and ultrasound. Ultrasound confirmed the silicon agent was placed in the correct position and there was an increase in maximum anal resting and squeeze pressures. The results showed after 18 months, 5 out of 6 patients had a marked improvement(57).

Expandable microballoons have been used previously for the treatment of urinary incontinence however in a study was used to treat patients with faecal incontinence problems. 6 patients (4 male) with average age of 43 with severe faecal incontinence received expandable microballons in the submucosa of the anal canal. Anal manometry was used to assess the outcomes. The results showed that the anal pressure at rest was not improved in any patient when compared before and after treatment. Anal

implantation of expandable microballoons is a safe and effective method however it seems to be more efficient with urinary rather than faecal incontinence patients(58).

Additionally autologous fat has been injected as a treatment for faecal incontinence. In a study 14 patients aged between 38-62 years old received 60 ml of fat harvested from the abdominal wall and injected submucosally in the rectal neck. The patient were remained continent during the first 2-3 months post-surgery but at the 6th month only 3 out of the 14 patients remained continent. Perianal injection of fat from the same patient is a simple and cost effective technique in comparison with other bulking agents however the results were not so convincing. Further investigation is required (59). Finally, glutaraldehyde cross-linked (GAX) collagen was also used as injectable bulking agent. 17 patients who suffered from faecal incontinence were injected with GAX. The evaluation was assessed with anorectal physiology and endoanal ultrasound before and after the injections. All patients tolerated the treatments without side effects. The results showed that 11 out of the 17 patients marked a significant improvement and 4 out of 17 no significant improvement. (60).

Although several potential treatment options have been developed, none have been shown to provide long-term efficacy. If the condition of the patient has been improved at this stage, further invasive procedures will be incorporated.

1.5.3 Invasive Procedures

Restoration of continence to patients when traditional treatment fails, or when traumatic or neurogenic injuries are extensive, remains a challenge. Options available to such patients include dynamic graciloplasty, an artificial anal sphincter, and sacral nerve stimulation.

1.5.3.1 Sacral Spinal Nerve Stimulation

Patients with chronic fecal incontinence in whom conservative treatments had failed are consulted to have sacral nerve stimulation. It includes the implantation of a stimulator subcutaneously, which delivers an electrical stimulation to the sacral nerve. Sacral nerve modulation appears to offer a valid treatment option for some patients with fecal incontinence and functional defects of the internal anal sphincter or of the striated muscle(6)

Previous studies that have used sacral nerve stimulation in a group of 6 patients. The results showed that incontinence was improved in all patients. The Wexner score decreased from a mean of 17 to 2 and the maximum squeeze pressure increased from a mean of 48.5 mmHg to 92.7 mmHg and median squeeze pressure increased from a mean of 37.3 mmHg to 72.5 mmHg. One patient has complaint of discomfort and the electrical stimulator was removed after 5 months. Long-term sacral spinal nerve stimulation improves continence and increases striated anal sphincter function in patients with fecal incontinence (61). In another sacral nerve stimulation study, 10 patients have received an electrode into the S3 or S4 foramen. The electrode was left in situ for a minimum of one week with chronic stimulation. The results showed that 7 patients were became continent, 1 patient was significantly improved and 1 patient observed no difference. The maximum squeeze pressure was increased but not the resting pressure as showed by anorectal manometry (62). Similarly in 16 patients (4 males; average age; 51.4 years old) received an electrode in the S2 (1 patient), S3 (14 patients), or S4 (1 patient) sacral foramen. The results showed an increase in mean maximal pressure at rest of 37.7 mmHg and with the electrode 49.1 mmHg and in mean maximal pressure during squeeze prestimulation 67.3 mmHg and with the electrode 82.6 mmHg (63). Similarly, 5 patients (age 41-68 years) who underwent

sacral nerve stimulation, the results showed significant improvement for all patients. Continence scores were improved (scale 0-20) from 16 before surgery to 2 after surgery. No early complication or side effects were observed. Only 1 patient required lead replacement after 12 months. The quality of life assessment improved in all patients. The resting pressure increased in four patients, but there was no consistent measured physiologic change that could account for the symptomatic improvement (62).

In a qualitative approach, the effect of sacral nerve stimulation was investigated in 37 patients. The assessment was performed with daily bowel diaries over a period of 3 weeks with a disease-specific American Society of Colon and Rectal Surgeons (ASCRS) questionnaire. The results showed that incontinence was improved in all 4 ASCRS scales (64).

Finally a long-term study of sacral nerve stimulation was performed in 120 patients (110 women; mean age, 60.5 years). The patients were followed up 3,6 and 12 months after the devise implantation. Patients were assessed with a 14-day bowel diary and Fecal Incontinence Quality of Life and Fecal Incontinence Severity Index questionnaires. Seventy-six of these patients (63%) were followed a minimum of 5 years. Fecal Incontinence Quality of Life scores also significantly improved for all 4 scales between baseline and 5 years and 27 of the 76 patients (35.5%) required a device revision, replacement, or explant (65).

Sacral nerve stimulation greatly improves continence and quality of life in selected patients with morphologically intact or repaired sphincter offering a treatment for patients in whom treatment options are limited. The results have shown that short-term sacral nerve stimulation notably decreases episodes of faecal incontinence but this treatment does not have long-term functional improvement.

1.5.3.2 Artificial Anal Sphincter

Anal sphincter replacement (AAS) is a treatment option if the problem is severe and not easy to repair it. Patients receive an artificial anal sphincter when previous methods have failed. The causes include obstetric damage, surgical damage, imperforate anus and spina bifida. It is the only surgical option for treatment of anal incontinence in patients with neurologic disease that affects the pelvic floor and the muscles of the lower limb. The AAS is an innovative approach where the artificial anal sphincter maintains continence via a fluid-filled cuff that surrounds and compresses the anal canal. The patient controls the device via a pump placed in the scrotum or labia majora. Squeezing the pump 9-12 times it forces the fluid from the cuff into a reservoir balloon, which is implanted behind the pubic bone in preperitoneal tissues. Once the cuff is deflated, the anal canal is open, allowing the passage of stool. The cuff then gradually re-inflates to close the anal canal until defecation is again desired (6-8).

The ASS has been used previously. In an Italian study the Action artificial anal sphincter (Acticon Neosphincter, American Medical Systems, Minneapolis, MN, USA) was introduced in 28 patients who suffered from faecal incontinence. The results showed that early infection were occurred in 4 patients requiring the removal of the device and the cuff was accidently broken in another patient and had to be installed a new one. The rest of the patients showed a significant improvement. The anorectal manometry results showed that the median resting anal pressure increased from 27 mmHg before surgery to 32 mmHg after operation. Preoperative squeeze pressure was 42 mmHg while maximum postoperative anal pressure with the activated device was 67 mmHg. (66). Similarly, in another study the Action artificial anal sphincter was introduced in 13 patients. The results have shown that 1 patient had infection of the perineal wound and the devise was removed. In two patients the device was removed

because of late infection (7 months) and erosion through the skin respectively (3 months). The rest of the patients who had the devise incorporated successfully resulting in a full continence to solids and lquids. In a different study, the Action artificial anal sphincter was introduced in 13 patients. The results showed that 1 patient had infection of the perineal wound and the devise was removed. In 2 patients the device was removed because of late infection (7 months) and erosion through the skin respectively (3 months). The rest of the patients the devise was incorporated successfully resulting in a full continence to solids and lquids. (67). In another study 24 patients (7 men; average age 44 years old) receive the ASS for a minimum of 6 months. The assessment was performed with continence scores (as 0 been normal and 120 been incontinent) and anal manometry preoperatively and postoperatively at a 6 month interval. The results showed that 7 patients had their devices explanted and the rest of the patients continued with the treatment up to the 20^{th} month. The rest of the patients showed a significant decrease in the faecal insentience scores at the 6^{th}, 12^{th} and 20^{th} month. However, difficulties on empting the bowel was observed in 9 patients. Additionally, median anal pressures at rest on manometry increased significantly from 28 mm Hg preoperatively to 60 mm Hg (68). In a different clinical trial, an ASS was implanted in 115 patients (86 females- average age 49). Patients were evaluated with anal physiology, endoanal ultrasound and faecal incontinence scoring. The patients underwent follow up 6 and 12 months post surgery. The results showed 99 patients were reported a potentially adverse effect of the devise. 51 patients underwent revisional operations. 37 patients have had their devises completely explanted of which 7 have had successful re-implantations. In patients with a functioning sphincter, improvement in quality of life and anal continence was documented. A successful outcome was achieved in 85% of patients with a functioning

device however; morbidity and the need for revisional surgery are high (69). Finally the long-term effects of ASS implantation were investigated. 17 patients were received an ASS and their evaluation was followed 5 years post surgery. The results showed that 2 patients died within the first year post surgery from unrelated causes, 3 patients had the devise removed due to infection. Also the devise was removed from 4 patients because of malfunction and only in 5 patients had the devise successfully positioned. These 5 patients had regular follow up for the following 5 years post surgery. Out of these 5 patients, continence was restored in 4 patients completely and only one had occasionally leakage of solid stool. (70).

Implantation of ASS provides a solution for patient who suffered from severe faecal incontinence. The results have shown that approximately half of the patients have an adequate long-term result. Early infection and rectal erosion, together with difficulty in evacuating, are still major concerns with this technique. Longer follow-up is needed to determine the extent of problems with infection, erosion, and mechanical failure

1.5.3.3 Dynamic Gracioplasty

Dynamic gracioplasty has been advocated as therapy for refractory fecal incontinence and for anorectal reconstruction to avoid colostomy.

In a dynamic gracioplasty study 139 patients were recruited. Intramuscular leads and neurostimulators were implanted to stimulate transposed gracilis or gluteus muscle. The results have shown that 70% of the patients had a reduction in solid stool incontinence however 1/3 of graciloplasty patients experienced a major wound complication, with therapy failing in 41% (71). Similarly, in a different study 123 patients were treated with dynamic gracioplasty. Continence was assessed preoperatively and postoperatively with the use of 14-day diaries. The results showed that 1 patient had died unexpectedly for unrelated reasons, 91 patients (74%) had

adverse effects and 49 patients (40%) required one or more operations to treat complications (72).

Dynamic gracioplasty might be a solution for people who suffer from severe faecal incontinence. However, the procedure has significant morbidity that can lead to functional failure.

1.5.3.4 Colostomy

If none of the previous treatments have been successful, more aggressive surgical treatments were incorporated such as colostomy. Colostomy certainly does not restore continence, but it does restore control of bowel evacuation and allows the patient to return to a normal life (6).

In a study colostomy was performed in 27 patients. Patients that didn't undergo stoma were used as control. The Cleveland Clinic Incontinence Score and anal physiology was assessed. The results showed that incontinence scores were improved significantly in both groups, no differences were found between the two groups (stoma/no stoma). The anorectal physiology results showed that the maximum resting pressure and maximum squeeze pressure increased significantly only in the no-stoma group. Stoma-related complications occurred in 7 of 13 patients having a stoma such as hernia, and wound infection at the closure site (73). In a different study at the Royal Prince Alfred Hospital (Australia), 57 female patients underwent sphincter repair primarily and then a colostomy was performed. All patients were assessed preoperatively and postoperatively with endoanal ultrasound, with a questionnaire, including a four-point Likert scale of continence level, the St. Mark's incontinence scoring system (range, 0-13), the Pescatori incontinence scoring system. 21 patients were received a colostomy in conjunction with an overlapping anal sphincter repair. After 18 months post surgery the continence scores had been improved for the St.

Mark's incontinence scoring (from 13 to 3) and the Pescatori incontinence scoring (from 6 to 2). Also, 49 of 57 (86%) repairs have been successful, and 8 are considered to be failures. Improved or normal continence was achieved in 17 of 21 (81%) patients with a stoma and overlapping anal sphincter repair and in 32 of 36 (89%) patients with an overlapping anal sphincter repair alone (74).

Colostomy is an extremely invasive procedure. Infections and morbidly are the main negative causes.

1.6 Regenerative Medicine Applications

Sphincter muscles are prone to degenerative process in the same way with other muscles. The pathophysiology of the incontinence is usually a damage occurring at the sphincter muscle at the cellular level. Manometric measures often fail to distinguish the cellular processes responsible for the damage. Regenerative medicine aims to restore function of the damaged sphincter with either restore sphincter innervations, or restore the sphincter itself (25, 75).

The delivery of stem cells in the sphincter area in order to restore function has been investigated previously. In a study muscle-derived stem cells were delivered into the sphincter muscle of a 3-week female Sprague-Dawley rats where previously was cryoinjured and served as a model faecal incontinent in order to investigate if the functional properties could be improved. The experiments were divided in 3 groups: 1) control (no injection, no injection), 2) cryoinjured (no injection) and 3) cryoinjury+muscle derived stem cells (aprox 3,000,000 cells). All groups were subsequently subjected to contractility. The results showed that the contractility in the cryoinjured group was significantly lower compared to the control group and in the muscle-derived stem cell group contraction had significantly increased compared to the cryoinjured group. The stem cells were detected in all sphincters. Stem cells were

differentiated and α-actin and myosin heavy chain was stained as indication of differentiation (76). Similarly, the ability of human umbilical cord matrix (hUCM) and rabbit marrow (rBM) stem cells to improve anal sphincter incontinence due to injure defects without surgical repair. hUCM were harvested from human Wharton's jelly and rBM stem cells from rabbit femurs and tibias. The rabit sphincter was cryoinjured and used a model for faecal incontinence. The experiment is divided in 5 groups: 1) control, 2) injection of hUCM cells+RPMI medium, 3) injection of rBM cells+RPMI medium, 4) RPMI medium only, 5) saline only. Transplanted cells were tracked in the injured sphincters by pre-labeling with bromodeoxyuridine. Electromyography was performed before and 2 weeks after the external anal sphincterotomy, and 2 weeks after cell transplantation. We also evaluated the proliferation and differentiation of injected cells with histopathologic techniques. The results showed a significant improvement in sphincter function 2 weeks after the injection of rBM stem cells compared to control values. Moderate improvement was observed with hUCM stem cells. Cells with incorporated bromodeoxyuridine were detected at the site of injury after transplantation for both population of cells. Histopathologic evaluation showed normal or muscle-dominant sphincter structure in all animals receiving rBM and fibrous-dominant sphincter structure in most animals receiving hUCM. Stem cell injection at the site of injury can enhance contractile function of the anal sphincter without surgical repair (77).

Finally the construction of a bioengineered 3D sphincter for potential replacement of the entire sphincter was investigated. The 3D bioengineered sphincter was constructed with smooth muscle cells isolated from the sphincter tissue of rabbits and the cells were seeded in a culture on top of a loose fibrin gel where they migrated and self-assembled in circumferential alignment. As the cells proliferated, the fibrin gel

contracted around a 5-mm-diameter SYLGARD mold, resulting in a 3-D cylindrical ring of sphincteric tissue. The 3D bioengineered tissue was subjected to electrophysiology testing. The results showed that that 1) the bioengineered IAS rings generated a spontaneous basal tone, 2) stimulation with 8-bromo-cAMP (8-Br-cAMP) caused a sustained decrease in the basal tone (relaxation) that was calcium-independent, 3) upon stimulation with acetylcholine, bioengineered IAS rings showed a calcium- and concentration-dependent peak contraction at 30 seconds that was sustained for 4 min and 4) addition of 8-Br-cAMP induced rapid relaxation of ACh-induced contraction and force generation of IAS rings. This is the first report of a 3-D in vitro model of a gastrointestinal smooth muscle IAS. Bioengineered IAS rings demonstrate physiological functionality and may be used in the elucidation of the mechanisms causing sphincter malfunction (78).

Regenerative medicine approaches hold a great promise, however, the studies conducted require further investigation. More research is necessary to be conducted in order to be safe for clinical applications.

1.7 Current Magnetic Stimulation Approach

The magnetic stimulation approaches include a magnetic devise called the Magnetic Anal Sphincter (MAS) a recent innovation for severe faecal incontince. The MAS was previously used for the treatment of gastroesophageal reflux disease. At the moment has not define its place in the treatment algorithm of faecal incontinence as seen in Figure 1.2 but is considered between minimally invasive and invasive technique.

The MAS was placed around the anal canal in 14 patients (female, average age 62.8 years old). The results showed that 7 patients had adverse effects and 3 patients are no longer implanted with a device, 2 devices were removed and 1 passed spontaneously

following a separation at the suture connection. Five patients with 6-month follow-up demonstrated a mean reduction in the number of average weekly incontinence episodes from 7.2 to 0.7 (90.9%) and a mean reduction in Wexner Continence Score from 17.2 to 7.8 (54.7%). Compared with baseline, quality of life improved in all 4 domains of the fecal incontinence quality of life (FIQoL) scoring system. No patients have reported that their condition has worsened. Two patients at 1-year follow-up both reported perfect continence. (79). Also, the same group has compared MAS with sacral nerve stimulation in 12 female patients (average age 65 years old). As control 16 females were implanted with a permanent SNS pulse generator during the same period, of similar age, preoperative function scores, aetiology and duration of incontinence, served as a reference group. The duration of hospital stay, complications, change in incontinence and quality of life scores and anal physiology were compared in the two groups. Four patients with MAS experienced a 30-day complication and there was 1 device removal in each group. A significant improvement in incontinence and quality-of-life scores occurred in both groups. Mean anal resting pressure increased significantly in patients implanted with MAS (80).

MAS is a promising new technique. Implantation is simple and it requires no adjustments from the physician or patient once the device is implanted. The results are not very conclusive and the number of patients is very low. Also, there is no study investigating the long-term effects and the only comparable study with sacral nerve stimulation demonstrated that MAS is effective as sacral nerve stimulation based in in improving continence and quality-of-life, with similar morbidity.

Therefore, there is still a need for developing new technologies or interventions to improve faecal incontinence. This will help incontinent people to reach a normal level

of faecal continence. Ideally new interventions should use minimal or non-invasive and cost effective methods that people can easily access.

1.8 Magnetic Regulation of Sphincter Smooth Muscle Cells as a New Potential Therapy for Faecal Incontinence

Smooth muscle cells have the ability to shift between a contractile or proliferative phenotype. This phenotypic continuum has been controlled previously; 1) chemically and 2) mechanically.

In this study, the phenotypic continuum of smooth muscle cells will be controlled magnetically. This approach would be in the semi-invasive spectrum and would offer an alternative treatment for faecal incontinence.

1.9 Physiology of Smooth Muscle Cells and Phenotypic Continuum

Smooth muscle cells (SMC) constitute the muscular part of the gastrointestinal tract from the distal oesophagus to the internal anal sphincter (81). Their length is between 200 to 300 μm and the width between 5-15 μm (82) which makes them smaller compared to a skeletal fibre which has width 10-100 μm. One of the main differences of smooth muscle cells compared with cardiac and skeletal muscle is the lack of cross striation (hence the name smooth) and also that contraction is under involuntary control because they receive neural innervations from the autonomic nervous system, whereas skeletal muscle is innervated by from the somatic nervous system (83). Contractile filaments and the dense bodies occupy ~80% of the cell interior. The dense bodies are electron dense portions of smooth muscle in which thin filaments (actin and tropomyosin namely) bind. It is presumed that the dense bodies operate similarly to the Z-lines in skeletal muscle. Smooth muscle and skeletal cells have the same amounts of actin and tropomyosin, however smooth muscle does not have troponin. Instead it has

different proteins such as caldesmon and caponin. Caldesmon is an 87 kDa protein and has binding sites for myosin, actin, tropomyosin and Ca^{2+}-calmodulin. Calponin is a 34 kDa protein and has binding sites for actin, tropomyosin and Ca^{2+}calmodulin. Both proteins are inhibiting the actin-activated ATPase activity of phosphorylated smooth muscle myosin (84).

Smooth muscle contains three types of filaments: 1) the thin actin filaments, 2) the thick myosin filaments, and 3) and the intermediate filaments.

Actin filaments contain actin a 42 kDa globular protein (G-actin) which polymerises and forms a two stranded helical filament (F-actin) (82). The thick filaments contain myosin molecules, which are further divided in two pairs of myosin light chain (MLC) and one pair of heavy chain (MHC). The heavy chains are coiled together making a helix and at the end of the strand a globular head is formed by the two pairs of myosin light chain. Its head has a binding site for actin (82). Smooth muscle is rich in intermediate filaments that contain two specific proteins, desmin and vimentin.

Smooth muscle cells can change their phenotype from a quiescent contractile to a synthetic phenotype. During the proliferation/synthetic phase, smooth muscle cells proliferate and produce more extracellular matrix. This can be a limitation for tissue engineering applications for example a bioengineered vascular graft seeded with smooth muscle cells due to Intimal Hyperplasia (IH), a vascular condition where smooth muscle cells lose their contractile proteins and an increase their proliferation, migration and production of extracellular matrix has been observed. For vascular tissue engineering promotion of a well-differentiated smooth muscle cells is the main goal in order to minimize IH and also to understand the molecular mechanisms, which underlie this process.

When culturing *in vitro,* proliferative smooth muscle cells acquire a spread shape that grows on top of each other in a "hill and valley" morphology. They have a wide rough endoplasmic reticulum, Golgi and ribosomes and also lack contractile bundles. Contractile smooth muscle cells have minimal rough endoplamic reticulum, Golgi and ribosomes. In culture, these cells possess a dense fusiform morphology (85). Several genes play a role in the proliferation and differentiation of smooth muscle cells such as caldesmon, smooth muscle actin, calponin, SM22, α- and β- tropomyosin and α1 integrin. These genes are transcriptionally regulated and controlled by the binding of a serum response factor (SRF). This factor binds to a cis-regulatory element known as CArG box (CCAAAAAAGG) which is responsible for the transcriptional activation of contractile genes mentioned before (81).

1.10 Mechanisms of Regulating the Phenotypic Continuum of Smooth Muscle Cells

1.10.1 Chemical Stimulation

Extracellular signals play a role in the shift between the synthetic to contractile phenotype. A wide variety of signalling factors have been implicated in the transition of SMC into the proliferative synthetic phenotype.

Table 1.2 summarizes all the soluble factors that are involved in this process.

Stimulation towards a synthetic/proliferative phenotype	**Stimulation towards a contractile phenotype**
Platelet-derived growth factor (PDGF	Heparin
Basic fibroblast growth factor (bFGF	Transforming growth factor beta 1 (TGF-b1)
Insulin-like growth factors (IGFs),	Ang-II,
Epidermal growth factor	IGF-1
a-Thrombin	
Factor Xa	
Ang- II	
Endothelin-1	
Unsaturated lysophosphatidic acids	
Fetal bovine serum (in vitro)	

Table 1.2 Soluble Factors Responsible for Smooth Muscle Cell Plasticity

1.10.2 The Application of Mechanical Stimulation to Cells

1.10.2.1 Mechanisms of Mechanotransduction

Smooth muscle cells are able to sense external mechanical loads and translate it into a biochemical intracellular cascade of events- a process called as mechanotransduction. Understanding the biophysical factors that make the cell change phenotype and also their intracellular signals that control this change is very important for tissue engineering applications. Mechanotransduction is the conversion of a mechanical signal or stimuli into an intracellular biochemical signal. An example type of mechanical signal is stretching, which results in changes to the cell morphology, differentiation and proliferation (86).

Cells use mechanoreceptors to detect a mechanical signal/stimulus and then transmit the message inside the cells. Once the mechanical signal has been detected the cell uses the cytoskeleton and a biochemical pathway to transmit the signal until it reaches its target, which will eventually cause a change in the cell phenotype.

Examples of different mechanoreceptors that will respond to extracellular signals are:

- Integrins- transmembrane proteins that link the ECM with the cytoskeleton.
- Stretch-activated ion channels-ion channel proteins across the cell membrane connecting the ICM with the ECM.
- Cell surface receptor proteins- they are classified into G protein-linked or enzyme-linked cell surface receptors. These receptors respond to extracellular signal molecules such as proteins, hormones, and peptides.

Mechanical stimulation can be delivered to cells *in vitro* using a variety of physical processes conditions including:

- Compression loading: this is a method of compressing the existing air in a culture system that results in hydrostatic pressure applied to the cells.
- Stretching: it is a common approach that involves the use of a flexible membrane where the cells are attached and deform this membrane by applying uniaxial or biaxial strain. Also cyclic and static strain can be applied.
- Fluid flow: it is a method in which shear stress is applied to cells as a way of mechanical stimulation. This can be achieved using viscometers and flow chambers (87).

1.10.3 Effects of Mechanical Strain on Smooth Muscle Cell Phenotype

Vascular smooth muscle cells (VSMC) in the arterial wall experience mechanical strain during the cardiac cycle. There are two main forces that act on the vascular wall: a) fluid shear stress, which affects mostly the endothelium because it acts parallel to the direction of the blood flow, and b) cyclic mechanical stretch, which acts on the vascular smooth muscle cells. Mechanical strain can influence the behaviour of the VSMC phenotype, shifting it from a differentiated/contractile phenotype to a synthetic/proliferative phenotype. The proliferative phenotype is seen in atherosclerotic lesions and is characterized by increased proliferation, matrix secretion, and decrease in the contractile proteins such as smooth muscle myosin heavy chain (88).

Williams *et al* suggested that no stretch or static culture can lead to a loss of the contractile phenotype and the initiation of a proliferative phenotype, however, excessive stretch can also lead to a proliferative phenotype and increased matrix formation (88).

In a study by Bonacci *et al*, the effects of collagen type I and laminin on bovine airway smooth muscle cells (ASM) was investigated in response to mechanical strain. The study demonstrated that the combination of a collagen coated surface with strain enhanced the proliferation of ASM (89).

In a similar study human cardiac stem cells were seeded into a fibronectin coated silicon chamber and mechanical strain was applied with 60 cycles per minute and 120% elongation by using a mechanical stretch system (STB-140-10, STREX) (stretching conditions that mimic the heart rate and 20% fractional shortening). Non-stretched cells were used as controls. Cell growth, proliferation, and apoptosis, release of different growth factors and cell differentiation were investigated after 24 hours and

again after 3 days of culture. The release of different growth factors after 12 hours of stretching was investigated to determine how mechanical strain affected the release of different growth factors. Results showed there was a 1.9-fold and 29.5-fold increase in the concentration of VEGF and bFGF in the stretched group compared with the non-stretched group (90).

1.11 Application of Magnetic Field to Cells

The application of magnetic fields to cells is not a new concept. In 1949 Crick et al, used magnetic fields to investigate the properties of the cytoplasm under an applied stress (91). Currently magnetic actuation research has involved the tagging of cells with magnetic particles allowing the manipulation of cell function or movement by an external magnetic field regardless of its location in the tissue. This advantage makes the technique useful for *in vivo* applications. Studies using magnetic actuation include the delivery of magnetically tagged cells to an area of interest (92-94) and magnetic seeding of cells to optimize attachment to a substrate (95-97).

Recent work has shown that it is possible to target specific ion channels or surface receptors of different types of cells and change their behavior. This technique offers a great potential in the field of tissue engineering and regenerative medicine (98).

1.11.1 Techniques of Magnetic Nanoparticle Actuation

There are different techniques of manipulating a cell's phenotype using magnetic actuation (Figure 1.2). These techniques include magnetic twisting cytometry and magnetic tweezers. Magnetic twisting cytometry produces a mechanical torque between the magnetic particle and the cell surface at a vertical position. This mechanical torque drives the particle to twist on the cell surface. The magnetic particle is bonded to a receptor or a ligand and this twisting action produces a shearing force at

this particular receptor/ligand. The second technique is magnetic tweezers where a magnetic field pulls the magnetic particles attached to the cells. In both techniques the force generated by the cells can be measured (99).

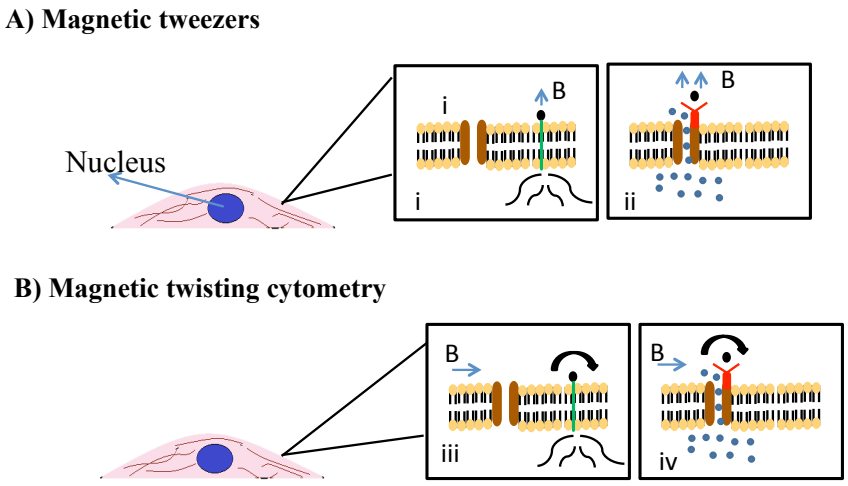

Figure 1.3 Schematic Representation of the Different Techniques of Magnetic Actuation: a) Magnetic tweezers: micromagnetic particles coated with RGD peptides attached on the plasma membrane (i) or with an antibody against an ion gated channel (ii) an external magnetic field (B = magnetic field vector) is applied to the particles vertically by pulling the particles. The mechanoreceptors are pulled towards the field source that initiates an intracellular signalling. b) Magnetic twisting cytometry: micromagnetic particles coated with RGD peptides attached on the plasma membrane (iii) or with an antibody against an ion gated channel (iv) an external magnetic field is applied to the particles making them "twist''.

One of the early studies using magnetic twisting cytometry by Wang *et al* investigated if extracellular matrix receptors such as integrins provide a molecular path for mechanical signal transfer to the cytoskeleton. In that study, endothelial cells were incubated with spherical micromagnetic beads that have been previously coated with an RGD sequence (Arg-Gly-Asp) known for binding to integrin receptors. A twisting magnetic field was applied providing a mechanical stress to the cells of 68 dyne/cm^2. The mechanical properties of cells were measured based on their angular strain (the average bead rotation) before and after disrupting the cytoskeleton with cytochalasin D (a metabolite that disrupts actin polymerisation). The angular strain of cells tagged

with RGD magnetic beads were increased after exposure to cytochalasin D for 15 minutes. Following these findings and also the fact that the cell's framework consists of microfilaments, microtubules and intermediate filaments which respond dynamically as a single unit when stress is applied, it was suggested that the mechanical behaviour of the cytoskeleton in response to mechanical force can be explained with tensengrity (firstly introduced as a concept in architecture) rather than compressional continuity and hypothesised that cells might use tensegrity to mediate mechanotransduction within cytoskeleton (100).

Several studies have used lab based magnetic bioreactors that mimic the action of magnetic twisting cytometry or magnetic tweezers to manipulate the cells for specific applications. The development of bioreactors is crucial for *ex vivo* tissue engineering. One of the paradigms of tissue engineering suggests that autologous cells from a patient growing on a scaffold within a bioreactor need to experience mechanical forces similar to those experienced in the body. These mechanical forces are considered to be crucial to initiate a cascade of signalling events inside the cell. Currently there are some constraints on the use of compressive loading or tensile loading bioreactors to mechanically stimulate 3D bioengineered scaffolds containing cells. However, magnetic actuation directed at specific mechanoreceptors has the potential for tissue engineering, particularly for the manipulation of scaffold/cells that are implanted into the patient (101, 102).

In a study by Glogauer *et al,* magnetic force was applied to study force-induced changes in the cytoskeleton. Fibroblasts were incubated with ferric oxide bead-like microparticles (Fe_3O_4) coated with collagen and attached to the surface of cells via receptors of the integrin family. A static magnetic force was applied to fibroblasts using a permanent magnet. The results showed that when force was applied

continuously for 30 minutes there was an increase in F-actin (103).

Hughes *et al* presented one of the first studies that demonstrated direct ion channel activation with the use of magnetic actuation. Magnetic particles with diameters between 250 nm to 2.7 μm were targeted with either monoclonal antibodies or complexes of nickel and nitrolotriacetic acid. An 80 mT magnetic field was applied to the cells with a frequency of 1 Hz in cyclical fashion. The results showed that manipulation of magnetic particles attached to the extracellular loop region of TREK-1 resulted in an increase in the expression of TREK-1. The technique of tagging ion channels with magnetic particles allows applying highly localized forces to specific region of the cells (104).

Similarly in another study, TREK-1 was used to differentiate stem cells in vitro and in vivo. Silica magnetic particles 250 nm in diameter with COOH coating (Micromod) were tagged with an anti-TREK (transmembrane ion channel stretch activated potassium channel) antibody and an RGD peptide. These particles were then applied to human bone marrow stromal cells (HBMSCs) and an oscillating magnetic field (1 Hz) was used to deliver force of 1-100 pN per particle. Cells were stimulated for 1 hour every day for a period of 7 days. The cells expressed an up-regulation of mRNA expression for Sox9, core binding factor alpha 1(Cbfa1) and osteopontin, indicating manipulation by magnetic actuation can induce the differentiation of osteoprogenitor cell populations toward an osteogenic lineage (102).

Additionally, carboxyl ferromagnetic microparticles with a size range of 4-4.5 μm, coated with L-arginyl-glycyl L-aspartic acid (also known as RGD) were tagged to mesenchymal stem cells (MSCs) via integrin receptors. An external magnetic field oscillating at a frequency of 1 Hz was used to deliver 6 pN of force per cell via the microparticles attached to the cell surface integrins. The results showed that the

membranes of MSCs were depolarized in response to force delivered by the magnetic field and that this response was mediated by big potassium (BK) channels and release of intra-calcium (105).

Magnetic actuation has also been used to control the differentiation of cells. A study by Hu *et al* examined the possibility of controlling differentiation by mechanically activating the PDFG receptor α and β of HBMSCs with a bioreactor. The objective of the study was to identify whether magnetic fields applied to nanoparticle-bound PDGF receptors could regulate the phenotype of human bone marrow stromal cells. Magnetic particles with a diameter of 250 nm (Micromod) were conjugated with anti-human PDGF-α and β antibodies (R&D Systems). The conjugated particles were incubated with cells and magnetic force was applied. The protein levels of smooth muscle α-actin expression (SMA) were estimated using immunocytochemistry. There was an increase in protein levels after 3 hours of continuous magnetic actuation. Additionally by performing real time PCR there was an up regulation of SMA mRNA levels after 3 hours of continuous magnetic actuation (106).

Similarly Glossop *et al* investigated the differentiation of mesenchymal stem cells (MSCs) by actuation using magnetic particles. MSCs were incubated with 250 nm superparamagnetic iron oxide particles (Nanomag-silica;Micromod) and an oscillating magnetic field of 90 mT applied for 1 hour at 1 Hz. The results showed no change in the mRNA expression of MAP3K8 and IL-1B both following magnetic actuation. One of the limitations of the study stated by the authors was the short period of the duration of the experiment (24 hours) (107).

1.12 Magnetic Fields and Superparamagnetism

Magnetism is a physical phenomenon that is mediated by magnetic fields. All materials have atoms (electron, proton and neutrons). The electrons are in a constant

spin around the nucleus. Electrons carry a negative electrical charge and produce a magnetic field as they move through space. A magnetic field is produced whenever an electrical charge is in motion. The strength of this field is called the magnetic moment**.** Since all the materials have atoms are affected at some extent by a magnetic field, However, not all materials react the same way(108).

When a material is placed under a magnetic field of strength H, the magnetic forces of the materials electrons will be affected. This is the Faraday's law of induction.

$$B = \mu 0(H + M)$$

Where μ0 is the permeability of free space, and the magnetization M = m/V is the magnetic moment per unit volume, where m is the magnetic moment on a volume V of the material.

Not all materials behave the same in the presence of a magnetic field. Materials that their electrons paired together in opposite direction cancel each other therefore the magnetic field is zero. However other materials with unpaired electrons will expose a net magnetic field and make them more attractable to an external magnetic field. All materials are magnetic to some extent, with their response depending on their atomic structure and temperature. They are categorized in terms of their volumetric magnetic susceptibility, χ, where M = χH, describes the magnetization induced in a material by H (109).

The materials could be classified as paramagnetic, ferromagnetic or diamagnetic. Paramagnetic materials have a small susceptibility to magnetic fields in comparison to diamagnetic which have a weak magnetic susceptibility. These materials are slightly attracted to an external magnetic field but when the field is removed the materials do not retain the magnetic properties and the χ ranges between 10^{-6} to 10^{-1}.

Diamagnetic materials have a weak susceptibility to magnetic fields and are slightly

repelled by a magnetic filed therefore the material does not retain the magnetic properties when the external magnetic field is removed therefore the χ ranges between 10−6 to 10^{-3}. Finally the ferromagnetic materials have a large susceptibility to an external magnetic field. Materials exhibit strong attraction towards an external magnetic field and are able to retain the magnetic properties even after the removal of the external magnetic field. Ferromagnetic materials have some unpaired electrons so their atoms have a net magnetic moment. They get their strong magnetic properties due to the presence of magnetic domains. In these domains, large numbers of atom's moments (10^{12} to 10^{15}) are aligned parallel so that the magnetic force within the domain is strong. When a ferromagnetic material is in the un-magnetized state, the domains are nearly randomly organized and the net magnetic field is zero. When a magnetizing force is applied, the domains become aligned to produce a strong magnetic field within the part. The susceptibility in ordered materials depends not just on temperature, but also on H, which gives rise to the characteristic sigmoidal shape of the M–H curve, with M approaching a saturation value at large values of H as showed in Figure 1.4 (108) (109).

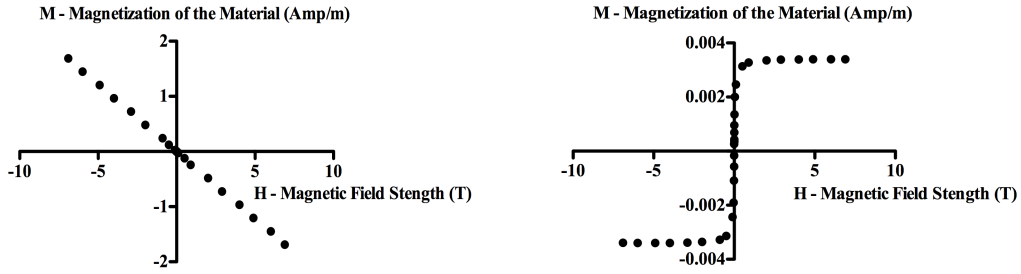

(a) (b)

Figure 1.4 The magnetic response of SPION loaded HRSMC. (a) HRSMC alone (no SPION), the M-H curve are shown for diamagnetic and (b) SPION-loaded cells (1000 μg/ml), the M-H curve has the characteristic sigmoidal shape indicating the presence of a superparamagnetic material.

The magnetic force that experience a magnetic material (magnetic dipole-m) when exposed to a magnetic field could be described by the following equation:

$$Fm = (m \cdot \nabla)B$$

Where is Fm is the force, ∇ is a symbol used in mathematics to denote the geometrical differentiation with respect to the direction of m with hypothetical coordinates m=(0,0) on the z-axis (110) (109).

1.13 Superparamagnetic Iron Oxide Nanoparticles (SPION)

Superparamagnetic particles consist of either magnetite (Fe_3O_4) or maghemite (γ-Fe_2O_3). Both magnetite and maghemite are members of the iron oxide family. The internal structure of ferromagnetic materials is composed of magnetic domains, which are regions grouping magnetic moments with the same orientation. Under the action of an external magnetic field, the domains with an orientation closer to that of the field tend to grow at the expense of those with a dissimilar orientation. This is regarded as the magnetization process. When the dimensions of the material are progressively reduced down to a certain size, which ranges from tens to hundreds of nanometers and is characteristic of each substance, the formation of magnetic domains is no longer favourable and the material becomes a single domain. In this state all the magnetic moments have the same orientation, and the magnetization of the particle can be represented by a single "giant" magnetic moment. If the size is further reduced, there will be a value from which the thermal energy overcomes the magnetic one, and the magnetisation of each particle will be continuously fluctuating between two limiting orientations separated by an energy barrier. It is then said the system has entered into a superparamagnetic regime (111).

1.14 Synthesis of Iron Oxide Nanoparticles

Superparamagnetic iron oxide nanoparticles can be prepared by various methods that affect the size distribution, shape and surface chemistry of the particles, which in turn affect the magnetic behaviour of the nanoparticles (112). Figure 1.3 summarizes the different processes available.

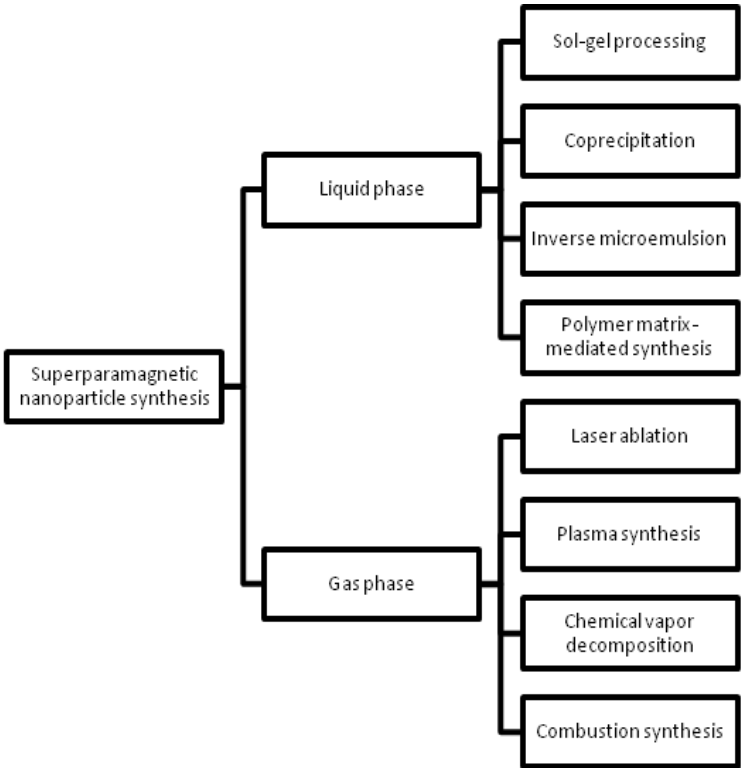

Figure 1.5 A diagram that summarized the different methods of SPION Synthesis

1.14.1 Co-Precipitation

Co-precipitation is a common method for manufacturing magnetic nanoparticles. In an aqueous solution Fe^{3+} and Fe^{2+} salts are mixed with alkaline because of the low reaction temperature and the hydrophilic surface properties of the resulting particles. Magnetite is synthesised by addition of ammonia to the aqueous mixture of Fe^{3+} and Fe^{2+} chloride (ratio 2:1) with the pH between 8 and 14. It is possible to control the size

and the shape, composition of the nanoparticles by changing the pH, ionic strength, temperature and nature of the salts, or the Fe(II)/Fe(III) concentration ratio (112).

Maghemite (γFe_2O_3) is formed from magnetite (Fe_3O_4) in the presence of oxygen, as described in the following reaction (112).

$$2Fe_3O_4 + O_2 \rightarrow 2\gamma Fe_2O_3$$

1.15 Research Hypothesis

Previous research have described that cyclic mechanical strain could regulate the phenotypic continuum of smooth muscle cells. It could shift the cells towards a contractile or proliferative phenotype (89). For example a study by Bonacci et al where airway smooth muscle cells (ASM) were subjected to cyclic strain with a Flexcell system resulted in an increase in the proliferation of ASM.

Additionally, the possibility of regulating the phenotype of different type of cells from distance with the use of an external magnetic field was also investigated previously (106). Specifically, a study by Hu *et al* where the possibility of controlling the differentiation of human bone marrow stromal cells (HBMSC) by mechanically activating the PDFG receptor α and β with the use of an external magnetic field. The results showed an increase in the gene and protein expression of smooth muscle actin.

Therefore, the combination of delivering a cyclic mechanical strain (mimicking the flex cell system) by an external oscillating magnetic field and SPION could have an effect on the phenotypic continuum of the cells. The SPION will be endocytosed by the cells rather than tagged to different proliferative or contractile receptors as have seen previously. This approach could potentially have a therapeutic application.

In this study, it was hypothesized that mechanical stretching of an external oscillating magnetic field could change the phenotypic continuum (proliferation or differentiation) of SPION-loaded HRMSC.

1.16 Thesis Aims and Objectives

The research described in this thesis aimed to investigate the feasibility of applying an external oscillating magnetic field to SPION-loaded HRSMC to regulate the phenotypic continuum of the cells.

The objectives of the research were:

1. To load HRSMC with SPION and localise them inside the cells; this objective will be explored with superconducting quantum interference device (SQUID) which quantifies the amount of magnetic material inside the cells and the localization of SPION with Tramission electron microscopy (TEM).

2. To investigate the biocompatibility of SPION-loaded HRSMC in response to an external magnetic field. This objective will be investigated with lactate dehydrogenase (LDH) toxicity assay, caspase 3-7 apoptosis assay and reactive oxygen species(ROS) assay.

3. To explore the effects on cell phenotype when an external magnetic field was applied to SPION loaded HRSMC; this objective will be investigated with cell proliferation bromodeoxyuridine (BrdU) assay, CyQUANT® Cell Proliferation Assay, immunocytochemistry and real-time PCR of different contractile or proliferative markers such as smooth muscle actin, myosin heavy chain, calponin and caldesmon.

4. To investigate whether an oscillating external magnetic field could change the shape of the cells by stretching the plasma membrane; this objective will be explored with time-lapse microscopy and scanning electron microscopy.

1.17 Thesis overview

Chapter 2: Materials and Methods

This chapter provides an overview of the materials and methods used throughout the research project.

Chapter 3: Preliminary Investigation of SPION Effects on HRSMC

The aim of this chapter was to explore the interaction of SPION with cell culture medium; the loading efficiency of SPION by HRSMC; the localization inside the cells after endocytosis had occurred; and finally the effects of different concentrations of SPION on the phenotype and biocompatibility of HRSMC.

Chapter 4: Chapter 4: Effect of Magnetic Actuation on the Phenotype of SPION-Loaded HRSMC

The aim of this chapter was to investigate the effects of applying external magnetic fields to HRSMC loaded with SPION. This included exploring the effect of a magnetic field on the cell phenotype. Additionally, the effect of applying a magnetic field on cell toxicity, release of reactive oxygen species, and apoptosis were investigated.

Chapter 5: Membrane Deformation of SPION-Loaded HRSMC in Response to an Externally Applied Magnetic Field

The aim of this chapter was to investigate whether application of an external magnetic field to SPION-loaded HRSMC results in an observable change to the cell shape by stretching the plasma membrane.

Chapter 6: Thesis Summary, Conclusion and Future work

Chapter 2

General Materials and Methods

2.1 Materials

2.1.1 Mammalian Cells

Primary human rectal smooth muscle cells (HRSMC) isolated from foetal rectal tissue of a healthy donor were obtained from the TCS CellWorks, UK (Catalog Number: 2980).

2.1.2 Cell Culture Medium

- **Proliferation Medium.** Minimum Essential Medium Eagle (MEME; Sigma Aldrich, UK). The medium was supplemented with 10% foetal bovine serum (FBS) (Sigma Aldrich, UK). In addition the medium was also supplemented with 1x non-essential amino acids (NEAA), 2 mM glutamine, 50 U/ml penicillin and 50 µg/ml streptomycin (all purchased from Sigma Aldrich, UK).
- **Differentiation Medium.** Dulbecco's Modified Eagle Medium DMEM (Sigma Aldrich, UK). The medium was supplemented with 1x NEAA, 2 mM glutamine, 50 U/ml penicillin and 50 µg/ml streptomycin (all purchased Sigma Aldrich, UK) and 2 ng/ml transforming growth factor (TGF)-β (PerproTech EC Ltd, UK) (113-115).

2.1.3 Cell Culture Solutions

Trypsin-ethylenediaminetetraacetic acid (EDTA) 1x solution 0.25% trypsin and 0.1% EDTA (Sigma). Dulbecco's phosphate buffered saline (PBS) (Sigma).

2.1.4 Superparamagnetic Iron Oxide Nanoparticles (SPION)

- SPION (fluidMAG-UC/A anionic charged SPION; 50 nm particles with a magnetite core suspended in water with a stock concentration of 25 mg/ml and particle density of ~1.3x1016 particles/g; Chemicell GmbH, Berlin, Germany).

- SPION (fluidMAG-UC/A anionic charged SPION; 200 nm particles with a magnetite core suspended in water with a stock concentration of 25 mg/ml and particle density of ~ 2.2 x 10^{14} particles/g; Chemicell GmbH, Berlin, Germany).

2.2 Methods

2.2.1 Cell Culture

2.2.1.1 Cell Culturing Conditions

HRSMC were maintained in proliferation medium. The cells were cultured in vented 75cm^2 tissue culture flasks (Nunclon^{TM}, Delta treated flask, Denmark). Cell cultures were incubated at 37ºC with 5% CO_2 in a humidified atmosphere (MCO-18AIC; UV; Sanyo CO_2; incubator, Japan).

2.2.1.2 Cell Subculture

HRSMC cultured in tissue culture flasks were not allowed to exceed 70-80% confluence so as to avoid contact inhibition and loss of their ability to proliferate. Sub-culturing was performed aseptically inside a class II microbiological safety cabinet (Walker Safety Cabinets Ltd, UK). The monolayers attached to the base of the flasks were washed with 10 ml of 1 x sterile PBS followed by the addition of 2 ml trypsin/EDTA. The flask was incubated for 2 minutes to facilitate enzymatic detachment of the cells. When the cells were fully detached (confirmed by viewing the contents of the flask with an inverted microscope) 10 ml of fresh proliferation medium was added to the flask and the contents transferred to a sterile 30 ml container (Sterilin Limited, UK). The container was centrifuged at 1000 rpm for 5 minutes to pellet the

cells in the bottom of the container. The supernatant was removed and the pellet was re-suspended in fresh culture medium.

2.2.1.3 Cell Counting

To quantify the number of cells in a suspension 10 µl of the cell suspension was placed into a haemocytometer (Neubauer Clear Sight, Hawksley, UK) and a coverslip placed on top.

The mean number of cells was calculated from the central squares located on both sides of the haemocytometer and the following equation was used to calculate the number of cells per ml.

Number of cells/ml = mean number of cells per central square x 10^4.

2.2.1.4 Cell Cryopreservation

Cells were cryopreserved to retain a sufficient stock of cells from similar passage numbers for future experiments. After trypsinization and centrifugation, the cell pellet was re-suspended in 1ml of Bambanker (Anachem, UK) freezing solution. The solution was transferred in to 2 ml cryogenic vials (Nalgene, Nalgene Company, USA). The samples were then stored in a -80^0C freezer (New Brunswick scientific ultra-low temperature freezer; Wolf laboratories Limited, UK).

2.2.1.5 Cell Resuscitation

The cryovials were thawed at 37^0C for 5 minutes. To avoid contamination of the cells, the vial was transferred into the class II microbiological safety cabinet and sprayed with 70% industrial methylated spirit (industrial methylated spirit; Scientific & Chemicals Supplies Ltd, UK) in water. The cell suspension was transferred into a 30

ml container containing 10 ml of cell culture medium. The cells were centrifuged for 5 minutes at 1000 rpm in order to remove the Bambanker (Anachem, UK). The supernatant was discarded and the pellet was re-suspended in 10 ml of fresh culture medium. The solution was transferred to a 75 cm^2 cell culture flask (Nunclon^{TM} delta treated, Denmark) and incubated at 37^0C in 5% CO_2.

2.2.2 Measurement of Cellular Loading with Superparamagnetic Iron Oxide Nanoparticles

2.2.2.1 Superconducting Quantum Interference Device (SQUID)

The magnetometers are measuring the magnetic properties of materials. The magnetometers could be classified according to the method used to measure the magnetic properties of the materials. This could be magnetometers: 1) that require motion of the sample within a coil (vibrating magnetometers-superconducting quantum interference device-SQUID) and 2) those that require force or torque in which the sample is kept static while the field is rotated for example (Faraday balance, Gouy method).

A SQUID magnetometer was used in this study to measure the amount of iron loaded per cell. The SQUID is a magnetometer that measures very small magnetic fields, down to 5 x 10^{-18} T. SQUID uses a Josephson junction, which is made out of two superconductors separated by an insulating layer, thin enough so that electrons can pass through. SQUID is usually made of lead alloy or niobium. The coils are kept within the vacuum space of a liquid helium-filled chamber that allows cooling of the coils to 9 K. The coils have a 2.02 cm diameter, and the total length of the coil system is 3.04 cm. The SQUID is moving the sample through a superconducting coil. As the sample moves the magnetic dipole moment of the sample induce an electric current in

the detection coils (the magnetic moment of the sample in recorded in electromagnetic units-emu). The SQUID converts the current to voltage, therefore determines the magnetic moment of the sample by measuring the voltage of the detection system. The changes in the voltage are directly proportional to the changes of the magnetic flux as the sample moves through the coil.

The sample is exposed to different temperatures and magnetic fields. Initially the sample is exposed to zero magnetic fields and the temperature is dropped up to 9K. Then temperature stabilizes, a magnetic field is applied to the sample and the temperature rises. The behaviour of the sample is recorded constantly at all different magnetic fields and temperatures (116-119).

(i) $5x10^5$ HRSMC were seeded in a 75 cm^2 culture flask. The flasks were incubated at 37^0C, in a humidified atmosphere and 5% CO_2 for 24 hours.

(ii) Medium was removed and experimental media containing SPION particles was added, as specified for each experiment.

(iii) Following incubation, the cells were washed 5x with 10 ml of PBS.

(iv) 2 ml of trypsin was added to each flask and incubated at 37^0C, 5% CO_2 for 1 minute.

(v) 10 ml of fresh media was added to each flask and the detached cells were collected in a 30 ml container.

(vi) Samples were centrifuged at 1000 rpm for 5 minutes, the supernatant was removed, and the pellet was re-suspended in 10 ml of PBS. This procedure was repeated once.

(vii) Supernatant was removed and the pellet was re-suspended in 1 ml of PBS. A cell count was performed as described in section 2.2.1.3. The samples were transferred in a 1.5 ml micro-centrifuge tube (Kartell SPA, Italy). The lid of the

tube was pierced using a needle (BD microlane TM 3; 18G 2'', 1.2 X50 mm) to allow air to escape from the tube during the freeze dry process.

(viii) The samples frozen at -80°C (New Brunswick Scientific ultra low temperature freezer Wolf laboratories Ltd, UK).

(ix) The samples were placed into a freeze drier (Edwards Modulyo, UK) and lyophilized for 24 hours.

(x) The freeze-dried pellets of cells were transferred to SQUID capsules (QD-P125E; Quantum Design, USA).

(xi) Samples were analysed with a Quantum Design SQUID-VSM magnetometer (Quantum Design Inc, San Diego, CA). An MH curve was generated at 300 K using a field between +/- 7T.

2.2.3 Ultrastructural Localisation of SPION

2.2.3.1 Preparation of Samples for Electron Microscopy

Transmission electron microscopy (TEM) was used to determine the cellular localisation of SPION.

(i) HRSMC were seeded in 25 cm^2 tissue culture flasks and incubated as specified for each experiment.

(ii) Media were removed and experimental media containing SPION particles were added, as specified for each experiment.

(iii) Following incubation, the cells were washed 5x with 10 ml of PBS.

(iv) To detach cells from the flask, 2 ml of trypsin was added and the flasks were incubated at 37^0C, 5% CO_2 for 1 minute.

(v) 10 ml of fresh media was added to each flask and the detached cells were

collected in a 30 ml container.

(vi) Cells were centrifuged at 1000 rpm for 5 minutes, the supernatant was removed, and the pellet was re-suspended in 10 ml. The procedure was repeated once.

(vii) The sample was centrifuged at 1000 rpm, the supernatant was removed and 1 ml of 2.5% v/v *glutaraldehyde* (Sigma, UK) was added to the pellet to fix the cells inside a fume cupboard.

(viii) The solution was transferred in a 1.5 ml micro-centrifuge tube and incubated overnight.

(ix) After removing the fixative the samples were washed in 0.5 ml of PBS and centrifuged at 1000 rpm 3x for 1 minute.

(x) The samples were post fixed with 2% osmium tetroxide (OsO_4) (Ceimiglinited, UK) for 1 hour inside a fume cupboard.

(xi) The cell pellet was washed 3x with 0.5 ml of PBS for 10 minutes and centrifuged at 1000 rpm for 1 minute.

(xii) The cell pellet was dehydrated in a progressive series in water/ethanol mixtures:

a. 25% v/v ethanol 4 minutes
b. 50% v/v ethanol 4 minutes
c. 75% v/v ethanol 4 minutes
d. 95% v/v ethanol 4 minutes
e. 100% v/v ethanol 4 minutes
f. 100% ethanol over sieves 20 minutes (the last step was repeated 5 times).

(xiii) Propylene oxide (Agar Scientific, UK) was added to the cell pellet for 20

minutes to act as a transition solvent before the embedding stage.

(xiv) Propylene oxide was removed and a mixture containing 1:1 v/v propylene oxide: embedding resin (Araldite CY212 resin;Agar Scientific, UK) was added for 20 minutes.

(xv) 1:1 propylene oxide was removed and 1:3 propylene oxide:embedding resin was added for 1.5 hours.

(xvi) The final propylene oxide:resin was removed and 100%resin was added.

(xvii) The samples were transferred to capsules (Beem Inc, USA) and placed on a hot plate at 60ºC for 24 hours.

(xviii) The resin blocks containing the samples were thin sectioned (70 nm) with an ultramicrotome (Reichertjung ultracut E, Germany) and directly collected onto copper grids for its examination under a JEOL JEM 1200EX TEM operating at 80 Kv.

2.2.4 Cellular Techniques to Investigate Changes in the Phenotype

2.2.4.1 Protein Expression of Smooth Muscle Contractile Markers

2.2.4.1.1 Immunocytochemistry

Immunocytochemistry was used to detect the expression of different contractile smooth muscle markers such as actin, myosin heavy chain, caldesmon and calponin.

(i) HRSMC were seeded in a Fluorodish Cell Culture Dish – 35 mm (World Precision Instruments, USA) and incubated as specified for each experiment.

(ii) The medium was removed gently and cells were fixed in 4% formaldehyde in PBS for 10 minutes at room temperature.

(iii) Cells were washed 3x with PBS.

(iv) Then cells were blocked with 3% BSA + 0.1% triton X-100 in PBS for 1 hour at room temperature.

(v) The solution was removed and the primary antibody was added to each well. Cells were incubated for 1 hour.

Primary antibody	**Description**
Actin (1:1000)	Monoclonal Anti-a Smooth Muscle Actin, Clone 1A4, 15mM Product No. A2547 (Sigma)
Myosin Heavy Chain (1:500)	Monoclonal Anti-Myosin (Smooth), Clone hSM-V produced in mouse, 15 mM, Product No. M7786 (Sigma)
Caldesmon (1:500)	Monoclonal Anti-Caldesmon (Smooth) Mouse Ascites Fluid Clone hHCD, 15 mM, Product No. C4562 (Sigma)
Calponin (1:1000)	Monoclonal Anti-Calponin Clone hCP produced in mouse, 15 mM, Product No. C2687 (Sigma)
Primary antibody (Isotype control)	
Actin (1:500) **Caldesmon (1:500)** **Calponin (1:500)**	Mouse IgG1,κ (MOPC-21), Purified Immunoglobulin, Mouse Isotype Control, 15 mM, Product No. M5284 (Sigma)
Myosin heavy chain (1:500) 1:500)	Mouse IgG2a Isotype Control; Clone UPC-10 purified immunoglobulin, 15 mM, Product No. M5409 (Sigma)

(vi) After the incubation period, cells were washed 3x with PBS.

(vii) Cells were incubated with the secondary antibody for 1 hour.

Secondary antibody	Description
Actin (1:500) **Myosin Heavy chain (1:500)** **Caldesmon (1:500)** **Calponin (1:500)**	Anti-mouse IgG (whole molecule) FITC conjugate, Antibody developed in Goat IgG, 15 mM, Product No. F 9006 (Sigma)

(viii) Cells were washed 3x with PBS.

(ix) Cells were mounted onto glass slides (Thermoscientific, Menzel-Glaser Superfrost® plus, UK) with DAPI (Vectashield® Mounting Medium with DAPI, Vector Laboratories Ltd, UK).

(x) An upright fluorescence microscope (BX51 Olympus, GX Optical, UK) was used to acquire images.

2.2.4.2 Quantification of Gene Expression of Smooth Muscle Contractile and Proliferative Markers

2.2.4.2.1 RNA Extraction from Cells

For the RNA extraction step, an RNeasy mini kit was used (Qiagen, UK). The RNeasy mini kit purifies RNA from animal cells, animal tissues and yeasts and cleans up RNA from crude RNA steps and enzymatic reactions (e.g DNase digestion, proteinase digestion, RNA ligation and labelling reaction).

(i) $3x10^5$ cells were seeded in a 75 cm^2 culture flask. The flasks were incubated at 37°C in a humidified atmosphere and 5% CO_2 for 24 hours.

(ii) Medium was removed and experimental media containing SPION particles was added, as specified for each experiment.

(iii) Following incubation, the cells were washed 5x with 10 ml of PBS.

(iv) 10 ml of differentiation medium was added in each flask and incubated for 7

days.

(v) On day 7, 2 ml of trypsin was added to each flask and incubated at 37^0C for 1 minute.

(vi) 10 ml of fresh media was added to each flask and the detached cells were collected in a 30 ml container.

(vii) Samples were centrifuged at 1000 rpm for 5 minutes, the supernatant was removed, and the pellet was re-suspended in 10 ml of PBS. This procedure was repeated once.

(viii) Supernatant was removed and the pellet was re-suspended in 350 ml of lysis solution/β-mercaptoethanol (10 µl of β-mercaptoethanol per 1 ml of buffer) in 1 ml of PBS. The samples were transferred in a 1.5 ml micro-centrifuge tube (Kartell SPA, Italy).

(ix) 350 µl of 70% ethanol was added to the homogenised lysate and mixed by pipetting. The sample was transferred to an RNeasy column.

(x) Samples were centrifuged at 10,000 rpm for 15 seconds with a centrifuge (Eppendorf Micro Centrifuge 5410) and the 'flow throw' remaining at the bottom of the tube was discarded. 700 µl of RW1 buffer (containing ethanol) provided with the kit was added to the tube and the sample was centrifuged for 15 seconds at 10,000 rpm.

(xi) The 'flow throw' remaining at the bottom of the tube was discarded and 500 µl of RPE Buffer (washing buffer) provided with the kit was added. The samples were centrifuged for 15 seconds at 10,000 rpm, the 'flow throw' was discarded, and a further 500 µl of RPE buffer was added and the sample was centrifuged for 2 minutes. The second centrifugation stage was longer than the first in order to completely remove liquid from the column membrane to ensure that no

ethanol was carried over during the RNA elution step that may interfere with downstream reactions.

(xii) To avoid carryover of the RPE buffer the RNeasy spin column was replaced with a 2 ml collection tube. The sample was centrifuged for 1 minute at 10,000 rpm.

(xiii) 30 µl of RNase free water was added to elute the RNA from the spin column membrane.

(xiv) The samples were stored in a -80°C freezer until further analysis.

2.2.4.2.2 RNA quantification

A NanoDrop ND-1000 spectrophotometer (Thermoscientific, UK) was used to quantify the amount of RNA present in the samples. The spectrophotometer measures the RNA samples up to 3200 ng/ml with a spectrum range from 220 to 750 nm.

(i) 1 µl of RNA was pipetted onto the receiving fibre and a second fibre ('source fiber') was placed on top. A pulsed xenon flash lamp provided the light source, which passed through the sample. The data were analysed using the ND-1000 spectrophotometer software.

2.2.4.2.3 cDNA Libraries

Complementary DNA (cDNA) libraries are a combination of cloned cDNA fragments inserted into a host cell, which together constitute some portion of the transcriptome of the organism. cDNA is produced from fully transcribed mRNA found in the nucleus and therefore contains only the expressed genes of an organism.

(i) The following reagents from a cDNA synthesis kit (Applied Biosystems, UK) were added to a 1.5 ml micro centrifuge tube and mixed: 10 µl of reverse transcription buffer, 4 µl of deoxynuclotide triphosphates (dNTPs), 10 µl of random primers, 5 µl of reverse transciptase and 61µl of RNA free water.

(ii) 90 µl of the above solution and 10 µl of extracted RNA sample were added to a fresh 1.5 ml micro centrifuge tube and mixed.

(iii) The samples were heated at 25^0C for 10 minutes, 37^0C for 120 minutes, and 85^0C for 5 minutes and finally cooled at 4^0C using a DNA Thermal Cycler Model 480 Perkin Elmer Cetus, UK). After the last step the samples were stored at -20°C.

2.2.4.2.4 Real-Time Polymerase Chain Reaction

Real time polymer chain reaction (PCR) was used to quantify the amount of cDNA present in the sample. The advantage of using real time PCR is that it enabled monitoring of the progress of the PCR reaction as it occurred by precisely measuring the amount of each amplicon at each cycle during the PCR process. The signal produced was directly proportional to the amount of PCR product in the reaction.

The expression of six genes was investigated along with GAPDH as the house keeping gene. These were actin (ACTA2), myosin heavy chain (MYH11), caldesmon (CALD1), calponin (CNN1), vimentin (VIM) and tropomyosin 4 (TMP4) (Applied Biosystems, UK). The characteristics of all the different markers are summarized in the following table:

Marker	Description
Actin (ACTA2)	Is a 43 kDa cytoskeletal protein associated with cell motility (myosin heavy chain as well). Additionally, is also involved in other cellular processed such as locomotion, secretion, cytoplasmic streaming, phagocytosis and cytokinesis. Six distinct actin isotypes have been identified in mammalian cells(120).
Myosin Heavy Chain (MYH11)	Skeletal muscle Myosin is 200–204 kDa protein that generates force to drive muscle contraction. It is comprised of two heavy chains and four light chains. Most organisms produce many muscle MHC isoforms with temporally and spatially regulated expression patterns. The globular head of each MHC molecule protrudes from the thick filament and binds actin of thin filaments in an ATP-dependent fashion(120-122).
Caldesmon (CALD1)	It is a 120-150 kDa protein and regulates smooth muscle contraction. Two types of isoforms exist h-caldesmon expressed in smooth muscle cells and i-caldesmon expressed in non-muscular tissue. Caldesmon could be found in either proliferative or synthetic smooth muscle cells. H-Caldesmon is an actin and calmodulin-binding protein that regulates cellular contraction, exocytosis, endocytosis, cell movement and cell shape change(123-127).
Calponin (CNN1)	Is a 34 kDa protein which modulates the myosin ATP-ase activity. The modulation of the ATP-ase is occurred with phosphorylation of either caldesmon or calponin. It is located in the same region with actin filaments and is involved in smooth muscle cell contraction. (128, 129)
vimentin (VIM)	Is a 52-58 kDa protein expressed in smooth muscle cells but also other type of cells such as fibroblasts, lymphocytes, and endothelial cells. It maintains cell shape and integrity of cytoplasm one of the most common markers for proliferative cells(130-135)
Tropomyosin 4 (TMP4)	Is a 30 kDa protein and is expressed in smooth muscle cells. It regulates actin binding and is involved in smooth muscle contraction. It is expressed in low levels in contractile smooth muscle cells but high levels of tropomyosin 4 could be found in proliferative smooth muscle cells(136-138).

Table 2.1 A table that summarizes all the genes used in this study

(i) The following reagents were added to a 1.5 ml micro centrifuge tube and mixed: 12.5 µl of Taqman universal master mix (Applied Biosystems, UK), 1.25 µl of primer and 6.25 µl of RNA free water and 5 µl of cDNA sample.

(ii) The mixtures were transferred to a 384 well plate (MicroAmp^{TM,} Applied Biosystems) and sealed with a film lid. The plate was centrifuged for 1 minute at 10,000 rpm and then was placed in a LightCycler 480, (Roche, UK) for the real time PCR reaction to occur. At the end of the real time PCR reaction the sample was normalised according to the housekeeping gene GAPDH.

2.2.4.3 Aspect Ratio

The aspect ratio is the ratio of the width of a cell to its length. The aspect ratio of muscle cells differentiated towards a contractile phenotype is typically greater than the aspect ratio of cells in a proliferative state and can be used as an indicator of the phenotypic status of cells in culture. The aspect ratio was therefore used to investigate whether proliferation or differentiation medium affected the morphology of SPION-loaded HRSMC.

(i) HRSMC were seeded in tissue culture plates and incubated as specified for each experiment.

(ii) The medium was removed and the cells were fixed with 1 ml of 2.5% gluteraldehyde for 10 minutes at room temperature.

(iii) The solution was removed and the cells were washed 3x with 1 ml of PBS.

(iv) The cells were imaged using a phase contrast inverted microscope (AmScope 40x-900X Phase Contrast Inverted Microscope with 3M Camera, USA).

(v) The aspect ratio was calculated using image analysis software (Image J, national

Institute of Health, USA).

2.2.4.4 Determination of Cell Proliferation

Four methods were used to investigate cell proliferation.

2.2.4.4.1 Cell Proliferation BrdU Assay

The proliferation of cells was measured with a colorimetric BrdU ELISA Assay (Roche, UK). 5-bromo-2'-deoxyuridine (BrdU) is a nucleoside and thymidine analogue. BrdU incorporates into the newly synthesized DNA of replicating cells substituting for thymidine. The assay involves labelling cells with concentration of 100 µM followed by detection using a mouse monoclonal antibody directed against BrdU.

(i) Human rectal smooth muscle cells were seeded in tissue culture plates and incubated as specified for each experiment.

(ii) After the incubation period the medium was removed from each well and replaced with fresh medium containing BrdU label (100 µM) and incubated for 2 hours at 37^0C, 5% CO_2.

(iii) Labelling medium was removed by inverting the plate and tapping off.

(iv) A sufficient volume of fixative and denaturing solution provided with the assay was added to the wells to cover the cells, as specified for each experiment. The plate was incubated for 30 minutes at room temperature.

(v) Fixative denaturing was removed from all the wells by inverting and tapping off and anti-BrdU-peroxidase monoclonal antibody was added to each well and incubated for 90 minutes at room temperature.

(vi) Antibody conjugated solution was then removed by inverting the plate and tapping off the solution. The wells were rinsed 3x with PBS/washing solution.

(vii) A sufficient volume of substrate solution provided with the assay was added to each well and incubated for 30 minutes at room temperature.

(viii) Transfer 100 µl to a 96 well plate (Nunclon TM, Delta surface, Denmark).

(ix) 25 µl/well of 1 M H_2SO_4 stop solution was added to each of the wells.

(x) The optical density of the reaction product in the wells was read with a colorimetric plate reader (Multiskan FC; Thermoscientific, UK) at 450 nm with a reference wavelength at 690 mm.

2.2.4.4.2 Measurement of Cellular DNA Content Using the CyQUANT® Assay

The proliferation of cells was also measured with the CyQUANT® Cell Proliferation Assay Kit. It is a rapid proliferation assay compared to the BrdU assay described in section 2.2.4.4.1. It is based in a fluorescent dye (CyQUANT® GR), which exhibits strong fluorescence when bound to cellular nucleic acids. After the addition of the dye, the fluorescence could be measured directly. The amount of fluorescent product generated is proportional to the amount of the fluorescent dye (CyQUANT® GR) present in the sample.

(i) HRSMC were seeded in tissue culture plates and incubated as specified for each experiment.

(ii) The medium was removed and 200 µl was added of Cyquant NF dye reagent (in 1x HBSS buffer).

(iii) It was incubated at 37^0C, 5% CO_2 using a plate shaker (Stuart mini orbital shaker SSM1, Bibby Sterilin Ltd, UK) at speed 70 for 1 hour.

(iv) After the incubation period, 100 µl of the solution were transferred in a black plate (Costar®, black with clear flat bottom, Corning B.V, Amsterdam).

(v) The fluorescence was measured using a fluorescence plate reader (TECAN

SpectraFluor, USA) at an excitation wavelength of 485 nm and an emission wavelength at 530 nm.

2.2.4.4.3 Direct Cell counts

Direct cell counts were performed in order to investigate the cell proliferation of HRSMC.

(i) HRSMC were seeded in tissue culture plates and incubated as specified for each experiment.

(ii) After the incubation period the medium was removed and the cells were washed 1x with 1 ml PBS.

(iii) 1 ml of trypsin was added to each well and incubated at 37^0C, 5% CO_2 for 1 minute.

(iv) 5 ml of fresh medium was added in each well and the detached cells were collected in a 15 ml container.

(v) Samples were centrifuged at 1000 rpm for 5 minutes, the supernatant was removed and the pellets were re-suspended in 1ml of fresh media.

(vi) A cell count was performed as described in section 2.2.1.3.

2.2.4.4.4 Cell Metabolic Activity Assay

The metabolic activity of HRSMC cells was determined by using the CellTiter 96 Aqueous Non-Radioactive Cell Proliferation Assay (Promega, UK). This colorimetric assay is composed of solutions of a tetrazolium compound [3-(4,5-dimethylthiazol-2-yl)-5-(3-carboxymethoxyphenyl)-2-(4-sulfophenyl)-2H-tetrazolium, inner salt; MTS] and an electron coupling reagent (phenazine methosulfate; PMS). MTS is bioreduced by cells into a formazan product that is soluble in tissue culture medium. The conversion of MTS into aqueous, soluble formazan is accomplished by dehydrogenase

enzymes found in metabolically active cells. The quantity of formazan product was measured by the amount of 490 nm absorbance which was directly proportional to the number of living cells in culture.

(i) HRSMC were seeded in tissue culture plates and incubated as specified for each experiment.

(ii) After the incubation period the medium was removed and replaced with fresh medium containing 20 µl MTS/PMS combined solution which was added to the wells and incubated for 2 hours at 37^0C, 5% CO_2.

(iii) Absorbance of the formazan was measured at 490 nm with colorimetric reader Multiskan FC (Thermoscientific, UK).

(iv) All optical densities of test samples were normalised with the control and expressed as a percentage change with the value measured for control cells.

2.2.5 Cellular Techniques to Investigate Changes in the Biocompatibility of Cells

Three techniques were used to investigate cellular biocompatibility:

2.2.5.1 Reactive Oxygen Species

The generation of reactive oxygen species (ROS) occurs in all aerobic organisms. However, in stressed cells it happens at a non-controlled rate. The over-production of ROS creates changes in the protein and nucleic acid formation. Diseases associated with ROS include atherosclerosis, carcinogenesis, ischemic reperfusion, and aging.

The ROS generation in cells was investigated with the Image-iT™ LIVE Green Reactive Oxygen Species Detection Kit. The assay is based in the expression of a fluorescent marker on 5-(and-6)-carboxy-2′,7′-dichlorodihydrofluorescen diacetate (carboxy-H2 DCFDA). To induce apoptosis, tert-butyl hydroperoxide (TBHP) was used. To stain the nucleus of the cells Hoechst 33342 was used. Using this

combination of fluorescent dyes the detection of ROS in stressed or non-stressed cells is distinguished with fluorescence microscopy. The fluorescent marker (carboxy-H2 DCFDA) DCFDA has excitation/emission maxima of approximately 495/529 nm and the Hoechst 33342 has excitation/emission maxima of approximately 350/461 nm.

(i) HRSMC were seeded in a Fluorodish Cell Culture Dish - 35mm (World Precision Instruments, USA) and incubated as specified for each experiment.

(ii) Before the test was started the medium was removed and cells were washed 1x with HBSS (Gibco, USA).

(iii) 25 μM carboxy-H2 DCFDA working solution (in Dimethyl sulfoxide-DMSO) was added for 30 minutes at 37^0C, 5% CO_2.

(iv) The last 5 minutes of the incubation period 1mM Hoechst 33342 stain (provided in the kit) was added.

(v) After the incubation period the cells were washed 3x with HBSS (Gibco, USA).

(vi) The cells were mounted with a drop of HBSS (Gibco, USA).

(vii) Images were taken using a fluorescent microscope (Leica DM2000, Germany).

2.2.5.1.1 Reactive oxygen species (Positive control)

(i) HRSMC were seeded in a Fluorodish Cell Culture Dish – 35 mm (World Precision Instruments, USA) and incubated as specified for each experiment.

(ii) To induce reactive oxygen species, 100 mM tert-butyl hydroperoxide (TBHP) solution (in water) were mixed with culture medium and added. The cell were incubated for 90 minutes at 37^0C, 5% CO_2.

(iii) Before the test was started the medium was removed and cells were washed 1x with HBSS (Gibco, USA).

(iv) 25 μM carboxy-H2 DCFDA working solution (in Dimethyl sulfoxide-DMSO) was added for the 30 minutes at 37^0C, 5% CO_2.

(v) The last 5 minutes of the incubation period 1 mM Hoechst 33342 stain (provided in the kit) was added.

(vi) After the incubation period the cells were washed 3x with HBSS (Gibco, USA).

(vii) The cells were mounted with a drop of HBSS (Gibco, USA).

(viii) Images were taken using a fluorescent microscope (Leica DM2000, Germany).

2.2.5.2 Cytotoxicity Assay - LDH Assay

The toxic effect of loading cells with SPION was determined by the CytoTox 96 Assay (Promega, UK). The assay quantitatively measures lactate dehydrogenase (LDH), a stable cytosolic enzyme that is released upon cell lysis. The quantity of LDH product was measured by the amount of 490 nm absorbance, which was directly proportional to the number of lysed cells.

(i) HRSMC were seeded in tissue culture plates and incubated as specified for each experiment.

(ii) After the incubation period the medium was removed from each well and transferred into a fresh 96 well plate (Nunclon^{TM}, Delta surface, Denmark).

(iii) 50 μl of medium was transferred into a fresh well and 50 μl of the LDH solution was added to each well.

(iv) Samples were incubated in the dark for 30 minutes.

(v) 50 μl of stop solution was added to each well and the optical density of the reaction produced in the well was read with a plate reader Multiskan FC (Thermoscientific, UK) at 490 nm.

2.2.5.2.1 Cytotoxicity Assay-LDH Assay (Positive Control)

(i) HRSMC were seeded in tissue culture plates and incubated as specified for each experiment.

(ii) 10 µl of lysis solution (10x) was added in each well per 100 µl of medium in order to lyse the cells.

(iii) The cells were incubated at 37^0C, 5% CO_2 for 45 minutes.

(iv) The plate was centrifuged at 250 x g (Stuart mini orbital shaker SSM1, Bibby Sterilin Ltd, UK) for 4 minutes.

(v) After the incubation period the medium was removed from each well and transferred into a fresh 96 well plate (Nunclon^{TM}, Delta surface, Denmark).

(vi) 50 µl of medium was transferred into a fresh well and 50 µl of the LDH solution was added to each well.

(vii) Cells were incubated in the dark for 30 minutes.

(viii) 50 µl of stop solution was added to each well and the optical density of the reaction produced in the well was read with a plate reader Multiskan FC (Thermoscientific, UK) at 490 nm.

2.2.5.3 Cell Apoptosis - Caspase-3/7

Cell apoptosis was measured with the Apo-ONE® Homogeneous Caspase-3/7 Assay. The Caspase-3/7 buffer lyses the cells and provides optimal caspase-3/7 enzymatic activity. The caspase-3/7 substrate rhodamine 110, bis-(N-CBZL-aspartyl-L-glutamyl-L-valyl-L-aspartic acid amide; Z-DEVD-R110), exists as a pro-fluorescent substrate prior to the assay. Both the buffer and the substrate were mixed together and added to the sample. Caspase-3/7 activity cleaves and removes the DEVD peptides with the excitation at 499 nm, which results in the rhodamine 110 leaving group becoming

intensely fluorescent. The emission maximum is 521 nm. The amount of fluorescent product generated is proportional to the amount of caspase-3/7 cleavage activity present in the sample.

(i) HRSMC were seeded in tissue culture plates and incubated as specified for each experiment.

(ii) The Substrate Z-DEVD-R110 was diluted (1:100 dilution) with the buffer to obtain the desired volume of Apo-ONE® Caspase-3/7 reagent.

(iii) The combined solution was added in each well and the plate was shaken at 300 rpm (Stuart mini orbital shaker SSM1, Bibby Sterilin Ltd, UK) at speed 70 for 30 seconds.

(iv) Then the cells were incubated at 37^0C, 5% CO_2 for 30 minutes.

(v) After the incubation period, 100µl of the solution were transferred in a black plate (Costar®, black with clear flat bottom, Corning B.V, Amsterdam).

(vi) The fluorescence of each well was measured with the optimal excitation wavelength for detection at 499 nm and the emission maximum at a wavelength of 521 nm.

2.2.6 Data Analysis

Data analysis was performed using GraphPad Prism version 5.00 for Windows (GraphPad Software, San Diego California USA). In order to compare if the differences between groups were statistically significant a one-way ANOVA and Tukey test was carried out. Any value was considered significant if $p< 0.05$.

Chapter 3

Preliminary Investigation of SPION Effects on HRSMC

3.1 Introduction

Loading cells with SPION is a requirement for achieving their magnetic actuation in the hypothesized manner using an externally applied magnetic field. To achieve this, SPION has to be delivered to cells efficiently whilst maintaining biocompatibility. Depending on the cell type and intended application there are different ways to achieve this.

Kyrtatos et al labelled the $CD133^{+}$ progenitor cells derived from human mononuclear cells (MNCs) with the FDA approved SPION Endorem® using 0.5 mg/ml SPION in growth medium. This was a direct loading regime where the SPION was mixed with the culture medium and directly applied to the cells relying on endocytosis mechanisms (92). Similarly in another study, human MNCs were labelled with three different types of particles: 45µl Endorem® with diameter 80-150 nm (concentration of 11.2 mg iron/ml), or 50 µl BioMag with a diameter 1.5 µm. (concentration 0.8 mg iron/ml) or 5 µl FluidMAG with a diameter of 200 nm (concentration of 48 mg iron/ml) added per ml of culture medium, and cells were incubated for 24 hours (93).

Another example of a loading regime was described in the study conducted by Vigor et al where three different types of SPION were investigated: i) 50 nm Nanomag coated with dextran, ii) 50 nm nanomag coated with dextran and PEG polyethylene glycol, and iii) 20 nm nanomag coated with dextran and PEG polyethylene glycol functionalized with recombinant single chain Fv (scFv) antibodies (specific for carcinoembryonic antigen-CEA) for the magnetic resonance imaging (MRI) of cancer cells. The results showed that the functionalised antibody-SPION bound specifically to CEA-expressing human tumour cells, generating selective image contrast for MRI (139).

SPION have many advantages in medicine. The particles exert magnetism only when an external magnetic field is applied (140). Due to their small size, cells are able to internalise these particles through endocytic pathways. Also the particles can be controlled by an external magnetic field; this ‘‘action at a distance’’ opens up many applications where magnetically tagged nanoparticles are functionalised to deliver an active load, such as an anticancer drug (141). Additionally, some SPION such as ferucarbotran and ferumoxide are approved by the FDA and have been used in clinical practice already as a magnetic resonance contrast agent as they offer higher contrast enhancement from the conventional gadolinium based contrast agents (142).

The aim of this chapter was to explore the effects of adding SPION to the cell culture medium, the loading efficiency of SPION by HRSMC, the localization of SPION inside the cells after endocytosis had occurred, and finally the effects of different concentrations of SPION on the phenotype and biocompatibility of HRSMC.

3.2 Materials and Methods

3.2.1 Preliminary Investigation of SPION

3.2.1.1 Transmission Electron Microscopy Analysis of SPION

Transmission electron microscopy (TEM) was used to determine the core diameter of the particle.

(i) 1 µl of SPION (31.25 µg/ml) was added to1000 µl of distilled water.

The sample was placed onto a carbon-coated copper grid and incubated at room temperature until it had dried. The sample was examined under a JEOL JEM 1200EX TEM operating at 80 kV. The average diameter of the clusters of iron oxide crystals was determined using image analysis.

3.2.1.2 Interaction between SPION and the Cell Culture Medium

3.2.1.2.1 Dynamic Light Scattering

Dynamic light scattering (DLS) measures Brownian motion and relates this to the size of the particles. The hydrodynamic particle size of SPION samples in water and culture medium (10% FBS) was measured by DLS.

(i) SPION at a concentration of 31.25 μg/ml was mixed with culture medium and water incubated at 37^0C and at 25^0C.

(ii) Samples were added in cuvettes and the measurements were performed using a Malvern 4700 spectrometer. The hydrodynamic diameter was measured for a period of 30 minutes.

3.2.2 Preliminary Investigation of SPION Effects on HRSMC

3.2.2.1 Incubation of HRSMC with SPION

Human rectal smooth muscle cells were seeded in 75 cm^2 tissue culture flasks (Nunclon^{TM} Delta treated, Denmark) at a cell density of 500,000 cells per culture flask. Cell cultures were incubated at 37^0C, 5% CO_2 for 24 hours. The medium was removed and experimental medium containing different concentrations (31.25, 250 and 1000 μg/ml) of SPION was added. After 24 hours the medium was removed and the cells were washed 5 times with 10 ml of PBS to remove unbound SPION following the addition of 2 ml trypsin/EDTA. The flasks were incubated for 2 minutes to facilitate enzymatic detachment of the cells. When the cells were fully detached 10 ml of fresh proliferation medium was added to the flask and the contents transferred to a sterile 30 ml container. The container was centrifuged at 1000 rpm for 5 minutes to pellet the cells in the bottom of the container. The supernatant was removed and the pellet was

re-suspended in fresh culture medium. A cell count was performed as described in section 2.2.1.3. Finally, the cells were re-seeded in proliferation medium and incubated for 24 hours at 37^0C, 5% CO_2 (as shown in Figure 3.1).

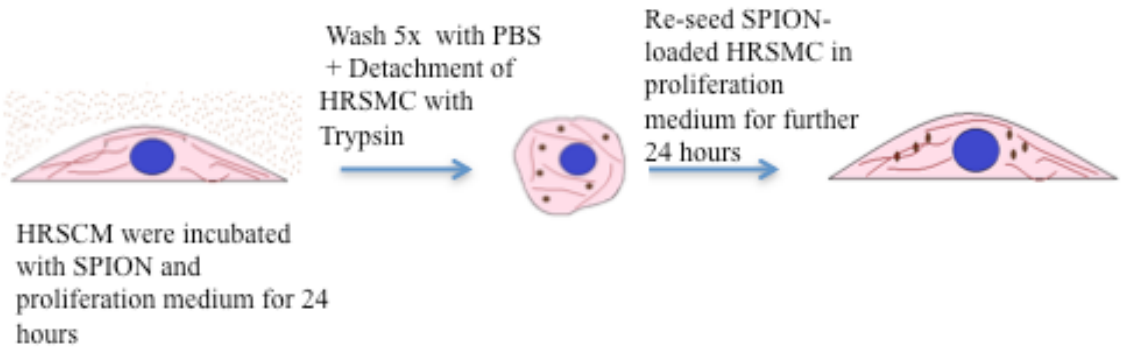

Figure 3.1 Incubation of HRSMC with SPION.

3.2.2.2 Light Microscopy of SPION-Loaded HRSMC

Light microscopy was used to determine the cellular localisation of SPION.

(i) $2x10^4$ HRSMC were seeded in a 25 cm^2 cell culture flask (Nunclon^{TM} Delta surface, Denmark) and incubated for 24 hours at 37^0C, 5% CO_2.

(ii) HRSMC were incubated with different concentration of SPION particles (31.25 µg/ml, 250 µg/ml and 1000 µg/ml) and incubated for 24 hours at 37^0C, 5% CO_2.

(iii) After the incubation period the culture medium was removed and the cells were washed 5x with 5 ml of PBS.

(iv) 1 ml of trypsin was added to each flask and incubated at 37^0C, 5% CO_2 for 1 minute.

(v) 5 ml of fresh media was added in each flask and the detached cells were collected in a 30 ml container.

(vi) Samples were centrifuged at 1000 rpm for 5 minutes, the supernatant was removed and the pellets were re-suspended in 1 ml of fresh media.

(vii) A cell count was performed and 25,000 HRSMC were placed into a 48 well plate (Nunclon^{TM}, Delta surface, Denmark) and incubated for 24 hours at 37^{0}C 5% CO_2.

(viii) The medium was removed and the cells were fixed with 200 µl 2.5% w/v glutaraldehyde in 0.01M PBS (Sigma-Aldrich Company Ltd, UK).

(ix) Images were taken with a 20x objective lens using a Leica DM IL Inverted Microscope (Leica, UK).

3.2.2.3 Transmission Electron Microscopy Analysis of SPION-Loaded HRSMC

Transmission electron microscopy was used to determine the ultrastructural cellular localisation of SPION.

(i) Steps i-vi from section 3.2.2.2 were followed for this experiment.

(ii) 2x10^{4} HRSMC were seeded in a 25 cm^{2} cell culture flask (Nunclon^{TM} Delta treated, Denmark) and incubated for 24 hours at 37^{0}C, 5% CO_2.

(iii) After incubation, the medium was removed and the cells were washed 5x with 10 ml of PBS.

(iv) 1 ml of trypsin was added to each flask and incubated at 37^{0}C, 5% CO_2 for 1minute.

(v) 5 ml of fresh medium was added to each flask and the detached cells were collected in a 30 ml container.

(vi) Steps vi-xviii from section 2.2.3 were repeated for the remainder of this experiment.

3.2.2.4 Quantification of Cellular Loading with SPION

Two techniques were used to quantify the amount of SPION in cells; SQUID and flow cytometry.

3.2.2.4.1 Determine the Cellular Loading with Different Concentrations of SPION Using SQUID

A Superconducting Quantum Interference Device (SQUID) was used to measure the amount of iron in cells following incubation with SPION as described in section 2.4.1.

(i) Steps i-vi from section 3.2.2.2 were followed for this experiment.

(ii) $5x10^4$ HRSMC were seeded in a 75 cm^2 culture flask and incubated for 24 hours at 37^0C, 5% CO_2.

(iii) Steps ii–xi from section 2.2.2 were then followed for the remainder of this experiment.

3.2.2.4.2 Granularity of SPION-Loaded HRSMC

Cells that have engulfed SPION are more granular. Therefore forward scatter (FS; a measurement of size) and side scatter (SS; a measurement of granularity) of SPION loaded cells were measured on a FACS Caliber flow cytometer (BD Biosciences). Forward scatter FS and SS intensities were digitalized on both linear and logarithmic scale. Cellular debris and SPION aggregates were eliminated by using a selection gate.

(i) Steps i-vi from section 3.2.2.2 were initially followed for this experiment.

(ii) A cell count was performed and 100,000 cells were extracted and placed into a 25 cm^2 cell culture flask (Nunclon^{TM} Delta surface, Denmark) and incubated at 37^0C, 5% CO_2 for 24 hours.

(iii) After the incubation period the medium was removed and the cells were washed 1x with 5 ml of PBS.

(iv) 1 ml of trypsin was added to each flask and incubated at 37^0C, 5% CO_2 for 1 minute.

(v) 5 ml of fresh media was added in each flask and the detached cells were collected in a 30 ml container.

(vi) The samples were centrifuged at 1000 rpm for 5 minutes, the supernatant removed and the pellet was re-suspended in 5 ml of FACS buffer (BD Bioscences, UK).

(vii) The sample was transferred to FACS collection tubes (BD Falcon, USA) and analysed using a FACS Calibur flow cytometer (BD Biosciences, UK).

3.2.2.5 The *In Vitro* Response of HRSMC to Different Concentrations of SPION

3.2.2.5.1 Cell Metabolic Activity Assay

(i) Steps i-vi from section 3.2.2.2 were initially followed for this experiment.

(ii) A cell count was performed and 10,000 cells were extracted and placed into a 96 well plate (Nunclon^{TM} Delta surface, Denmark) with a final volume of 100 µl per well and incubated at 37^0C, 5% CO_2 for 24 hours.

(iii) 20 µl/well MTS/PMS combined solution was added to all the wells and incubated for 2 hours at 37^0C, 5% CO_2.

(iv) Absorbance of the formazan product was measured at 490 nm with a colorimetric plate reader Multiskan FC (Thermoscientific, UK).

3.2.2.5.2 Cell Proliferation Assay

(i) Steps i - vii from section 3.2.2.2 were initially followed for this experiment.

(ii) 10 µl per well BrdU label (final volume of 100 µl) was added to all the wells and the plate was incubated for 2 hours at 37^0C, 5% CO_2.

(iii) Labelling medium was removed by inverting the plate and tapping off.

(iv) 200 µl of fixative and denaturing solution provided with the assay was added to the wells. The plate was incubated for 30 minutes at room temperature.

(v) Fixative denaturing was removed from all the wells by inverting the plate and tapping off the solution and 100 µl per well anti-BrdU-peroxidase monoclonal antibody was added to each well and incubated for 90 minutes at room temperature.

(vi) Antibody conjugated solution was then removed by inverting the plate and tapping off the solution. The wells were rinsed 3x with PBS/washing solution.

(vii) 100 µl of substrate solution provided with the assay was added to each well and incubated for 30 minutes at room temperature.

(viii) 25 µl of 1M H_2SO_4 stop solution provided with the assay was added to all the wells.

(ix) Optical density of the reaction produced in the well was read with a colorimetric plate reader Mutliskan FC (Thermoscientific, UK) at 450 nm with a reference wavelength at 690 nm.

3.2.2.5.3 Cytotoxicity Assay

(i) Steps i-vii from section 3.2.2.2 were initially followed for this experiment.

(ii) Supernatants of cells incubated with different concentrations of SPION (0 µg/ml, 31.25 µg/ml, 250 µg/ml and 1000 µg/ml) for 24 hours were collected and transferred to a fresh 96 well plate (Thermo Scientific, Nunc, Fisher Scientific, UK) accordingly.

(iii) 50 µl of medium was removed and placed in a new well and 50 µl of the LDH assay reagents was added to each well and the plate was incubated in the dark at room temperature for 30 minutes.

(iv) 50 µl of stop solution was added to each well and the optical density of the reaction produced in the well was read with a plate reader Multiskan FC (Thermoscientific, UK) at 490 nm.

3.2.2.5.3.1 Cytotoxicity Assay (Positive Control)

(i) Steps i - vii from section 3.2.2.2 were initially followed for this experiment.

(ii) 10 µl of cell lysis solution (provided with the assay) per 100 µl was added to all the wells.

(iii) The cells were incubated for 45 minutes at 37^0C, 5% CO_2.

(iv) The plate was centrifuged at 250 x g for 4 minutes.

(v) Supernatants of cells incubated with different concentrations of SPION (0 µg/ml, 31.25 µg/ml, 250 µg/ml and 1000 µg/ml) were collected and transferred to a fresh 96 well plate (Thermo Scientific, Nunc, Fisher Scientific, UK) accordingly.

(vi) 50 µl of medium was removed and placed in a new well and 50µl of the LDH solution was added to each well and the plate was incubated in the dark for 30 minutes.

(vii) 50 µl of stop solution was added to each well and the optical density of the reaction product in the well was read with a plate reader Multiskan FC (Thermoscientific, UK) at 490 nm.

3.2.2.5.4 Flow Cytometry

3.2.2.5.4.1 Propidium Iodide Staining of Dead Cells

Propidium iodide (PI) is commonly used to identify dead cells. PI binds to DNA by intercalating between the bases with little or no sequence preference and with a stoichiometry of one dye molecule per 4 - 5 base pairs of DNA. PI is membrane impermeant and generally excluded from viable cells.

(i) Steps i - vi from section 3.2.2.2 were initially followed for this experiment.

(ii) A cell count was performed and 100,000 cells were extracted and placed into a 25 cm^2 cell culture flask (Nunclon^{TM} Delta surface, Denmark) and incubated at 37^0C, 5% CO_2 for 24 hours.

(iii) After the incubation period the medium was removed and the cells were washed 1x with 5 ml of PBS.

(iv) 1 ml of trypsin was added to each flask and incubated at 37^0C, 5% CO_2 for 1 minute.

(v) 5 ml of fresh media was added in each flask and the detached cells were collected in a 30 ml container.

(vi) The samples were centrifuged at 1000 rpm for 5 minutes, the supernatant removed, and the pellet was re-suspended in 5 ml of PI/FACS buffer (BD Bioscences, UK) (PI 1:500 dilution in FACS buffer) was added 15 minutes prior the measurement.

(vii) Solution was transferred to FACS collection tubes (BD Falcon, USA). The samples were analysed using a FACS Calibur flow cytometer (BD Biosciences). Red "fluorescence intensities emitted by dead cells (measured at 610 nm) was digitalized on a logarithmic scale.

3.3 Results

3.3.1 Preliminary Investigations of SPION

3.3.1.1 Ultrastructural Analysis of SPION

Transmission electron microscopy (TEM) was used to determine the core diameter of the SPION used for loading cells. The images revealed that the SPION consisted of clusters of iron oxide crystals that were each approximately 20 - 30 nm in diameter (Figure 3.2).

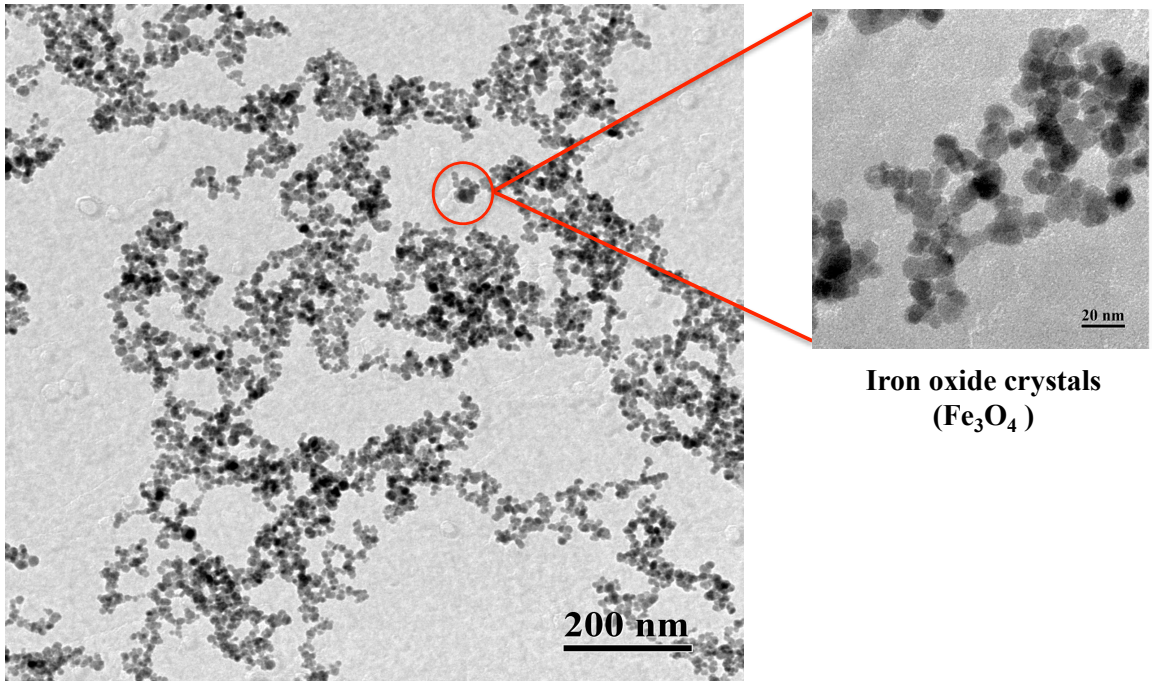

Figure 3.2 TEM images of SPION showing Clusters of iron oxide crystals

3.3.1.2 Analysis of the Interaction Between SPION and Cell Culture Medium

Dynamic light scattering (DLS) was used to investigate the interaction between SPION and the cell culture medium. The hydrodynamic particle sizes of SPION samples in distilled water or culture medium (proliferation medium described in section 2.1.2) were obtained by DLS. Culture medium or water was mixed with 31.25 µg/ml of SPION both at 37^0C and at 25^0C. The hydrodynamic diameter was measured for a

period of 30 minutes. It was not possible to perform DLS with concentrations of SPION above 31.25 μg/ml due to the particle density exceeding the detection limitations of the equipment. When SPION was mixed with culture medium containing 10 % FBS and incubated at 37^0C for 30 minutes there was an initial agglomeration of particles with a hydrodynamic diameter of 578.4 nm at 1 minute (Figure 3.3 a). As the incubation period increased, the hydrodynamic diameter fell to 475.7 nm. When SPION was mixed with water and incubated for 30 minutes at 37^0C, there was an increase in the hydrodynamic diameter (60.56 nm) the first minute of incubation. However, as the incubation period was increased the hydrodynamic diameter fell to 59.73 nm, which was close to the starting hydrodynamic diameter of the particles (50 nm). In order to determine if temperature was a critical factor for agglomeration of particles, SPION was mixed with culture medium and water for 30 minutes at 25^0C. Mixing SPION with culture medium at 25^0C (Figure 3.3 b) resulted in an increase in the average hydrodynamic diameter (546.9 nm), which then dropped to its lowest value after 30 minutes (512.1 nm). When SPION was mixed with water there was an increase in the hydrodynamic diameter (61.59 nm) but after 30 minutes it fell to an average hydrodynamic diameter of 56.51 nm.

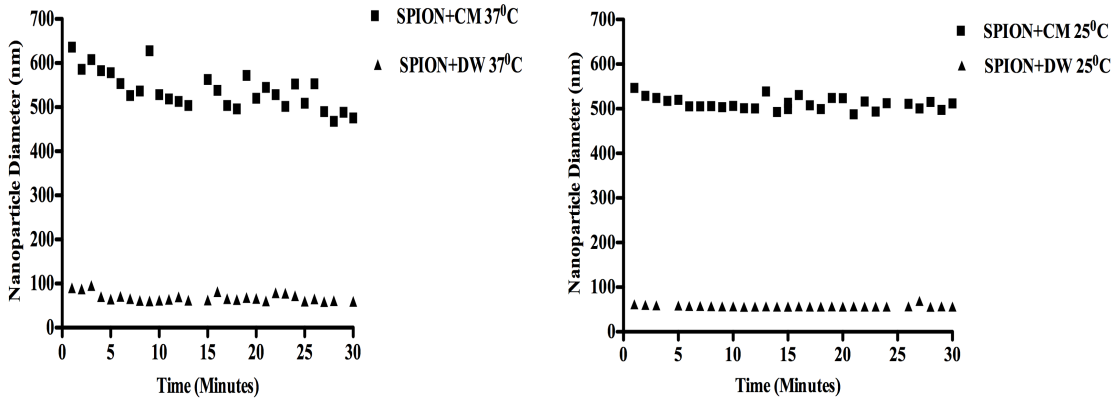

(a) **(b)**

Figure 3.3. **DLS Measurements for Culture Medium and SPION (CM+SPION) and Distilled Water and SPION (DW+SPION) at 37^0C and 25^0C.** (Nanoparticle diameter = average cluster diameter in nanometers)

3.3.2 Preliminary Investigation of SPION Effects on HRSMC

3.3.2.1 Light Microscopy of SPION-Loaded HRSMC

Images of HRSMC after loading with 31.25, 250 and 1000 µg/ml of SPION were taken using an inverted light microscope to investigate the localization of SPION. Images revealed that cells internalized SPION for all of the concentrations investigated and also retained their cell viability and characteristic spindle shape. The amount of SPION internalized appeared to correlate directly with the concentration of SPION. The uptake of SPION appeared to increase when HRSMC were incubated with 1000 µg/ml of SPION for 24 hours (Figure 3.4 c). Although the cells were washed extensively in PBS to remove unbound SPION, images showed SPION remaining attached to the plasma membrane (Figure 3.4 c). Additionally, the images revealed an apparent uneven distribution of SPION between the cells.

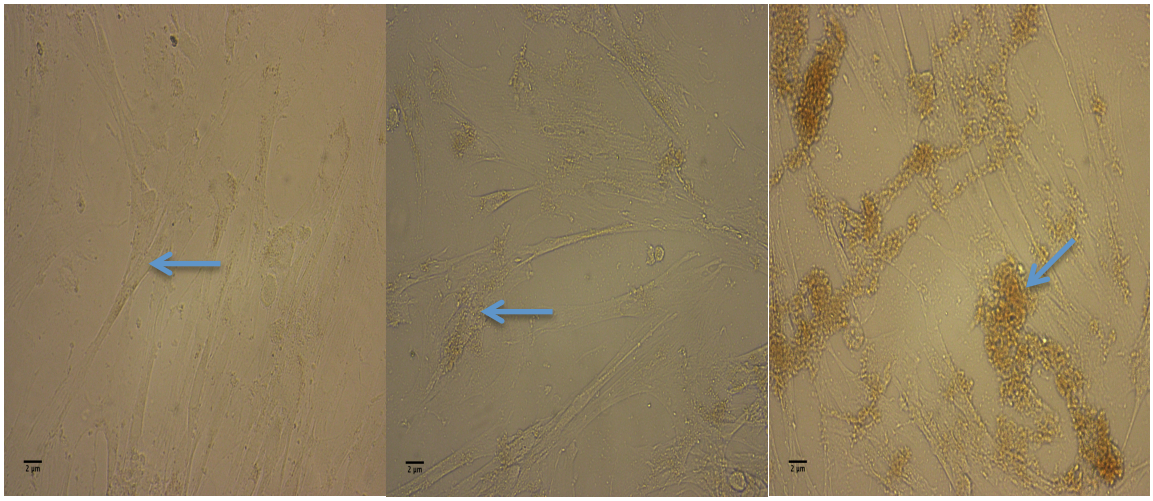

(a) **(b)** **(c)**

Figure 3.4. Light Microscopy Images of SPION-Loaded HRSMC Contained Incubated with Different Concentrations of SPION (31.25, 250 and 1000 µg/ml) at 20x Magnification. The cells maintained their cell viability and their spindle shape characteristic. Images showed the uneven distribution of SPION between the cultured HRSMC.

3.3.2.2 Ultrastructural Localization of SPION in HRSMC

The localization of SPION in HRSMC was determined using TEM. HRSMC were incubated with different concentrations of SPION (31.25, 250 and 1000 µg/ml) for a period of 24 hours. The images revealed that the cells internalized SPION, with the amount corresponding directly with the concentration of SPION used. Uptake of SPION increased when HRSMC were incubated with 1000 µg/ml of SPION for 24 hours (Figure 3.5 c). Although the HRSMC were washed extensively in PBS to remove unbound SPION, images showed SPION remained attached to the plasma membrane (Figure 3.5 a).

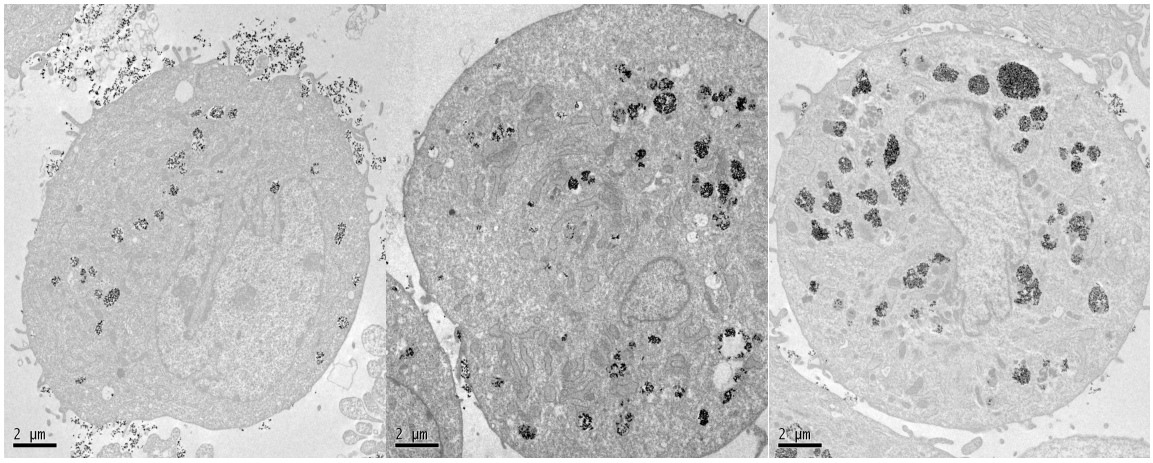

(a) **(b)** **(c)**

Figure 3.5. Transmission Electron Microscopy of SPION-Loaded HRSMC, (a) 31.25 µg/ml, (b) 250 µg/ml and (c) 1000 µg/ml), Incubated for a Period of 24 Hours. SPION became localized in discrete vesicles within the cytoplasm.

3.3.2.3 Determine the Cellular Loading of SPION

3.3.2.3.1 SQUID Magnetometry

SQUID magnetometry was used to quantify the amount of SPION in HRSMC. Cells were incubated with different concentrations of SPION (31.25, 250 and 1000 μg/ml) for a period of 24 hours. A doubling dilution was chosen for this experiment.

The SQUID measures the magnetic moment of a sample, in Am per meter. The average magnetization of the magnetic material (M) was plotted against the strength of the magnetic field (H) for all the different concentrations of SPION. The magnetic filed ranges between -7 T to 7 T. The graph of the control sample (no SPION-0 μg/ml) was diamagnetic confirming no presence of SPION (Figure 3.6-a), however, in the SPION-loaded samples (31.25-1000) the graphs had the characteristic sigmoidal shape indicating the presence of a magnetic material (Figure 3.6-b,c,d).

To convert the magnetization of the magnetic material (magnetic material inside the cells) to mass of particles per cell, the average magnetization per cell of the magnetic material was divided with the average magnetization (92 emu/g) of SPION alone (in water) and then was divided by the total number of cells (Figure 3.6).
This could be described as follows:

$$\text{Total mass per sample} = \frac{\text{Average Magnetization of Sample (31.25, 250 and 1000 μg/ml)}}{\text{Average Magnetization of SPION Alone (92 emu/g)}}$$

$$\text{SPION per cell} = \frac{\text{Total Mass per Sample}}{\text{Number of Cells}}$$

For example for cells incubated with 31.25 µg/ml (Figure 3.6-b):

Total mass per sample = $\frac{1.06 \times 10^{-4} \text{ emu}}{92 \text{ emu/g}} = 1.15 \times 10^{-6}$ g

SPION per cell = $\frac{1.15 \times 10^{-6} \text{ g}}{150000 \text{ cells}} = 7.66 \times 10^{-12}$ or 7.66 pg of SPION

The average SPION per cell in picograms (pg) of 3 different replicates (n=3) from each group was plotted against the concentration. The results showed that when cells were incubated with increasing concentrations of SPION there was a direct increase in the amount of SPION measured in the cells (Figure 3.7).

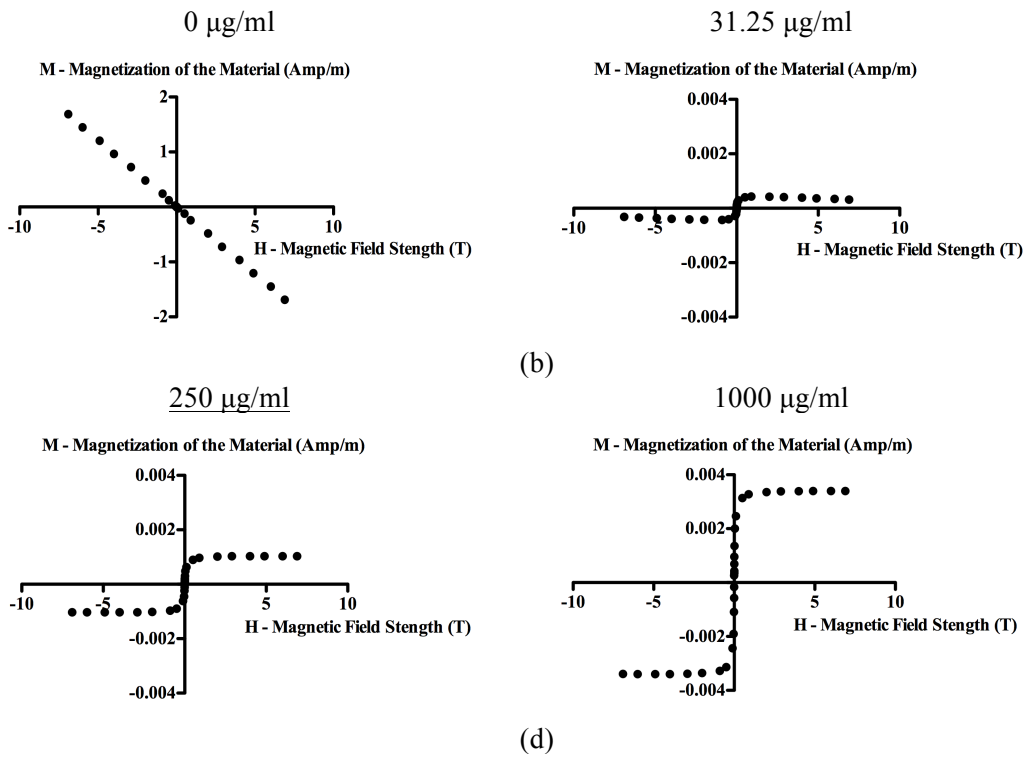

Figure 3.6. The average magnetization of the magnetic material was plotted against the magnetic field for all the different concentrations of SPION (31.25, 250 and 1000 µg/ml)

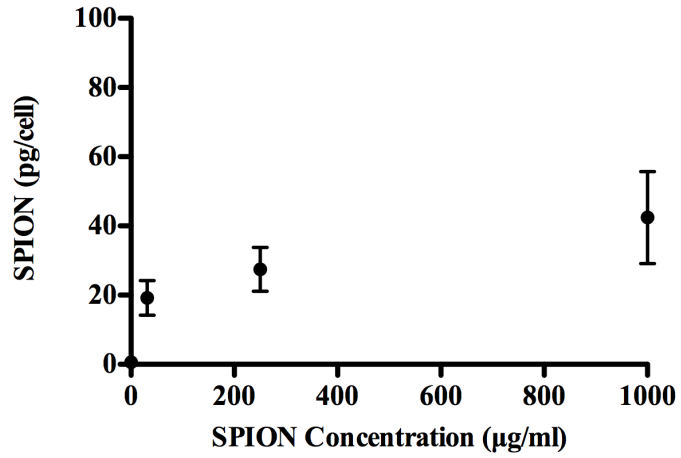

Figure 3.7. SPION Concentration per Cell After Incubation with SPION at Different Concentrations (31.25, 250 and 1000 µg/ml) as Calculated from SQUID Magnetometry (n = 3).

3.3.2.3.2 Cell Granularity After SPION-Loading

3.3.2.3.2.1 Flow Cytometry

To further investigate the cellular loading of SPION in HRSMC the forward light scatter (FS) and side light scatter (SS) of cells were measured using flow cytometry. The forward scatter indicates the size of the cells and the side scatter shows the granularity of the cells. This phenomenon was investigated as a technique for determining cell loading with SPION. Side scatter (Figure 3.8 a) showed a significant increase for all the concentrations of SPION loaded cells compared with unloaded control cells (31.25µg/ml $p<0.0001$; 250 µg/ml $p<0.0001$; and 1000 µg/ml $p<0.0001$). Forward scatter (Figure 3.8 b) showed a significant decrease for all concentrations of SPION loaded cells (31.25µg/ml $p<0.0001$; 250 µg/ml $p<0.0001$; and 1000 µg/ml $p<0.0001$).

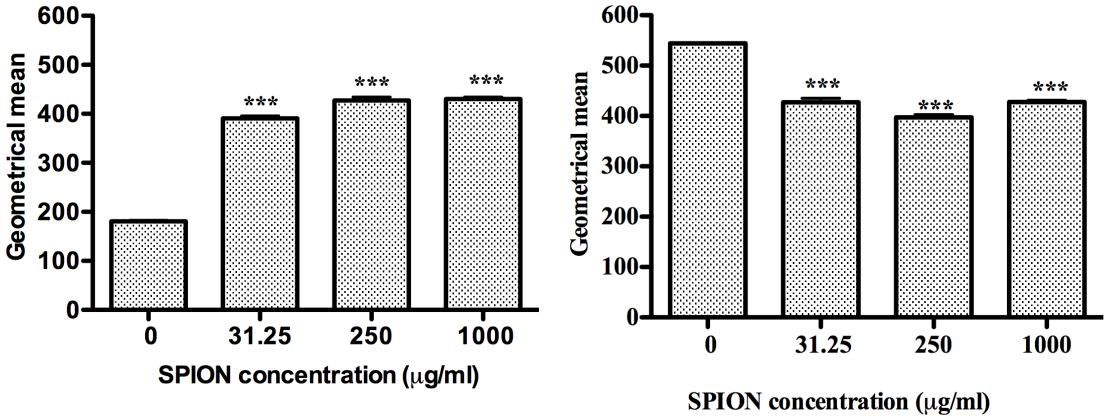

(a) **(b)**

Figure 3.8. The Side Scatter (a) and the Forward Scatter (b) of SPION-Loaded HRSMC (31.25 µg/ml, 250 µg/ml, and 1000 µg/ml) Plotted as their Geometrical Mean. For the forward scatter there was a continuous decrease and for the side scatter there was continuous increase. (*** $p<0.0001$ compared with unloaded control cells).

3.3.2.4 Effect of SPION-Loading on the Phenotype of HRSMC

3.3.2.4.1 The Effect of SPION-Loading on HRSMC Proliferation

A BrdU ELISA assay was performed to investigate the effect of SPION on cell proliferation. There was no significant change to the proliferation of cells incubated with 31.25 μg/ml and 1000 μg/ml of SPION (Figure 3.9) compared with the control cells ($p>0.05$). However, a significant increase was observed for cells incubated with 250 μg/ml ($p<0.01$).

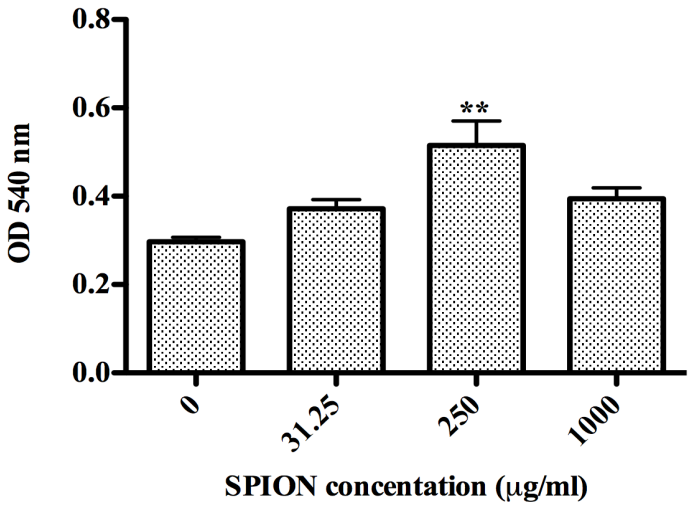

Figure 3.9. Cell Proliferation of HRSMC Incubated with Different Concentrations of SPION for 24 Hours. A significant increase in cell proliferation was observed at 250 μg/ml ($p<0.01$). (**$p<0.01$ compared with unloaded control cells).

3.3.2.4.2 Cell Metabolic Activity Following Incubation with SPION

In order to investigate the metabolic activity of HRSMC after culture with SPION an MTS/PMS assay was performed. A decrease was observed when cells were incubated with 1000 μg/ml of SPION (Figure 3.10) compared with unloaded control cells.

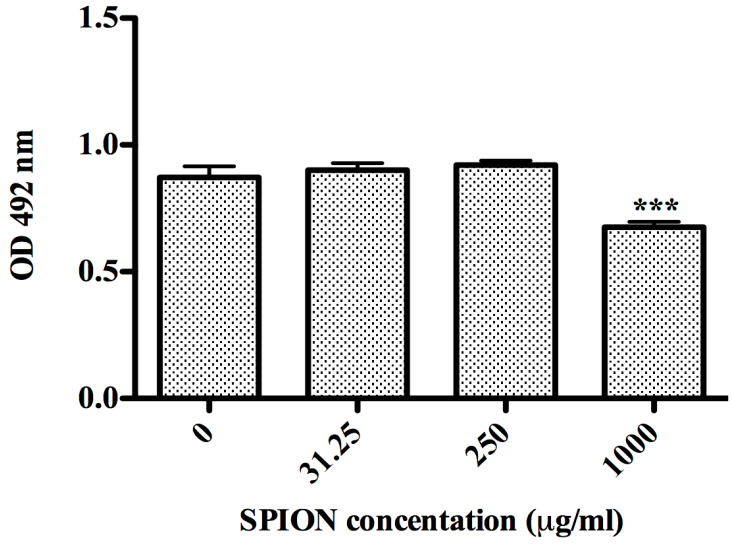

Figure 3.10. Metabolic Activity of Human Rectal Smooth Muscle Cells after 24 Hours Incubation with Different Concentrations of SPION. A decrease was observed when cells were incubated with 1000 μg/ml of SPION compared with unloaded control cells. (***$p<0.001$ compared with unloaded control cells).

3.3.2.5 Effect of SPION-Loading and Biocompatibility with HRSMC

3.3.2.5.1 Cell Toxicity Following Incubation with SPION Measurement of Lactate Dehydrogenase Release (LDH)

The cytotoxic effect of incubating HRSMC with SPION was investigated by measuring cellular release of LDH. Two types of controls were used: i) HRSMC with no SPION (0 μg/ml) and ii) a positive control (PC) was obtained by incubating HRSMC in a lysis solution (provided with the kit). The lysis solution lyses the cell membrane resulting in the maximum production of LDH in the supernatant (100% toxic). The detailed process was described in sections 2.2.5.2.1 and 3.2.2.5.3.1. No significant change was observed between HRSMC incubated with SPION (31.25-1000 μg/ml) and control cells (no SPION) as showed in Figure 3.11. The optical density of the positive control (PC) had approximately 20% increased.

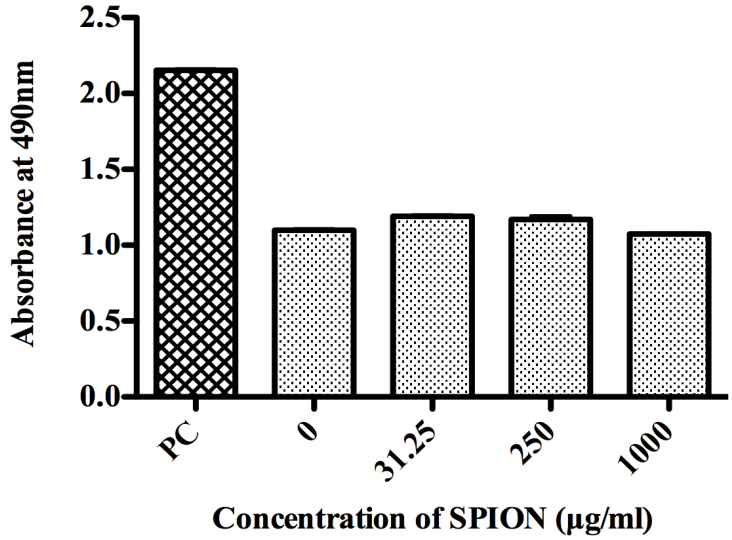

Figure 3.11. LDH Release in the Supernatant Collected from HRSMC Incubated with SPION for a Period of 24 Hours. No significant change was observed following incubation between 31.25, 250 and 1000 µg/ml SPION compared to control cells (no SPION). The was an apparent increase in the release of LDH in the supernatant in the positive control (PC)

3.3.2.5.2 Measurement of Cell Viability by Flow Cytometry

Flow cytometry of cells incubated with propidium iodide (PI) was used to investigate the proportion of dead cells after incubation with different concentrations of SPION (32.15 µg/ml, 250 µg/ml, 1000 µg/ml) for 24 hours. Unlabelled control cells (Figure 3.12 a) were acquired to set a gate based on the side scatter, which was subsequently used for acquiring PI labelled cells. The percentage of gated cells was used to quantify the number of cells stained with PI from 10,000 events. The quantities of cells stained with PI increased from 8 % in control cells to 11.23 % in cells incubated with 31.25 µg/ml SPION ($p<0.0001$). Similarly, an increase was observed from 8% in control cells to 12.71 % and 13.97% for cells incubated with 250 µg/ml and 1000 µg/ml compared with control cells ($p<0.0001$) (Figure 3.12).

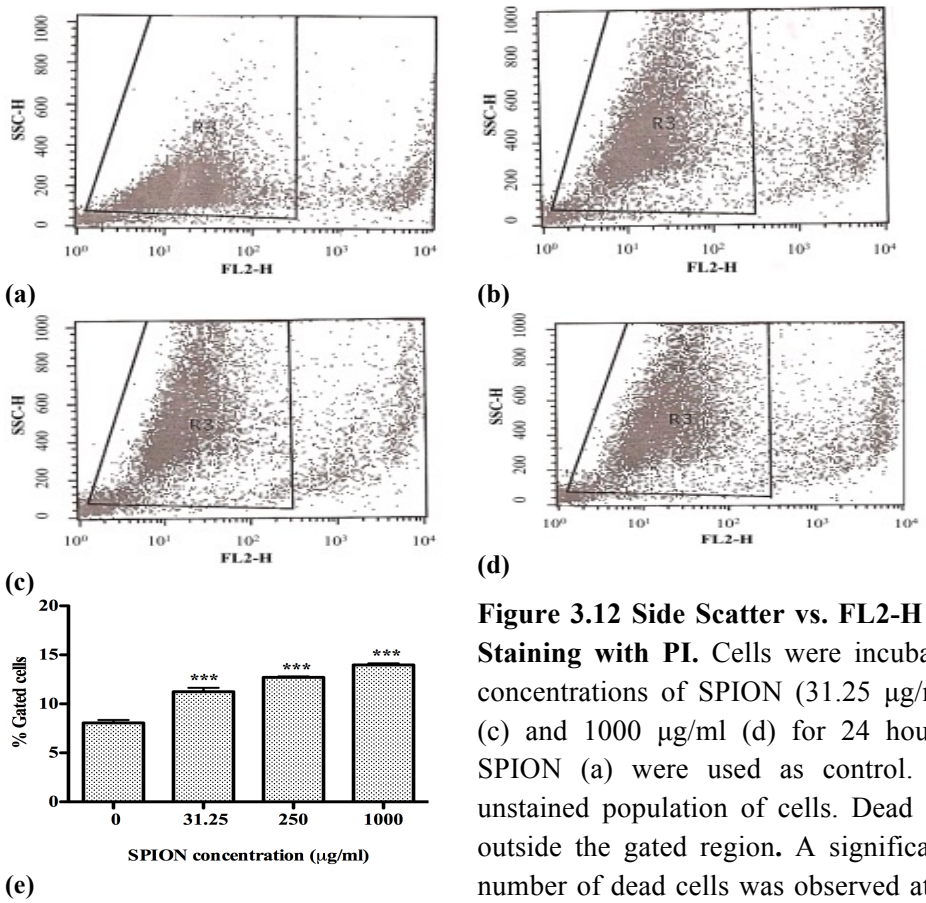

Figure 3.12 Side Scatter vs. FL2-H of HRSMC after Staining with PI. Cells were incubated with different concentrations of SPION (31.25 µg/ml (b), 250 µg/ml (c) and 1000 µg/ml (d) for 24 hours. Cells with no SPION (a) were used as control. R3 indicated the unstained population of cells. Dead cells were located outside the gated region**.** A significant increase in the number of dead cells was observed at 31.25 µg/ml, 250 µg/ml and 1000µg/ml after HRSMC stained with PI after 24 hours (e). (***p<0.001 compared with unloaded control cells.

3.4 Discussion

This chapter describes the preliminary investigations of the effects of SPION on HRSMC. It explores the effects of SPION in the culture medium used for this experiment, the localization of SPION inside HRSMC and the loading efficiency. Additionally, the biocompatibility of SPION with HRSMC was investigated.

Main findings

- SPION particles used in the experiments consisted of clusters of iron oxide crystals, each measuring approximately 20-30 nm in diameter. The iron oxide crystals formed clusters in aqueous solutions, with a hydrodynamic diameter of

approximately 50 nm in water and 500 - 600 nm in culture medium due to a corona effect.

- SPION were endocytosed by HRSMC and located inside endosomes in the cytoplasm.
- The amount of SPION internalised by cells was concentration dependent. However, for concentrations above 250 μg/ml loading saturation occurred.
- Incubation of HRSMC with 250 μg/ml SPION for 24 hours resulted in an increase in cell proliferation, no change in metabolic activity, and a small increase in release of LDH. An increase in propidium iodide staining occurred for all concentrations of SPION tested.

The properties and characteristics of the SPION were investigated. The nanoparticles used in this study were negatively charged uncoated iron oxide crystals, commercially available from Chemicell (Germany) and manufactured by chemical precipitation. SPION at a concentration of 31.25 μg/ml was mixed with culture medium or distilled water and incubated for 30 minutes at 37^0C and 25^0C. The results showed an increase in the hydrodynamic diameter of the particles for both temperatures when incubated with culture medium compared with distilled water. The hydrodynamic diameter of SPION incubated with culture medium at both temperatures dropped with time. This can be explained by the Brownian motion of the particles. During the first few minutes of incubation there was a vigorous movement of the particles, which eventually decreased with time. The initial increase of the hydrodynamic diameter of the particles is likely to have resulted from their agglomeration with culture medium constituents. This could be explained as the corona effect, where particles, surrounded by biological fluids such as the culture medium, are coated by a corona of serum proteins and

biomolecules or they aggregate to form clusters of various sizes. The corona that surrounds the nanoparticle is the primary contact to the cells therefore the type of coating or the charge of the nanoparticle is important (143-145).

To highlight the importance of surface charge, a previous study investigated iron oxide nanoparticles with a diameter of 8 nm, which were coated with two different types of coating materials with different charges. The first was coated with anionic citrate ions to create citrate coated particles (Cit-γ-Fe_2O_3), and the second was coated with a cationic compound poly(acrylic acid) (PAA_{2K}). Dynamic light scattering measurements revealed no change in the hydrodynamic diameter of the particles when they were mixed with phosphate buffered saline (PBS) after 2 hours of incubation. An increase in the hydrodynamic diameter from 20 nm to 50 nm within seconds was observed when Cit-γ-Fe2O3 were mixed with Roswell Park Memorial Institute medium (RPMI) containing 10 % fetal bovine serum (FBS), which continued to grow slowly up to 100 nm after 2 hours of incubation. Interestingly, no change in the hydrodynamic diameter of the PAA_{2K} was observed when mixed with RPMI with 10% FBS after 2 hours of incubation. The particles remained dispersed, forming a stable colloid and did not form a corona in the culture medium (145). This study could explain the increase in the hydrodynamic diameter observed in the current study, where it could be due to the culture medium constituents but also due to the negative surface charge of the particles used for this experiment.

After exploring the effects of SPION with the culture medium, the effect of SPION when incubated with cells was investigated, specifically the loading efficiency and biocompatibility. There are several possible methods to label cells with SPION. As described in section 3.1, cells could be labelled with a magnetically labelled antibody which targeted a specific protein of interest (92, 93) or with direct incubation intended

to load SPION inside the cells (139). For this study direct incubation of SPION with HRSMC was explored.

To investigate the loading and the localization of SPION in HRMSC, light microscopy, TEM, SQUID, and the side and forward light scatter from flow cytometry measurement were used. HRSMC monolayers were incubated with SPION as described in section 3.2.2.1. The cells were washed thoroughly with PBS in an attempt to remove unbound SPION. Light microscopy images of HRSMC loaded with a different concentration of SPION (0-1000 μg/ml) revealed that loading had occurred for all the concentrations of SPION; however, loading was concentration dependent. There was an apparent increase in the loading for 1000 μg/ml of SPION compared with 31.25 μg/ml and 250 μg/ml. SPION attached to the plasma membrane was observed for all concentrations even if the cells were washed extensively. This could be explained, possibly, by the membrane SPION being in the process of endocytosis when this process was disrupted. Alternatively, electrostatic forces between the negatively charged particles and positively charged components of the cell plasma membrane could account for this. An apparent clustering of non-internalised SPION was observed when HRSMC were incubated with 1000 μg/ml of SPION.

Similarly, TEM images revealed that loading had occurred for all concentrations of SPION investigated. Images of HRSMC incubated with different concentrations of SPION revealed that SPION was internalised, possibly by an endocytic process. Other studies have used TEM to demonstrate SPION internalization by the cells (146). In one study, dimercaptosuccinic acid magnetic nanoparticles (10 nm in diameter) were incubated with Sprague-Dawley rat aortic SMCs for 24 hours at a concentration of 0.1 mg/ml. Images revealed that the particles were endocytosed by SMC and were located into the lysosomes in the cytoplasm. Additionally the formation of aggregates were

observed outside the cells (147). Both findings were also observed in this study.

The exact endocytic process was not investigated in this study. It is likely that caveolae-mediated or caveolae-independent endocytosis occurs. This type of endocytosis creates 50 nm diameter vesicles to endocytose nanoparticles, similar in size to the magnetic nanoparticles used in this study. Caveolae-mediated or independent endocytosis fall into a broad category of endocytosis called pinocytosis, together with clathrin-mediated and independent endocytosis and macropinocytosis (148). However, according to the DLS results the hydrodynamic diameter of the particles was increased from 50 nm to 500-600 nm in culture medium and remained stable for 30 minutes of incubation. Therefore the particles were possibly endocytosed through clathrin-coated endocytosis (>150nm vesicles) or macropinocytosis (<1 μm). Recent reports suggest that there is not only one type of endocytosis responsible for SPION uptake but maybe a combination of more than one. Jing Li *et al* investigated the endocytic process of dimercaptosuccinic acid coated γ-Fe_2O_3 particles (10 nm in diameter) into macrophage-like cell line RAW264.7. Cells were incubated with a number of endocytic inhibitors such as 10 μg mL^{-1} chlorpromazine (an inhibitor of clathrin-dependent endocytosis), 5 μg mL^{-1} of filipin III and M-β-CD that disturb the caveolin-dependent endocytosis and 2.5 mmol L^{-1} of amiloride, which is a macropinocytosis inhibitor. The results showed that pre-treatment with these endocytic inhibitors and subsequent incubation of RAW264.7 with DMSA coated γ-Fe_2O_3 nanoparticles showed reduced SPION internalization for all the endocytic inhibitors suggesting that there is not a defined endocytic process but maybe a combination (149).

SQUID magnetography was used to quantify the amount of SPION loaded in the cells. HRSMC were incubated with different concentration of SPION (0 - 1000 μg/ml). The

results revealed that there was an increase in SPION internalisation as the concentration of SPION rises. These findings confirm the light microscopy and TEM results that SPION loading is concentration dependent. However, the SQUID results showed that the increase in the amount of SPION was not linear, instead plateauing, which suggests that saturation might have occurred. This is supported by light microscopy images where clustering of non-internalised SPION was evident outside the cell.

The internalisation process was also investigated using flow cytometry. Forward scatter indicates the size of cells and the side scatter the granularity. Cells were incubated with different concentrations of SPION. The results revealed that as the concentration of SPION increased the cells became more granular. Side scatter showed a significant increase for all the concentrations of SPION. This result indicated that as the SPION concentration was increased the cells became more granular, suggesting the cells had internalized more SPION. The apparent increase in side scatter corresponded with the SQUID results. Interestingly a decrease was observed in the forward scatter (cell size) for all the concentrations of SPION. This finding does not correspond with the light microscopy and TEM images, where no difference was observed in cell size. It is not certain that SPION loading affects the size of cells. A recent study suggested that when two different population of stem cells (human chorial villi and human amniotic fluid cells) were incubated with the same concentration of a dextran coated SPION (35 mg/ml; Endorem®) coupled to Poly-L-Lysine for 72 hours, the side scatter revealed that that there was no significant difference in cell size, even if both types of cells had internalised the same amount of SPION (150).

In this study, uncoated negatively charged SPION were directly incubated with HRSMC allowing the cells to take up the particles through endocytosis. The amount of

SPION internalised was estimated to be between 10–40 pg/cell for the different concentrations of SPION. In general many studies have used transfection agents in order to enhance the loading efficiency (151). Transfection agents could be polymeric compounds such as dextran or PLL, which have an electrostatic charge that can be used to transfect cells without the use of viruses. Previous studies have compared the loading efficiency of different transfection agents. An example is a study by Miyoshi where rat pheochromocytoma PC12 cells were loaded with Feridex (120 to 180 nm) using either inactivated HVJ-E vectors (GenomeOne, Japan) or a liposome agent, Lipofectamine 2000, in order to compare the loading capacity of 2 different transfection agents with the same magnetic particles. HVJ-Es were used to encapsulate Feridex particles. HVJ-Es containing Feridex at volumes of 3.2 μl or 10 μl were incubated with PC12 for six hours. Atomic absorption spectrophotometry demonstrated that HVJ-E transfection resulted in significantly greater iron content than L2000 transfection. The average iron content of cells labeled using HVJ-E transfection was 2.97 pg/cell for 3.2 μl and 10 μl of Feridex. The iron content of cells labelled using L2000 transfection was 0.21 pg/cell for 3.2 μl and 10 μl of Feridex, respectively. The viability studies showed that Feridex-loaded cells transfected with either HVJ-Es or L2000 did not affect the cell viability compared to unlabelled cells for all the different concentration of Feridex after 6 hours of incubation when an MTS and LDH assay was performed (152). In another example Ferumoxides (FE) (50 μg/mL) with a diameter approximately 80-150 nm were coated with a polycationic poly-L-lysine (PLL) transfection agent (The FE-to-PLL ratio was 1:0.06 or 1:0.03) and incubated with human cervical carcinoma (HeLa), human MSC and hematopoietic stem cells overnight. The iron concentration was measured with nuclear magnetic resonance (NMR) relaxometry. The results showed that the iron content is cell type and density

dependent. The lowest iron content was observed in hematopoietic cells with an average content of 1.53 pg and the highest iron concentration in MSC with 12.61 pg (both seeded with 20,000 cells/cm^2). Additionally, when different cell densities where compared the iron content was different. HeLa cells were cultured at different densities (2,000, 4000, 20,000, 40,000 and 80,000 cells/cm^2) and the amount of SPION internalized was 10.58, 10.11, 9.29, 7.42 and 4.15 pg/cell. (153).

The hypothesis that suspension cells such as hematopoietic stem cells internalize more SPION has been seen elsewhere (154). In a different study without the use of transfection agents, neural progenitor cells (NPC) were incubated with SPION (Feridex IV, Berlex, USA) at different concentrations (0-100 μg/ml) and at different time points (0.5, 24 and 48 hours). Electron microscopy revealed that SPION were endocytosed by the cells, most probably by endosomes or lysosomes. Prussian blue staining results showed that the higher the concentration the more labelling occurred. The amount of iron inside the cells was estimated 5.3 pg/cell for NPCs labelled with 75 μg/ml for 48 hours according to Inductively Coupled Plasma Atomic Emission Spectroscopy (ICP-AES) (155). All these studies have demonstrated that SPION internalization is time and concentration dependent, two factors that play a substantial role in the loading efficiency. Different types of cells and magnetic nanoparticles have been investigated, but sufficient loading has been achieved without affecting cell viability.

The biocompatibility of incubating HRSMC with different concentrations of SPION was investigated. The toxicity of SPION-loaded HRSMC were tested with an LDH assay. No significant change was observed between SPION-loaded and control cells. However, there was a decrease in the viability when SPION-loaded cells are stained with propidium iodide (PI). The decrease in cell number/viability observed when

HRSMC might be explained by the particles used not being coated with a polymer. In the literature, SPION coated with different polymers have shown substantial cell viability. For example, previous studies have demonstrated that SPION incubation did in fact affect the viability of cells. An example is a study by Kupta *et al*, where primary human fibroblasts were incubated with different concentration (0-2.0 mg/ml) of Pullalan coated magnetic nanoparticles (Pn-SPION) with a diameter between 40-50 nm. The MTT assay results showed that loading the cells with Pn-SPION did not affect the cell number in comparison with uncoated SPION where the cell number was decreased significantly (156). Similarly when polyvinyl alcohol (PVA) magnetic nanoparticles with a diameter of 86 nm were incubated with primary mouse connective tissue cells (L929 fibroblast) at a different concentration of SPION, no change was observed in the cell viability for all concentrations and time points investigated, indicating that PVA coated magnetic nanoparticles are safe in comparison to control cells (no SPION) (157). In a different study, Alamar blue assay was used to study cell viability. Human chondrocytes were loaded with Endorem and Lipofectamine 2000 (Invitrogen) at different concentrations. The results showed that SPION loading did not change the viability of cells for all the concentrations (158). In another study the cell viability was investigated with CellTracker™ Green CMFDA (5-chloromethylfluorescen diacetate, Invitrogen) for 24 hours. Three different types of cells were compared (human bone marrow stromal cells, neonatal chondrocytes and adult chondrocytes) by incubating with 0.5 mM Fe/ml Resovist. The cell viability images revealed no significant changes in comparison with control unlabelled cells. Additionally viability results revealed that SPION loading affected the morphology of all three types of cells compared with non-loaded cells. SPION-loaded cells appeared to be more stretched out compared with control non-loaded cells. (159). Based on the

previous studies it might be assumed that coating magnetic nanoparticles is crucial to avoid changes in the cell viability. It is important to be mentioned that many papers have used an MTT assay to examine the in vitro toxicity and others the viability or the proliferation. This is perhaps due to the fact that the assay allows rapid evaluation of cell viability, cell survival, cell growth and gives good reproducibility. MTS/PMS is a mitochondrial metabolic activity assay where MTS is bioreduced by cells into a formazan product that is soluble in tissue culture medium.

The increase in cell proliferation observed when HRSMC incubated with 250 μg/ml of SPION was not supported by the MTS/PMS assay. This finding could be explained in the literature by Saha *et al,* where the proliferation of three different types of cells were compared (human bone marrow stromal cells, neonatal chondrocytes and adult chondrocytes). A significant change in the proliferation of neonatal chondrocytes compared with non-loaded cells occurred after 2 days incubation. After 7 days of incubation no significant change was observed between SPION-loaded and control cells and finally after 14 days of incubation an increase in cell proliferation was observed between SPION-loaded compared with control cells. No change was observed in cell proliferation for HBMSCs and adult chondrocytes (159).

3.5 Conclusion

The increase in cell proliferation observed when HRSMC were incubated with 250 μg/ml of SPION could have therapeutic value in degenerated muscle. However, this finding needs to be investigated further. According to the SQUID results saturation was occurred in HRSMC loaded with SPION above 250 μg/ml. additionally loaded the cells with SPION did not affect the biocompatibility as demonstrated with the toxicity-LDH assay. Therefore the SPION concentration 250 μg/ml produced the most consistent results without detrimental cellular effects and finally that concentration was

selected for the magnetic actuation experiments (chapter 4) was selected for use in the following chapters because of the loading characteristics and less clustering on the plasma membrane compared with higher concentrations investigated.

Chapter 4

Effect of Magnetic Actuation on the Phenotype of SPION-Loaded HRSMC

4.1 Introduction

Previous studies have demonstrated it is possible to manipulate the cell phenotype remotely using magnetic actuation. The aim of this chapter was to investigate the effects of applying external magnetic fields to HRSMC loaded with SPION. This included exploring the effect of a magnetic field on the cell phenotype and the biocompatibility of applying a magnetic field to SPION-loaded HRSMC.

The concept of applying cyclic magnetic force to the cells with a frequency of 1Hz and 2 Hz was devised from previous experiments conducted in the department using a Flexcell system. The Flexcell provides a cyclic mechanical strain to cells previously seeded onto elastic membranes. The cells are stretched uniaxial and the strain is received by different mechanoreceptors and translated into a biochemical signal inside the cells. In these previous studies, HRSMC were subjected to cyclic strain (20% elongation) at a frequency of 1Hz for 1 hour every day over a period of 5 days resulting in an increase in cell proliferation determined by a BrdU ELISA (unpublished data). The magnetic actuation regime is based on the Flexcell study described earlier. An oscilating magnetic field delivers a cyclic strain to the cells at a frequency of 1 Hz and 2 Hz for a period of 7 days. However the main difference was that the cells were not seeded onto an elastic membrane but on a rigid bottom (6-well plate). Therefore the SPION-loaded endosomes ‘’magnetosomes’’ will physically move by dragging all the cytoskeletal components such as actin filaments, microtubules creating a stretching effect similar to the Flexcell system. this cytoskeletal movement will create a change in the phenotype of cells.

4.2 Materials and Methods

4.2.1 Materials

4.2.1.1 Magnetic Actuator

A prototype magnetic actuation device was designed to deliver magnetic force to cells loaded with SPION (Figure 4.1a+b+c). The device consisted of two components. A rectangular housing made from polyoxymethylene (Delrin) with external dimensions 100 mm (L) x 45 mm (W) x 45 mm (H) allowed tissue culture vessels to be placed on top. The centre of the long axis of the housing block was milled to provide a channel into which could be inserted a cylinder holding the magnets. The magnetic cylinder contained a pair of magnets asymmetrically housed in a Delrin rod (Figure 4.1 c+d+e). The two magnets were composed of neodymium-iron-boron (NdFeB;N50; MagnetSales, UK) with dimensions 6 mm x 8 mm x 12 mm. The direction of magnetisation was through their thickness (Figure 4.1 d+e). The magnets were placed 6 mm apart in a rectangular cavity in the Delrin rod, so that poles were facing the same direction. A soft steel plate (dimensions 3 mm x 8 mm x 30 mm) was positioned beneath the magnets in the Delrin rod to concentrate the magnetic field in a forward direction (Figure 4.1 d+e).

The magnetic actuator was driven by an external motor (Lego Technic 8293, UK) battery power pack (9V) and the rotational speed controlled by an infrared controller unit.

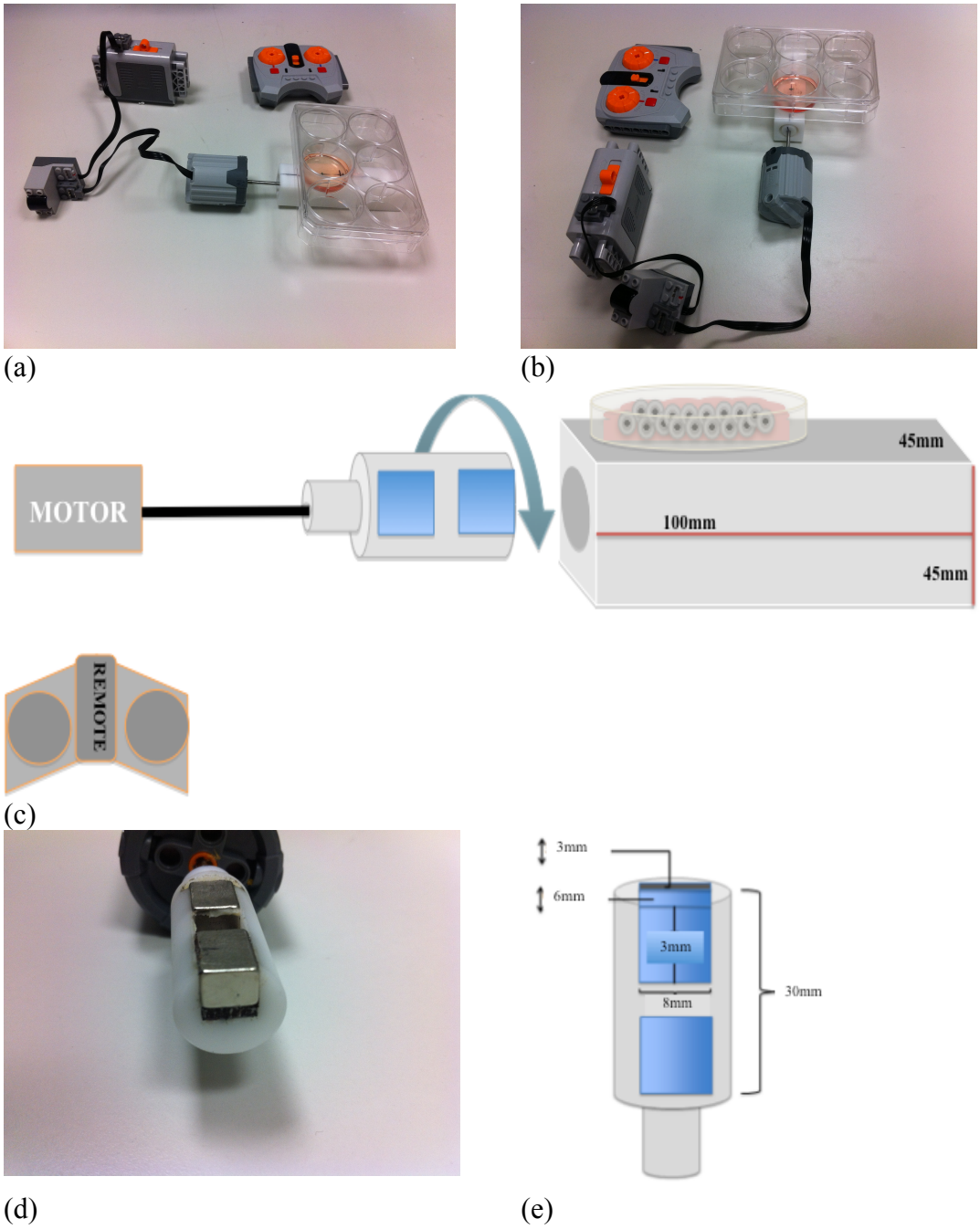

Figure 4.1. (a+b) the components of the prototype magnetic actuator for use with tissue culture plates (c) Diagrammatic representation of the magnetic actuator with all the dimensions. (d) The components of the magnetic cylinder (Part of the Magnetic Actuator) Located Inside the Delrin Housing. (e) Diagrammatic representation of the Dimensions of the Magnetic Cylinder

4.2.1.2 Localized Cell Retention in Tissue Culture Plate for Magnetic Actuation Experiments

In order to seed the cells in specific areas of tissue culture plates, silicone moulds were fabricated (Figure 4.2). 6 ml of silicone (Sylgard 184, Corning, UK) was poured into wells of a six-well tissue culture plate (Nunclon^{TM} Delta, Denmark). Each well had a diameter of 17.5 mm. A polystyrene container (7ml screw-capped Bijou; Greiner Bio-One, UK) with a diameter of 17 mm was positioned in the centre of the well of the tissue culture plate and the silicone was left for 48 hours to cure. The container was removed leaving a silicone disc with a central hole measuring 17 mm in diameter where the cells would be seeded.

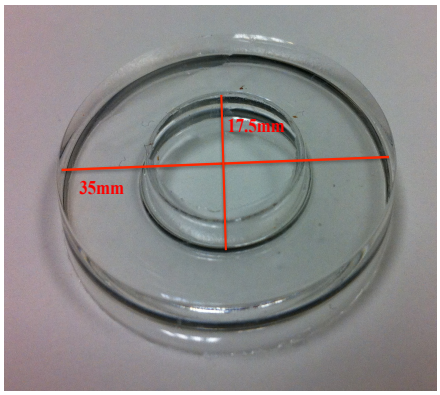

Figure 4.2.Silicone mould used to retain HRSMC in a designated area in the tissue culture plates.

4.2.2 Methods

4.2.2.1 Computer Modelling of Magnetic Fields Produced by the Actuator Device

Finite element modelling was used to model the magnetic field and magnetic force produced by the oscillating magnetic actuator described in this chapter. The modelling was performed by Mr George Frodsham (Department of Biochemical Engineering, University College London, London and Institute of Biomedical Engineering,

University College London).

Finite element modelling with Opera-3D (Version 12; Vector Fields, UK) was used to calculate the strength of the magnetic field produced by the magnetic actuator. The distance from the centre of the magnetic cylinder (with assigned co-ordinates x=0, y=0, z=0) to the base of the tissue culture plate was 14 mm. This included the diameter of the magnetic cylinder (8 mm), the thickness of the Delrin housing (4 mm), and the distance from the surface of the magnetic actuator housing to the inside surface of the tissue culture plate (2 mm) (Figure 4.3).

The force produced by the magnetic actuator on each SPION particle in the cells was calculated using mathematical software (MATLAB, MathWorks, Natick, MA, U.S.A), from which the net magnetic force per cell was calculated. For all calculations the direction of the force was assumed to be downward. The force applied to cells by the magnetic actuator was calculated for each SPION with a density of 1.25g/cm^3, diameter of 50 nm and weight of 6.545×10^{-4} pg at a distance of 14 mm away from the centre of the magnetic cylinder. Additional calculations were also made for the force generated by the magnetic actuator as it was rotated in the Delrin housing.

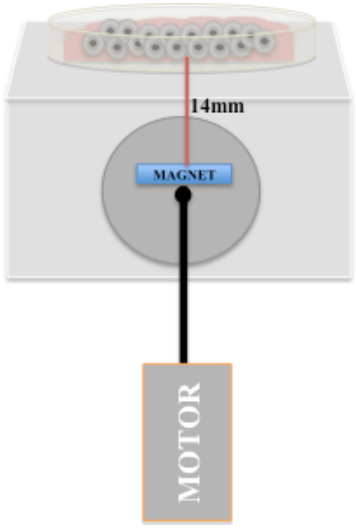

Figure 4.3 Horizontal View of Magnetic Actuator with the Culture Plate Located on its Top.

4.2.2.2 Visualization of the Magnetic Field with Micro Iron Microparticles

(i) Iron microparticles (150-300 μm and a density of 3.5g/cc; Guyson Flexgrain, Guyson International Limited, North Yorkshire, UK) were sprinkled into a 6 well tissue culture plate (Nunclon^{TM} Delta). The magnetic actuator was placed under the plate for 1 minute.

(ii) Images were taken using a digital camera (PowerShot SX260 HS digital *camera,* Canon).

4.2.2.3 Actuation of HRSM Loaded with SPION Using the Magnetic Actuator

The following steps are summarized in Figure 4.4 a, b.

(i) $2x10^4$ HRSMC were seeded in a 25 cm^2 cell culture flask (Nunclon^{TM} Delta surface, Denmark) and incubated for 24 hours at 37^0C, 5% CO_2.

(ii) The medium was removed and experimental (proliferation) medium containing 250 μg/ml of SPION (50 nm) was added and incubated at 37^0C, 5% CO_2 for 24

hours.

(iii) After the incubation period the medium was removed and the cells were washed 5x with 5 ml of PBS.

(iv) 1ml of trypsin was added to each flask and incubated at 37^0C, 5% CO_2 for 1minute.

(v) 5 ml of fresh media was added in each flask and the detached cells were collected in a 30 ml container.

(vi) Samples were centrifuged at 1000 rpm for 5 minutes, the supernatant was removed and the pellets were re-suspended in 1 ml of fresh medium.

(vii) A cell count was performed and 10,000 cells were extracted.

(viii) Silicone moulds described in section 4.2.1.2 were dipped in 70% alcohol to sterilise them and dried inside a class II safety cabinet (Walker safety cabinets Ltd, UK).

(ix) The moulds were placed inside a 6 well tissue culture plate (Nunclon^{TM} Delta treated, Denmark).

(x) Cells were extracted and seeded in the hole at the centre of the mould.

(xi) The plate was incubated at 37^0C %, 5% CO_2 for 24 hours.

(xii) Silicone moulds were carefully removed and the medium was replaced with differentiation or proliferation medium and incubated for 7 days at 37^0C, 5% CO_2. The medium was replaced every other day. A separate plate was incubated parallel to the incubation (day 1-control).

(xiii) The magnetic actuator was placed under the 6 well plate and cells were exposed to an oscillating magnetic field for 1hour each day at 1 Hz and 2 Hz for a period of 7 days at 37^0C, 5% CO_2.

(xiv) At the end of day 7 the medium was removed and kept at -80^0C for further

analysis.

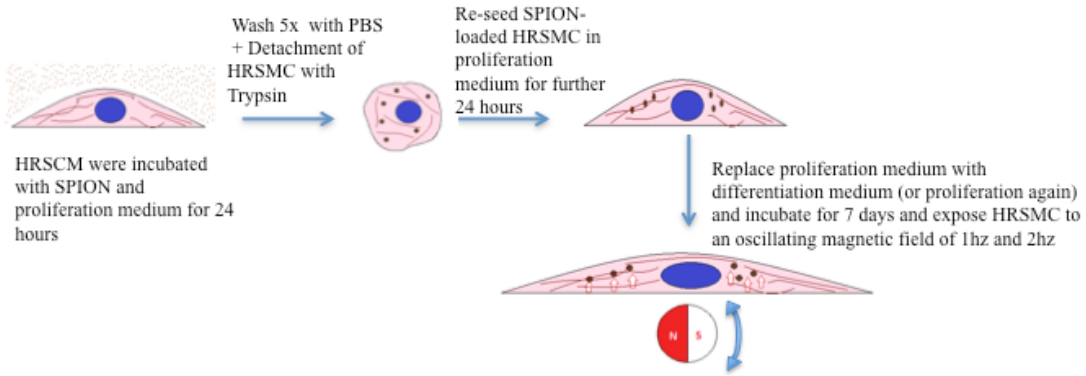

(a)

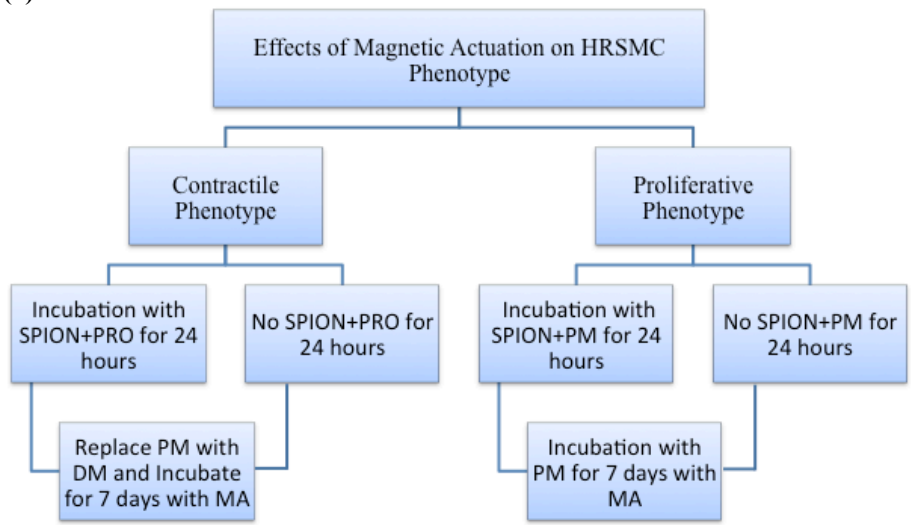

(b)

Figure 4.4 Magnetic Actuation of HRSMC. Incubation of SPION-Loaded HRSMC with Proliferation and Differentiation Medium. SPION-loaded HRSMC in proliferation or differentiation medium are referred to as PRO+SPION or DIFF+SPION, respectively.

4.2.2.4 Preparation of Cell Monolayers after Magnetic Actuation for Transmission Electron Microscopy

Transmission electron microscopy (TEM) was used to determine the cellular localisation of SPION after magnetic actuation. The method for this was described in section 2.2.3.1.

(i) Steps i- vi from section 4.2.2.3 were repeated for this experiment.

(ii) A cell count was performed and 50,000 cells were extracted and transferred to

a 24 well plate (Nunclon^{TM} Delta treated, Denmark).

(iii) Cells were incubated for 24 hours at 37^0C 5% CO_2.

(iv) The 24 well plate was placed on top of the magnetic actuator device for 1 hour under static or oscillating conditions.

(v) After 1 hour the supernatant was removed and 1ml of 2.5% v/v glutaraldehyde (Sigma, UK) in PBS was added to fix the cells inside a fume cupboard for 10 minutes.

(vi) Glutaraldehyde was removed and the samples were washed 2x with 1 ml of PBS.

(vii) The samples were post fixed with 2% osmium tetroxide (OsO_4) (Ceimig Limited, UK) for 1hour inside a fume cupboard.

(viii) The samples were dehydrated in a graded series of ethanol:water solutions.

a. 25% v/v ethanol 4 minutes

b. 50% v/v ethanol 4 minutes

c. 75% v/v ethanol 4 minutes

d. 95% v/v ethanol 4 minutes

e. 100% v/v ethanol 4 minutes (the last step was repeated 5 times).

(ix) The monolayers were scored with a scalpel blade creating squares of 5 mm x 5 mm.

(x) Propylene oxide (Agar Scientific, UK) was added to the samples in order to dissolve the plastic and detach the monolayers from the bottom of the well. Propylene oxide acts as a transition solvent before the embedding stage.

(xi) When the propylene oxide started to dissolve the plastic the cell monolayers were lifted with a wire loop and were transferred into fresh solutions of propylene oxide for 10 minutes each in order to allow the dissolved plastic to

diffuse out of the monolayers.

(xii) Propylene oxide was removed and the monolayers were transferred in a mixture containing 1:1 v/v propylene oxide: embedding resin (Araldite CY212 resin; Agar Scientific, UK) was added for 20 minutes.

(xiii) 1:1 propylene oxide was removed and 1:3 propylene oxide:embedding resin was added for 1.5 hours.

(xiv) The final propylene oxide:resin was removed and 100% resin was added.

(xv) The cell monolayers were transferred into a silicone rubber embedding moulds.

(xvi) The moulds were placed into an oven at 60ºC for 24 hours.

(xvii) The resin blocks containing the samples were thin sectioned (70 nm) with an ultramicrotome (Reichertjung ultracut E, Germany) and directly collected onto copper grids for its examination under a JEOL JEM 1200EX TEM operating at 80 Kv.

4.2.2.5 Quantification of Cellular Loading with SPION After Incubation with Proliferation and Differentiation Medium

A superconducting quantum interference device (SQUID) was used to measure the amount of iron inside the cells after a period of 7 days with proliferation medium or differentiation medium. The method for this was described in section 2.2.3.1.

(i) Steps i-vi from section 4.2.2.3 were followed from this experiment.

(ii) A cell count was performed and 200,000 cells were extracted and placed in a 25 cm^2 cell culture flask (Nunclon^{TM} Delta surface, Denmark) and incubated for 24 hours at 37^0C, 5% CO_2. A separate flask was incubated parallel to the incubation (day 1-control).

(iii) The medium was removed and proliferation or differentiation medium was replaced for 7 days. The medium was replaced every other day.

(iv) Steps iii-xi from section 2.2.2.1 were followed for this experiment.

4.2.2.6 Effect of Magnetic Actuation on the Phenotype of SPION Loaded HRSMC

4.2.2.6.1 Protein Expression of Contractile Markers of SPION-Loaded HRSMC Exposed to an Oscillating Magnetic Field

Immunocytochemistry was used to investigate the expression of proteins in HRSMC loaded with SPION following incubation in proliferation or differentiation medium. The method for this was described in section 2.2.4.1.1.

(i) Steps i-vi from section 4.2.2.3 were followed for this experiment.

(ii) 10,000 cells were plated in a Fluorodish and incubated at 37^0C, 5% CO_2 for 24 hours.

(iii) The medium was replaced with differentiation or proliferation medium and incubated for 7 days at 37^0C, 5% CO_2. The medium was replaced every other day. A separate plate was incubated parallel to the incubation (day 1-control).

(iv) The magnetic actuator was placed under the 6 well plate and cells were exposed to an oscillating magnetic field for 1hour each day at 1 Hz and 2 Hz for a period of 7 days at 37^0C, 5% CO_2.

(v) The medium was removed and the cells were fixed with 1 ml 4% glutaraldehyde (Sigma-Aldrich, USA) for 10minutes.

(vi) The cells were washed 3x with 1ml of PBS.

(vii) 500 µl of Triton X-100 (Sigma-Aldrich, USA) were added and the cells were incubated for 30 minutes.

(viii) After the incubation period the cells were washed 3x with 1 ml of PBS.

(ix) 500 µl of 5% BSA (Sigma-Aldrich, USA) was added and cells were incubated for 30 minutes at room temperature.

(x) The solution was removed and 500 µl of primary antibody (1:1000 for actin, 1: for 1:500 myosin heavy chain, 1:1000 for calponin, 1:500 for caldesmon all in PBS; Sigma-Aldrich, USA) and cells were incubated over night at 4^0C.

(xi) The antibody was removed and cells were washed 3x with 1ml of PBS.

(xii) 500 µl of secondary antibody (1:400) (Sigma-Aldrich, USA) was added and cells were incubated for 1 hour at room temperature.

(xiii) The solution was removed and cells were washed 3x with 1ml of PBS.

(xiv) The cells were mounted with a glass coverslip using drop of DAPI (Life Technologies, USA).

(xv) An upright fluorescence microscope (BX51 Olympus, GX Optical, UK) was used to acquire images.

4.2.2.6.2 Gene Expression of Contractile and Proliferative Markers of HRSMC Loaded with SPION Exposed to an Oscillating Magnetic Field

4.2.2.6.2.1 Real-Time Polymerase Chain Reaction

Real time polymerase chain reaction was performed for these experiments. The general methods used for this were described previously in section 2.2.4.2.1.

To complete the experiment:

(i) Steps i-xiii from section 4.2.2.3 were followed for this experiment.

(ii) Steps vi-xiv from section 2.2.4.2.1, step i from section 2.2.4.2.2, steps i-iii from section 2.2.4.2.3 and steps i-ii from section 2.2.4.2.4 were followed for this

experiment.

4.2.2.6.3 The Aspect Ratio of SPION-Loaded HRSMC Exposed to an Oscillating Magnetic Field

Aspect ratio measurements were performed for these experiments. The methods used for this were described previously in section 2.2.4.3.

To complete the experiment:

(i) Steps i-xiii from section 4.2.2.3 were followed for this experiment.

(ii) The medium was removed and the cells were fixed with 1 ml of 2.5% glutaraldehyde for 10 minutes at room temperature.

(iii) The solution was removed and the cells were washed with 3x with 1ml of PBS.

(iv) The cells were imaged using a Phase Contrast Inverted Microscope (AmScope 40X-900X Phase Contrast Inverted Microscope with 3M Camera, USA).

(v) The aspect ratio was calculated using an image analysis software (Image J, National Institute of Health, USA).

4.2.2.6.4 Cell Proliferation of SPION-Loaded HRSMC Following Incubation with Proliferation or Differentiation Medium

Four methods were used to investigate the effect of proliferation and differentiation medium of SPION-loaded HRSMC.

4.2.2.6.4.1 BrdU Assay

Cell proliferation-BrdU assay was performed for these experiments. The methods used for this were described previously in section 2.2.4.4.1.

(i) Steps i-xiii from section 4.2.2.3 were followed for this experiment.

(ii) Before the test was started the medium was removed and 1 ml of fresh medium was added.

(iii) 50 µl per well BrdU label (final volume of 500 µl) was added to all the wells and the plate was incubated for 2 hours at 37^0C 5% CO_2.

(iv) Labelling medium was removed by inverting the plate and tapping off.

(v) 500 µl of fixative and denaturing solution provided with the assay was added to the wells. The plate was incubated for 30 minutes at room temperature.

(vi) Fixative denaturing was removed from all the wells by inverting the plate and tapping off the solution and 500 µl per well anti-BrdU-peroxidase monoclonal antibody was added to each well and incubated for 90 minutes at room temperature.

(vii) Antibody conjugated solution was then removed by inverting the plate and tapping off the solution. The wells were rinsed 3x with PBS/washing solution.

(viii) 1000 µl of substrate solution provided with the assay was added to each well and incubated for 30 minutes at room temperature.

(ix) 100 µl of the solution was removed and plated in a fresh 96 well plate (Nunclon™ Delta surface, Denmark).

(x) 25 µl of 1M H_2SO_4 stop solution provided with the assay was added to all the wells.

(xi) Optical density of the reaction produced in the well was read with a colorimetric plate reader Multiskan FC (Thermoscientific, UK) at 450 nm with a reference wavelength at 690 nm.

4.2.2.6.4.2 Measurement of Cellular DNA Content Using the CyQUANT® Assay

The CyQUANT NF Assay was performed for these experiments. The methods used for this were described previously in section 2.2.4.4.2.

(i) Steps i-xiii from section 4.2.2.3 were followed for this experiment.

(ii) Before the test was started the medium was removed and 1 ml of fresh medium was added.

(iii) Remove medium and add 200 µl of CyQUANT NF dye reagent (in 1x HBSS buffer).

(iv) Incubate at 37^0C, 5% CO_2 using a plate shaker at speed 70 for 1 hour.

(v) After the incubation period, 100 µl of the solution was transferred in a black plate (Nunc™ F96 MicroWell™ Plates, Denmark).

(vi) The fluorescence intensity was measured using a fluorescence plate reader (TECAN SpectraFluor, USA) at an excitation wavelength of 485nm and an emission wavelength at 530 nm.

4.2.2.6.4.3 Direct Cell Count

Direct cell counts were performed for these experiments. The methods used for this were described previously in sections 2.2.4.4.3.

(i) Steps i-xiii from section 4.2.2.3 were followed for this experiment.

(ii) After the incubation period the medium was removed and the cells were washed 1x with 1ml of PBS.

(iii) 1 ml of trypsin was added to each well and incubated at 37^0C, 5% CO_2 for 1 minute.

(iv) 5 ml of fresh media was added in each well and the detached cells were collected

in a 15 ml container.

(v) Samples were centrifuged at 1000 rpm for 5 minutes, the supernatant was removed and the pellets were re-suspended in 1ml of fresh media.

(vi) A cell count was performed as described in section 2.2.1.3.

4.2.2.6.4.4 Cell Metabolic Activity Assay-MTS/PMS

Cell Metabolic Activity Assay-MTS/PMS was performed these experiments. The methods used for this were described previously in section 2.2.4.4.4.

(i) Steps i-xiii from section 4.2.2.3 were followed for this experiment.

(ii) Before the test was started the medium was removed and 1 ml of fresh medium was added.

(iii) 100 µl /well MTS/PMS combined solution was added to all the wells and incubated for 2 hours at 37^0C, 5% CO_2.

(iv) The regents were mixed using a plate shaker (Stuart mini orbital shaker SSM1, Bibby Sterilin Ltd, UK) at 70 speed at 37^0C %, 5% CO_2 for 2 hours.

(v) After the incubation period 100ul of the supernatant was transferred to a fresh 96 well plate (Nunclon^{TM} Delta surface, Denmark).

(vi) Absorbance of the formazan was measured at 490 nm with colorimetric reader Multiskan FC (Thermoscientific, UK).

4.2.2.7 Effect of Magnetic Actuation on the Biocompatibility of SPION- Loaded HRSMC

4.2.2.7.1 Reactive oxygen species

Measurement of reactive oxygen species release was performed for these experiments. The methods used for this were described previously in section 2.2.5.1.

(i) Steps i-vii from section 4.2.2.3 were followed for this experiment.

(ii) 10,000 cells were plated in a Fluorodish Cell Culture Dish - 35mm (World Precision Instruments, USA) and incubated at 37^0C, 5% CO_2 for 24 hours.

(iii) The medium was replaced with differentiation or proliferation medium and incubated for 7 days at 37^0C, 5% CO_2. The medium was replaced every other day. A separate plate was incubated parallel to the incubation (day 1-control).

(iv) The magnetic actuator was placed under the 6 well plate and cells were exposed to an oscillating magnetic field for 1hour each day at 1Hz and 2Hz for a period of 7 days at 37^0C, 5% CO_2.

(v) Before the test was started the medium was removed and cells were washed 1x with HBSS (Gibco, USA).

(vi) 500 µl of 25µM carboxy-H2 DCFDA working solution (in DMSO) was added for the 30 minutes at 37^0C, 5% CO_2.

(vii) The last 5 minutes of the incubation period 1 µl of (1mM) Hoechst 33342 stain (provided in the kit) was added.

(viii) After the incubation period the cells were washed 3x with HBSS (Gibco, USA).

(ix) The cells were mounted in a drop of HBSS (Gibco, USA).

(x) Images were taken using a fluorescent microscope (Leica DM2000, Germany).

4.2.2.7.1.1 Reactive Oxygen Species-Positive Control

A reactive oxygen species positive control was included in these experiments. The methods used for this were described previously in section 2.2.5.1.1.

(i) Steps i-vii from section 4.2.2.3 were followed for this experiment.

(ii) Cells were plated in a Fluorodish and incubated at 37^0C, 5% CO_2 for 24 hours.

(iii) The medium was replaced with differentiation or proliferation medium and incubated for 7 days at 37^0C, 5% CO_2. The medium was replaced every other day. A separate plate was incubated parallel to the incubation (day 1-control).

(iv) The magnetic actuator was placed under the 6 well plate and cells were exposed to an oscillating magnetic field for 1 hour each day at 1 Hz and 2 Hz for a period of 7 days at 37^0C, 5% CO_2.

(v) To induce reactive oxygen species, 500 µl of 100 mM TBHP (in water) were mixed with 1ml of culture medium and added. Cells were incubated for 90 minutes at 37^0C, 5% CO_2.

(vi) Before the test was started the medium was removed and cells were washed 1x with HBSS (Gibco, USA).

(vii) 500 µl of 25 µM carboxy-H2 DCFDA working solution (in DMSO) was added for the 30 minutes at 37^0C, 5% CO_2.

(viii) The last 5 minutes of the incubation period 1 µl of (1mM) Hoechst 33342 stain (provided in the kit) was added.

(ix) After the incubation period the cells were washed 3x with HBSS (Gibco, USA).

(x) The cells were mounted with a drop of HBSS (Gibco, USA).

(xi) Images were taken using a fluorescent microscope (Leica DM2000, Germany).

4.2.2.7.2 Cytotoxicity Assay-LDH Assay

Cytotoxicity Assay-LDH Assay was performed in these experiments. The methods used for this were described previously in section 2.2.5.2.

(i) Steps i-xiii from section 4.2.2.3 were followed for this experiment.

(ii) Before the test was started the medium was removed and 1 ml of fresh medium

was added.

(iii) Medium from SPION-loaded cells incubated with proliferation or differentiation medium were collected and transferred to a fresh 96 well plate (Nunclon^{TM} Delta surface, Denmark) accordingly.

(iv) 50 µl of medium was removed and placed in a new well and 50 µl of the LDH solution was added to each well and the plate was incubated in the dark for 30 minutes.

(v) 50 µl of stop solution was added to each well and the optical density of the reaction produced in the well was read with a plate reader Multiskan FC (Thermoscientific, UK) at 490nm.

4.2.2.7.2.1 Cytotoxicity Assay (Positive Control)

Cytotoxicity Assay-LDH Assay (Positive Control) was performed for these experiments. The methods used for this were described previously in section 2.2.5.2.1.

(i) Steps i-xiii from section 4.2.2.3 were followed for this experiment.

(ii) 10 µl of lysis solution (provided with the kit) per 100 µl was added to all the wells.

(iii) The cells were incubated for 45 minutes at 37^0C, 5% CO_2.

(iv) The plate was centrifuged at 250 x g for 4 minutes.

(v) Supernatants of SPION cells incubated with proliferation or differentiation were collected and transferred to a fresh 96 well plate (Nunclon^{TM} Delta surface, Denmark) accordingly.

(vi) 50 µl of medium was removed and placed in a new well and 50 µl of the LDH solution was added to each well and the plate was incubated in the dark for 30

minutes.

(vii) 50 µl of stop solution was added to each well and the optical density of the reaction produced in the well was read with a plate reader Multiskan FC (Thermoscientific, UK) at 490 nm.

4.2.2.7.3 Apoptosis - Caspase 3-7 Activity

Measurement of Caspase 3-7 activity was performed for these experiments. The methods used for this were described previously in sections 2.2.5.3.

(i) Steps i-xiii from section 4.2.2.3 were followed for this experiment.

(ii) The medium was removed and 200 µl of Apo-ONE® Caspase reagent was added and the cells were incubated for 30 minutes at room temperature.

(iii) After the incubation period 100 µl were transferred in a black plate (Nunc™ F96 MicroWell™ Plates, Denmark).

(iv) The fluorescence was measured using a fluorescence plate reader (TECAN SpectraFluor, USA) at an excitation wavelength of 485 nm and an emission wavelength at 530 nm.

4.3 Results

4.3.1 Modelling of the Magnetic Field and Forces Acting on SPION-Loaded HRSMC

The field plots in Figure 4.5 show the magnetic field produced at the base of the tissue culture plate 14 mm from the centre of the magnetic device. As the magnet rotated from 0 degrees (directly below the plate) to 180 degrees (farthest from the plate) the magnetic field became weaker. At 0 degrees the magnetic field acting on the particles was 82 mT and at 180 degrees the magnetic field dropped to 0 mT. The areas of the

plot coloured red indicated the magnetic field had its highest value and those coloured blue had the lowest value. The force plot (Figure 4.6) show that as the magnet rotated from 0 to 180 degrees the magnetic force also became weaker. At 0 degrees the force acting on each particle was 0.9 pico Newton (pN) and at 180 degrees the forces was 0.000007 pN. The calculations were made assuming each SPION was 50 nm diameter, had a density 1.25g/cm^3 and mass of 6.545x10^{-4} pg. Therefore, if the HRSMC were loaded with 50 pg of magnetic material the force acting on a cell at 0 degrees was:

$$50 \text{ x } 0.9 \text{ pN} = 45 \text{ pN}$$

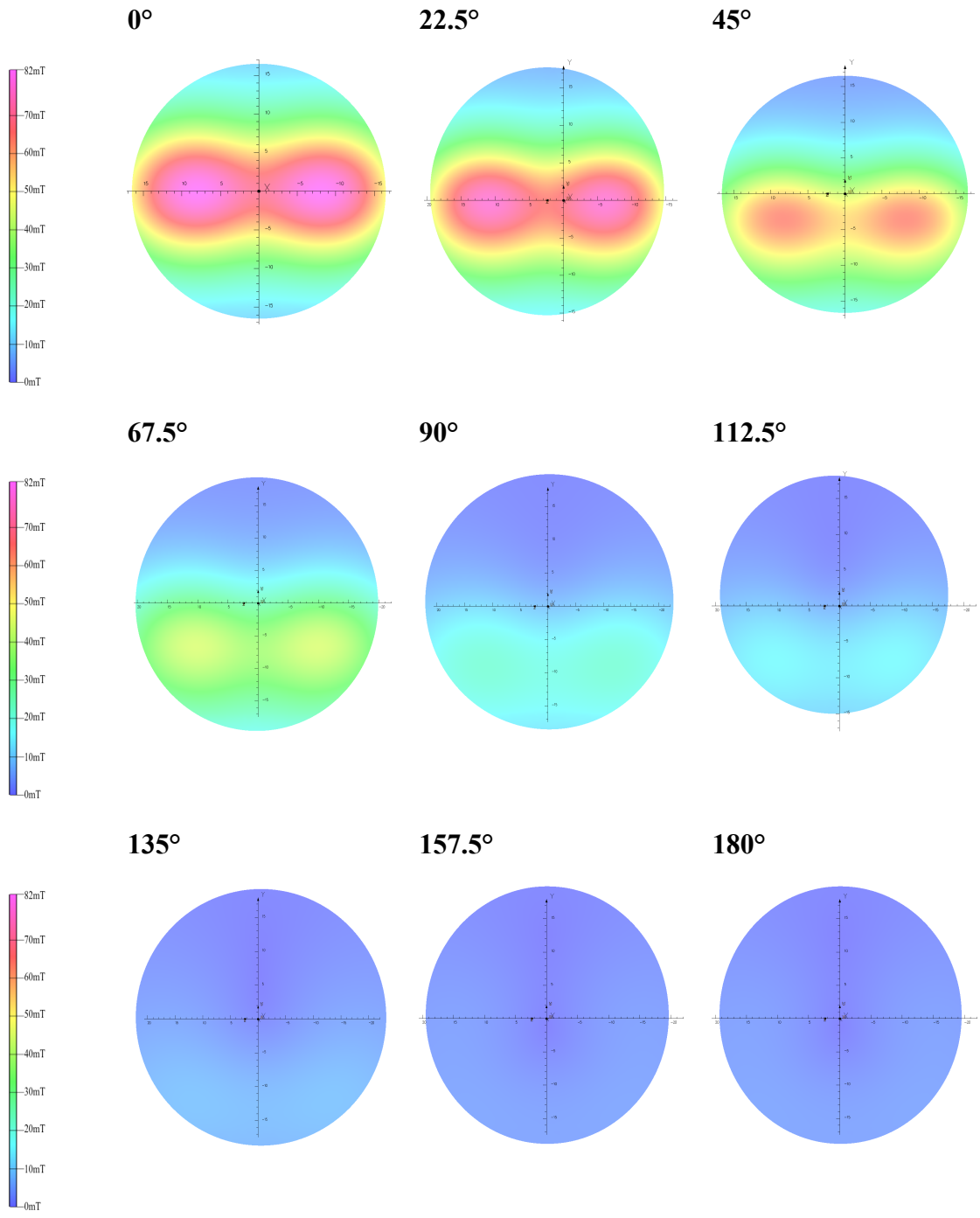

Figure 4.5 Magnetic Field Plots from the Magnetic Actuator. At 0 degrees the magnetic field had the highest value of 82 mT. As the magnet rotated from 0 to 180 degrees the magnetic field became weaker with lowest value of 0 mT.

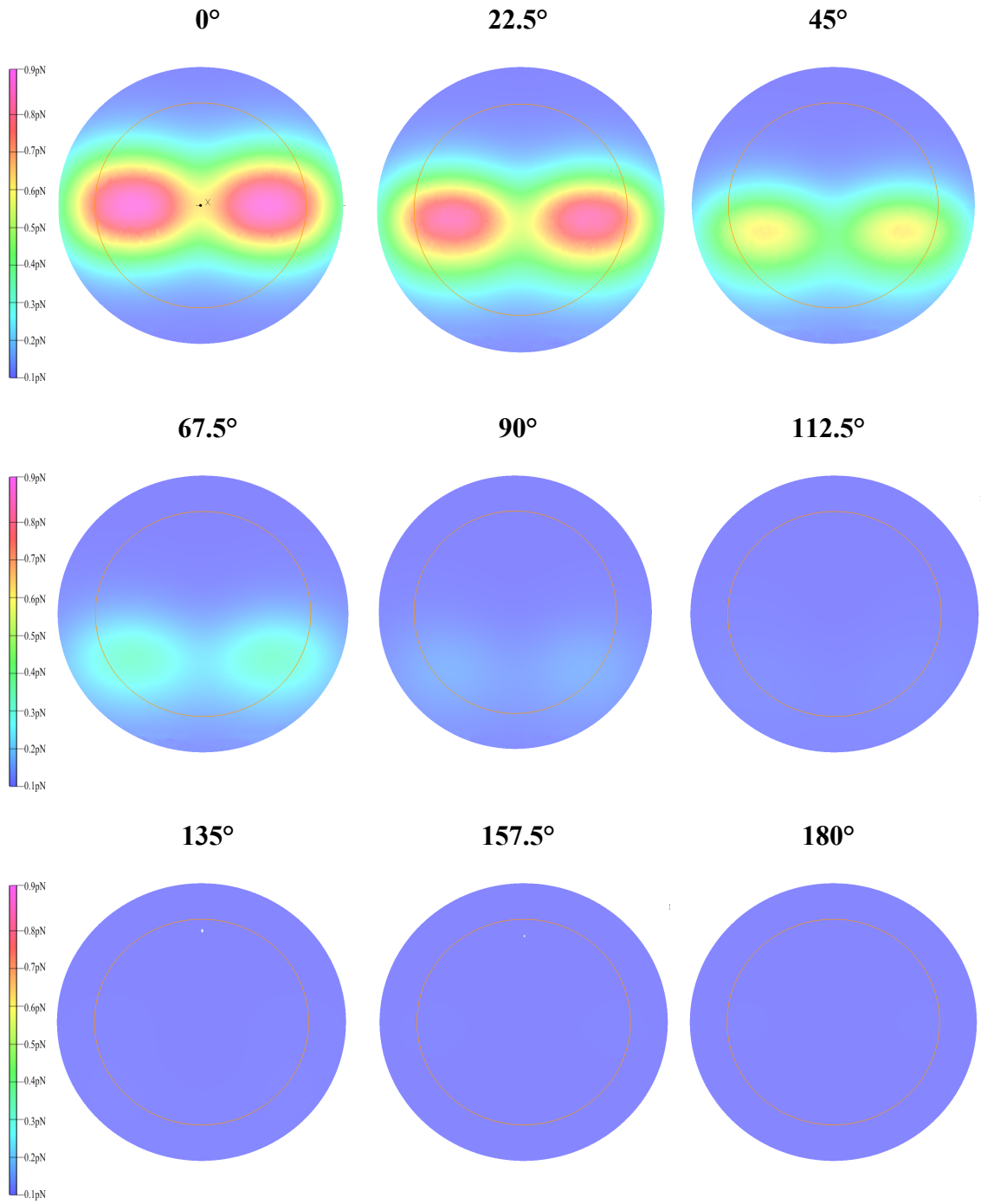

Figure 4.6 Magnetic Force Plots from the Magnetic Actuator. At 0 degrees the magnetic field produced the highest value of 0.9 pN. As the magnet rotated from 0 to 180 degrees the magnetic force became weaker with lowest value 0.000007 pN.

4.3.2 Visualization of the Magnetic Field with Iron Microparticles

Figure 4.7 (a) shows where the majority of iron filings were attached when a static magnetic field was applied to the base of the tissue culture plate. The majority of the iron filings were positioned to where the magnets were located. At this position (0 degrees) the magnetic field had its highest value as shown in Figure 4.7 (c).

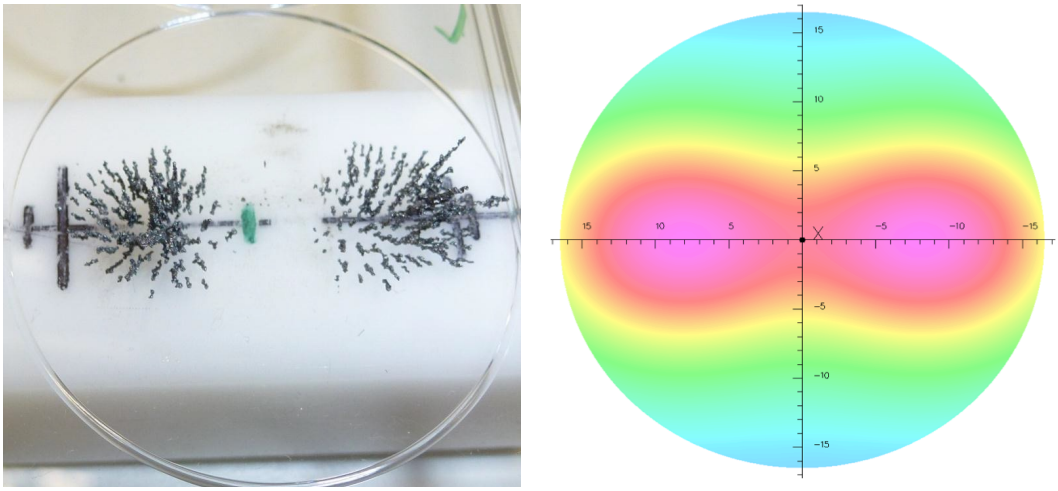

(a) **(b)**

Figure 4.7. (a) Distribution of Iron Filings under a Static Magnetic Field. (b) The Magnetic Field Plot Shows that the Field has its Highest Value directly above the Magnets.

4.3.3 Quantification of Cellular Loading with SPION After Incubation of HRSMC in Proliferation and Differentiation Medium

SQUID magnetometry was used to quantify the amount of SPION in HRSMC after the incubation in differentiation or proliferation medium for 7 days. The controls (Figure 4.8 a+b+c) were calculated in the same way like section (3.3.2.3.1). The results showed that SPION-loaded HRSMC incubated with proliferation medium for a period of 24 hours had approximately 16 pg of SPION per cell. However, SPION-loaded

HRSMC incubated with proliferation medium for 7 days had approximately 6 pg of SPION per cell, (Figure 4.9 a). The number of cells in the SPION-loaded HRSMC incubated in proliferation medium for 24 hours followed by incubation in differentiation medium for 7 days did not increase, whereas the cell number for SPION-loaded HRSMC incubated with proliferation medium for 7 days had increased by approximately three fold (Figure 4.9 b).

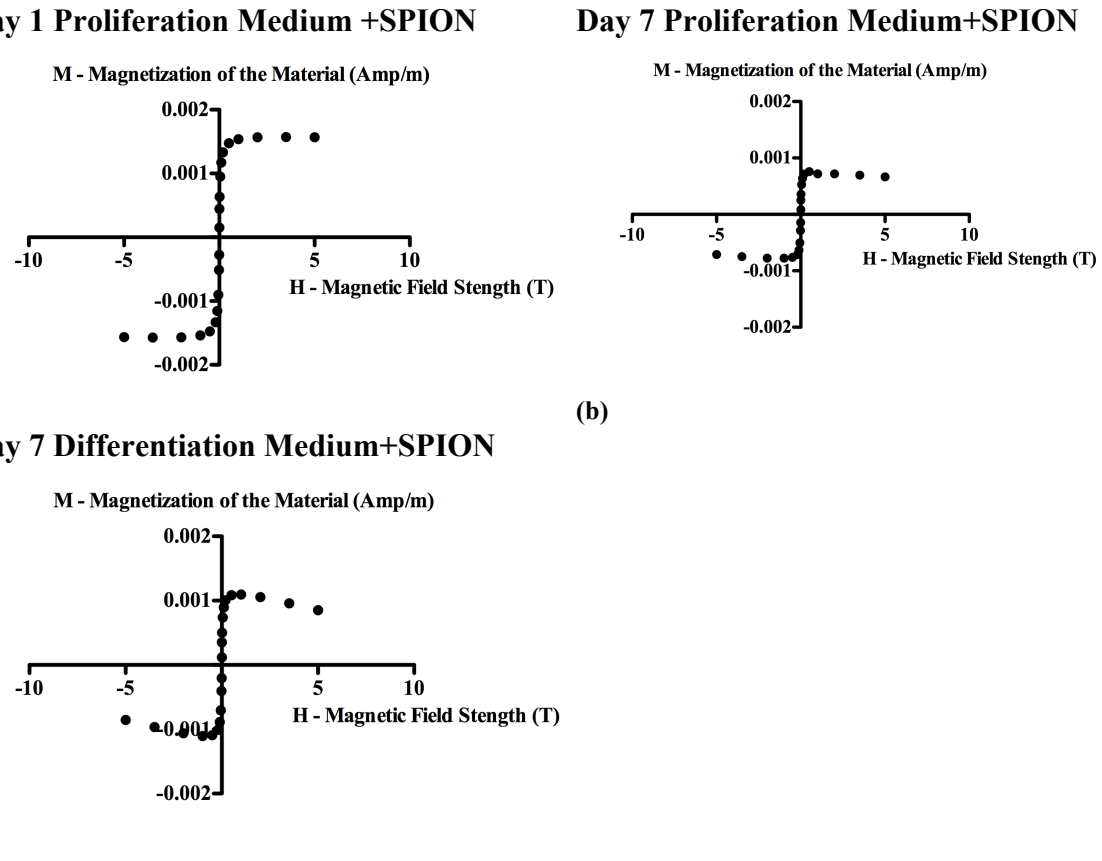

Figure 4.8 The average magnetization of the magnetic material was plotted against the magnetic field of cells incubated with 250 µg/ml. (a) the magnetization of HRSMC incubated with 250 µg/ml in proliferation medium for 24 hours, (b) the magnetization HRSMC incubated with 250 µg/ml in proliferation medium for 7 days and (c) the magnetization of HRSMC incubated with 250 µg/ml in differentiation medium for 7 days

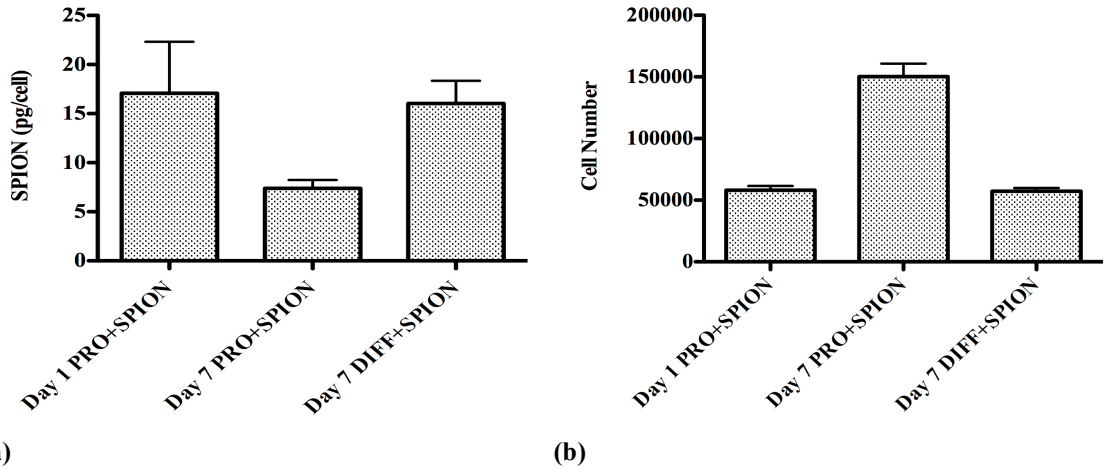

Figure 4.9 (a) SPION Concentration per Cell after Incubation with SPION (250µg/ml) for 24 Hours and 7 Days with Proliferation and Differentiation Medium. (b) Cell Number after Incubation in Proliferation or Differentiation Medium.

4.3.4 Cellular Localisation of SPION After Magnetic Actuation

TEM was used to investigate the cellular localization of SPION after exposure to magnetic actuation. HRSMC monolayers pre-incubated with culture medium containing 250 µg/ml of SPION for 24 hours were exposed to magnetic actuation for a period of 1 hour at 37^0C, 5% CO_2 (Figure 4.10 b). Electron micrographs of the actuated cells showed SPION-loaded endosomes inside the cells. The position of the endosomes inside the cells was similar to those of non-actuated SPION-loaded control cells (Figure 4.10 a).

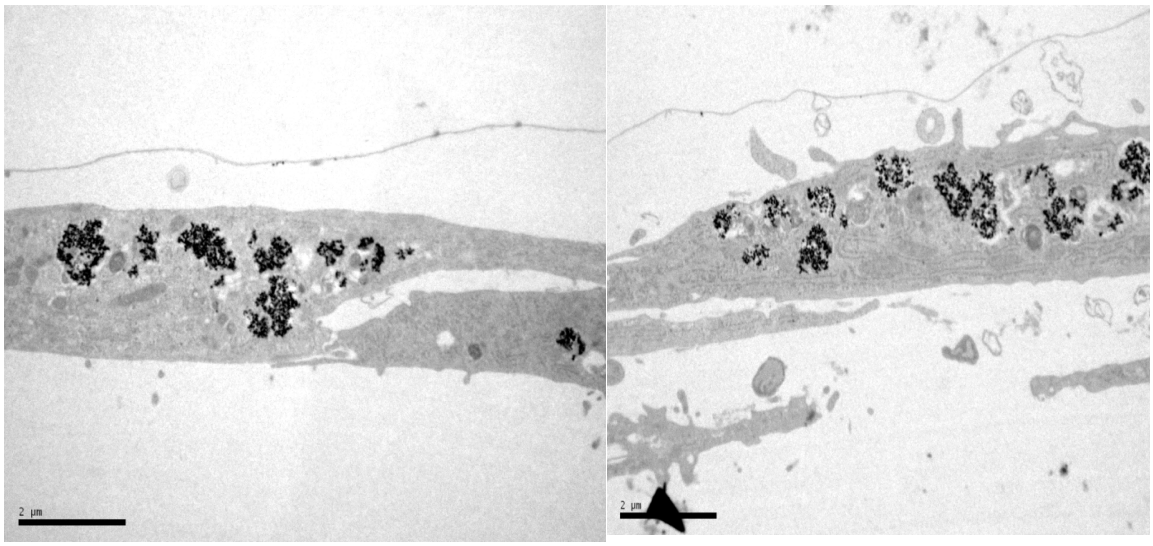

(a) **(b)**

Figure 4.10 Transmission Electron Microscopy Images of SPION-Loaded HRSMC Incubated in Medium Containing 250 µg/ml. (a) Non-actuated control cells (b) After actuation for 1 hour using a static magnetic field.

4.3.5 Effect of Magnetic Actuation on the Phenotype of SPION-Loaded HRSMC

4.3.5.1 Expression of Contractile Proteins in SPION-Loaded HRSMC Following Magnetic Actuation

Immunocytochemistry and fluorescence microscopy was used to investigate the expression of contractile proteins actin, myosin heavy chain, caldesmon, calponin in SPION-loaded HRSMC incubated in proliferation or differentiation medium and exposed to magnetic actuation. HRSMC were incubated with 250 µg/ml of SPION in proliferation medium for 24 hours and then switched to differentiation or proliferation medium for 7 days, whilst receiving exposure to magnetic actuation. Two types of controls were used: i) HRSMC without SPION and no actuation, incubated with proliferation or differentiation medium for 7 days, and ii) SPION-loaded cells incubated with proliferation medium for 24 hours, included as a pre-actuation control. After 7 days treatment the cells were stained with antibodies for the contractile protein markers such as actin, myosin heavy chain, caldesmon and calponin. The expression of

the proteins was detected using anti-mouse IgG FITC conjugated antibody, and the nuclei were counterstained blue with DAPI.

Fluorescence microscopy revealed SPION-loaded HRSMC incubated with proliferation medium for 24 hours without magnetic actuation had no detectable protein expression of myosin heavy chain and caldesmon compared with the control (cells in proliferation medium) (Figure 4.11 f, h and Figure 4.11 e, g).

Expression of actin and calponin in SPION-loaded HRSMC was visible after 24 hours incubation in proliferation medium (Figure 4.11 b, d), and the intensity and localization was comparable to that observed in the control (no SPION) cells, as shown in Figure 4.11 a, c.

The diffuse cytoplasmic expression of actin and calponin in SPION-loaded HRSMC after 7 days in proliferation medium (Figure 4.12 b, f) was similar to that observed for control cells (no SPION) (Figure 4.12 a, e). No visible difference existed for the expression and localization of actin and calponin in SPION-loaded cells incubated in proliferation medium for 7 days compared with SPION-loaded HRSMC incubated in proliferation medium after 24 hours.

SPION-loaded HRSMC incubated in proliferation medium for 7 days showed no visible expression of myosin heavy chain and caldemon (Figure 4.12 j, n), which matched that observed in control cells (no SPION) (Figure 4.12 i, m).

Incubating HRSMC with differentiation medium for 7 days appeared to result in the cells shifting from a proliferative to a contractile phenotype. There was a visible change in the localization of actin and calponin expression after 7 days incubation in differentiation medium for both SPION-loaded HRSMC (Figure 4.13 b and f) and

control cells (no SPION) (Figure 4.13 a, e). The staining distribution was notably more fibrillar compared with cell incubated in proliferation medium.

SPION-loaded HRSMC incubated in differentiation medium for 7 days showed no visible staining of myosin heavy chain and caldesmon (Figure 4.13 j and n) compared with control cells (no SPION) (Figure 4.13 i, m).

The expression of actin and calponin in SPION-loaded HRSMC after 7 days of actuation in differentiation medium (Figure 4.13 c, g, d, h) remained similar to that observed in the control cells (no SPION, no actuation) (Figure 4.13 a, e).

SPION-loaded HRSMC incubated in differentiation medium and actuated for 7 days at 1 Hz and 2 Hz showed no visible staining of myosin heavy chain and caldesmon (Figure 4.13 k, o, l, p) compared with control cells (no SPION, no actuation) (Figure 4.13 i, m).

The expression of actin and calponin in SPION-loaded HRSMC after incubation and 7 days of actuation in proliferation medium (Figure 4.12 c, g, d, h,) was similar to that observed for control cells (no SPION, no actuation) (Figure 4.12 a, e). Likewise, no observable difference existed for the expression of actin and calponin in SPION-loaded cells incubated in proliferation medium for 7 days compared with SPION-loaded HRSMC incubated in proliferation medium after 24 hours of actuation.

SPION-loaded HRSMC incubated in proliferation medium actuated for 7 days at 1 Hz and 2 Hz showed no visible expression of myosin heavy chain and caldesmon (Figure 4.12 k, o, l, p) which matched that observed in control cells (no SPION, no actuation) (Figure 4.12 i, m).

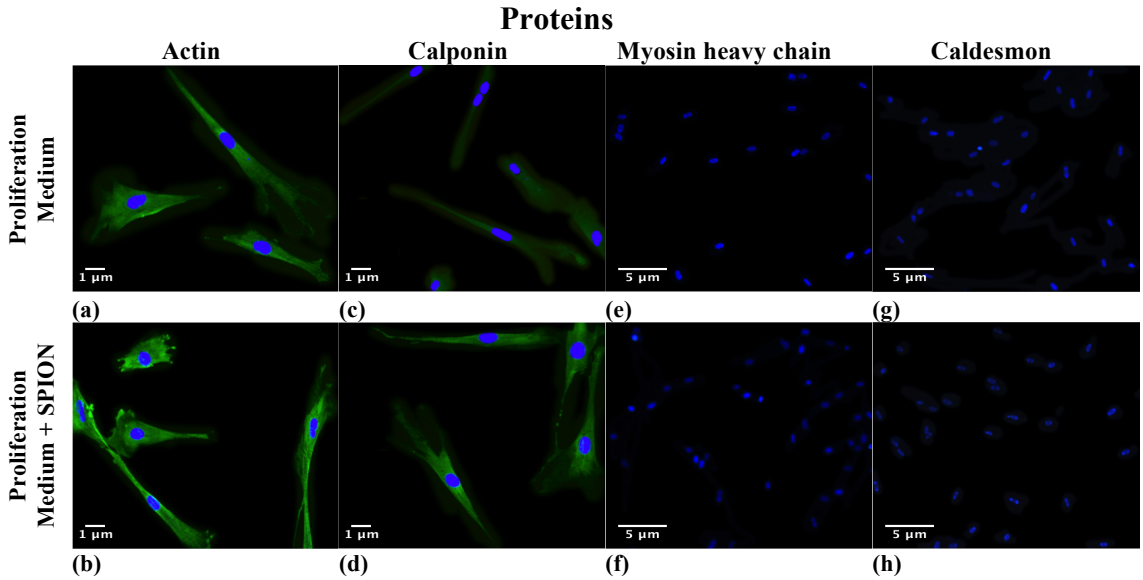

Figure 4.11 Immunofluorescence Microscopy Showing Expression of Contractile Markers Actin, Calponin, Myosin Heavy Chain and Caldesmon after Incubation of SPION-Loaded HRSMC in Proliferation Medium for 24 Hours. (a-d) Actin and calponin were visible in SPION-loaded HRSMC in proliferation medium after 24 hours, similar to that observed in control cells. (e-h) Staining for myosin heavy chain and caldesmon was not visible in SPION-loaded HRSMC after 24 hours of incubation in proliferation medium, nor in control cells.

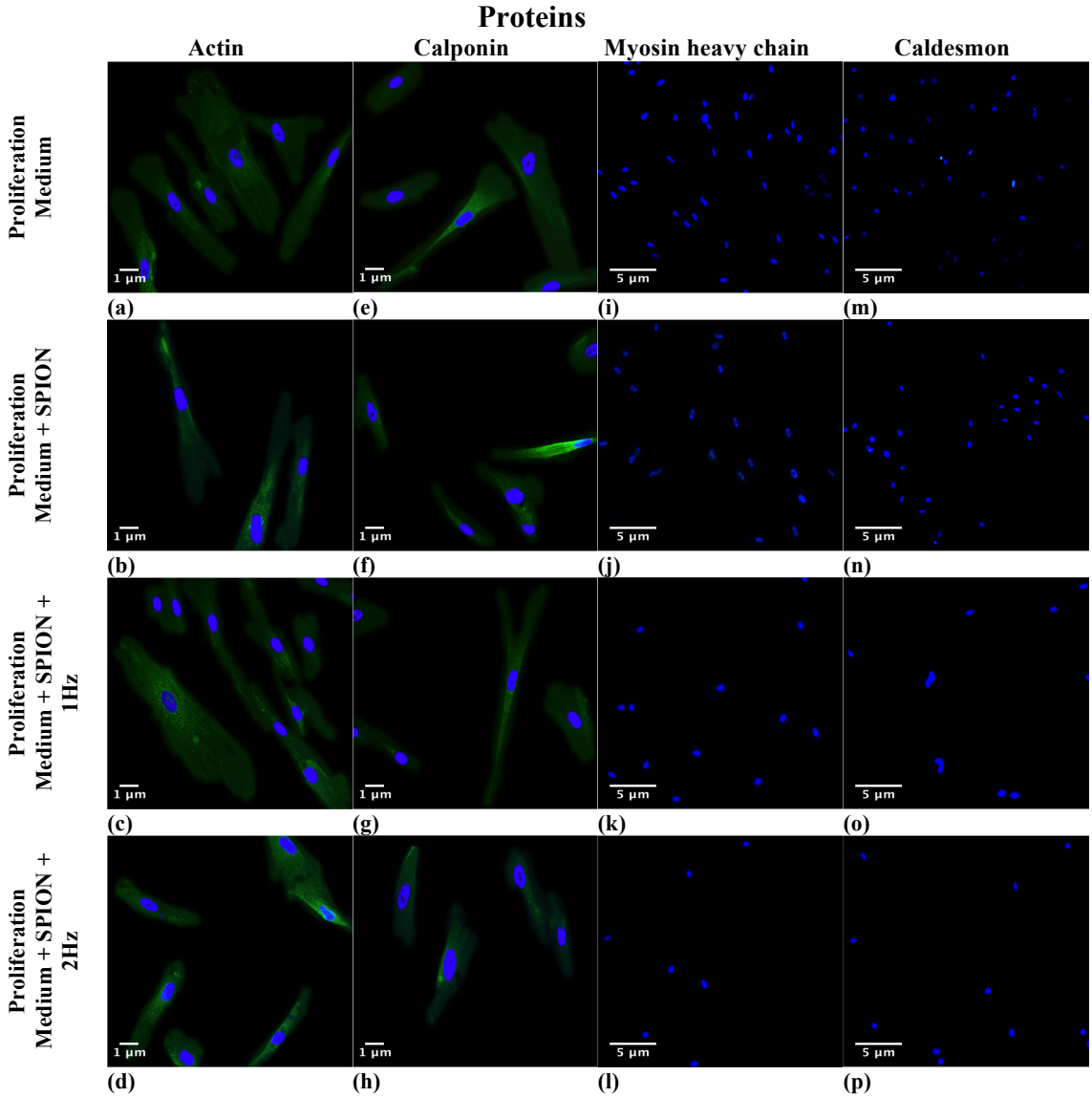

Figure 4.12 Immunofluorescence Microscopy Showing Expression of Different Contractile Markers Actin, Calponin, Myosin Heavy Chain and Caldesmon in SPION-Loaded HRSMC Incubated in Proliferation Medium for 7 Days with Magnetic Actuation (1 Hz or 2 Hz). (b, f) The expression of actin and calponin in SPION-loaded HRSMC after 7 days incubation in proliferation medium was similar to that observed in control cells (a, e). (j, n) Staining for myosin heavy chain and caldesmon was not visible in SPION-loaded HRSMC after 7 days in proliferation medium, nor in control cells (i, m). (c-h) The expression of actin and calponin in SPION-loaded HRSMC after 7 days of magnetic actuation in proliferation medium was similar to that observed in control cells (a, e). (k-p) Staining for myosin heavy chain and caldesmon was not visible in SPION-loaded HRSMC after 7 days of magnetic actuation in proliferation medium, nor in control cells (i, m).

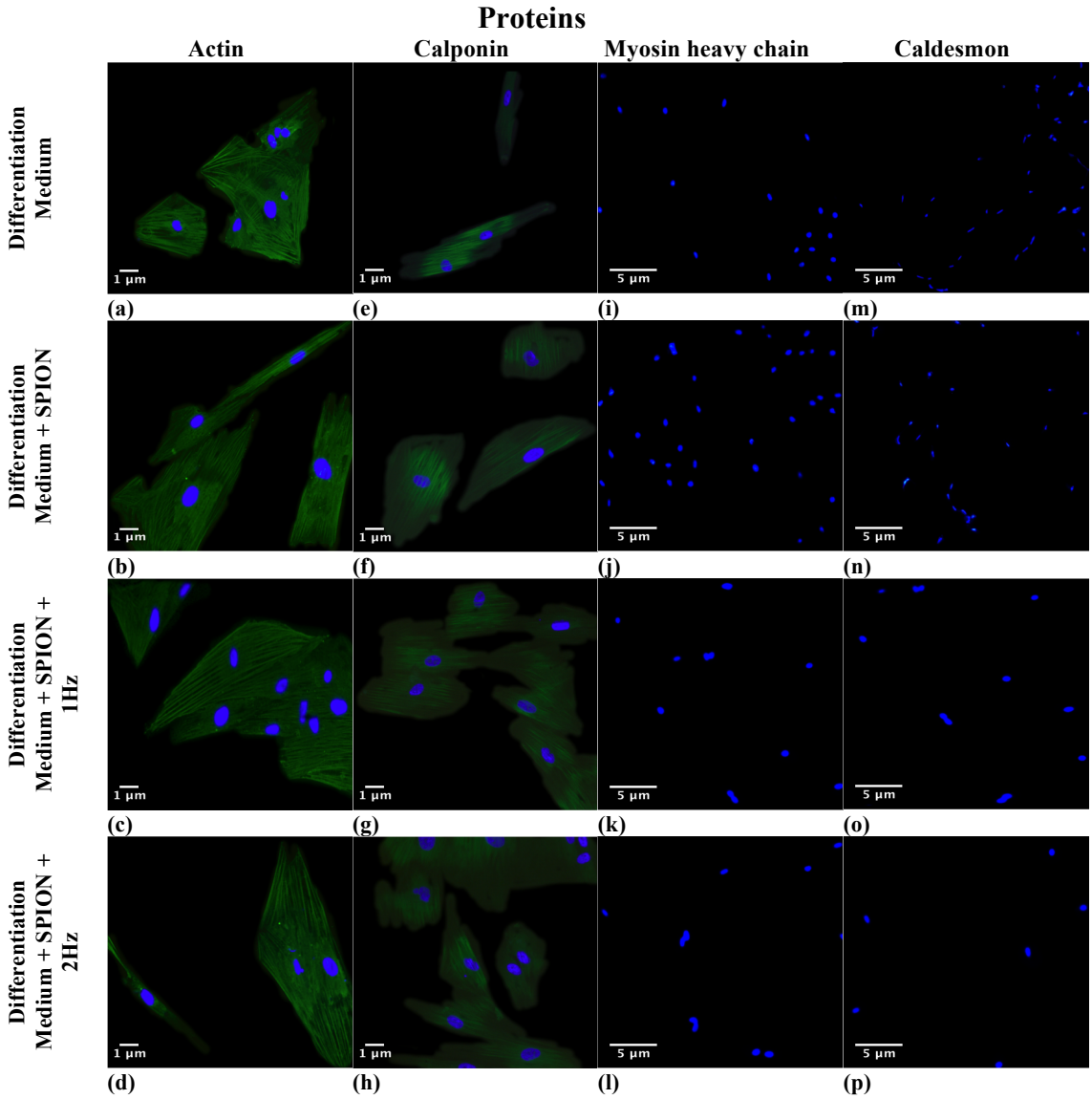

Figure 4.13 Immunofluorescence Microscopy Showing Expression of Contractile Markers Actin, Calponin, Myosin Heavy Chain and Caldesmon after 7 Days of Magnetic Actuation (1 Hz or 2 Hz) of SPION-Loaded HRSMC Incubated in Differentiation Medium. (b, f) The expression of actin and calponin in SPION-HRSMC after 7 days in differentiation medium was similar to that observed in control cells (a, e). (j, n) Staining for myosin heavy chain and caldesmon was not visible in SPION-loaded HRSMC after 7 days in differentiation medium, nor in control cells (i, m). (c-h) The expression of actin and calponin in SPION-HRSMC after 7 days of magnetic actuation in differentiation medium was similar to that observed in control cells (a, e). (k-p) Staining for myosin heavy chain and caldesmon was not visible in SPION-loaded HRSMC after 7 days of magnetic actuation in differentiation medium, nor in control cells (i, m).

4.3.5.2 Gene Expression of Contractile and Proliferative Markers of HRSMC Loaded with SPION Exposed to an Oscillating Magnetic Field

4.3.5.2.1 Real-Time PCR

Real-time PCR was used to investigate the expression of different contractile (actin, myosin heavy chain, caldesom and calponin) and proliferative (vimentin and tropomyosin) markers at the mRNA level in SPION-loaded HRSMC incubated in proliferation or differentiation medium and exposed to magnetic actuation.

HRSMC were incubated in proliferation medium containing 250 μg/ml of SPION for 24 hours and then switched to differentiation or proliferation medium for 7 days with the incorporation of magnetic actuation. Two types of controls were used: i) HRSMC without SPION and no actuation, incubated with proliferation or differentiation medium for 7 days, and ii) SPION-loaded cells incubated with proliferation medium for 24 hours, included as a pre-actuation control. After 7 days magnetic actuation the cells were tested for different contractile markers and proliferative markers. For abbreviation, SPION-loaded HRSMC in proliferation or differentiation medium was referred to as PRO+SPION or DIFF+SPION, respectively. Finally, all the values have been normalized according to cells in proliferation medium (PRO).

A decrease in the mRNA expression for actin ($p<0.01$), myosin heavy chain ($p<0.01$), caldesmon ($p<0.05$), vimentin ($p<0.05$) and tropomyosin 4 ($p<0.05$) in SPION-loaded HRSMC incubated in proliferation medium for 24 hours without magnetic actuation was observed compared with control cells incubated in proliferation medium, as shown in Figure 4.14 (a, b, c, e, f). No significant difference in mRNA expression was found for calponin compared with control cells, as shown in Figure 4.14 d.

There was no change in mRNA expression for any of the contractile markers (actin, myosin heavy chain, caldesmon and calponin) or the proliferative markers (vimentin and tropomyosin 4) in SPION-loaded HRSMC incubated in proliferation medium for 7 days compared with the control cells (no SPION) (Figure 4.15 a-f).

HRSMC incubated with differentiation medium for 7 days showed a significant increase in actin ($p<0.05$) and calponin mRNA expression ($p<0.01$) (Figure 4.15 a, d). However, SPION-loaded HRSMC incubated in differentiation medium for 7 days showed a significant decrease in actin and calponin mRNA expression ($p<0.05$) compared with control cells (no SPION), as shown in Figure 4.15 (a, d).

No change in myosin heavy chain, caldesmon, vimentin and tropomyosin 4 mRNA expression was observed in SPION-loaded HRSMC incubated in differentiation medium for 7 days compared with control cells (no SPION), as shown in Figure 4.15 (b, c, e, f).

There was no change in mRNA expression for any of the contractile markers (actin, myosin heavy chain, caldesmon and calponin) or the proliferative markers (vimentin and tropomyosin 4) in SPION-loaded HRSMC in proliferation medium after magnetic actuation for 7 days compared with the control cells (no SPION, no actuation) (Figure 4.15 a-f).

SPION-loaded HRSMC incubated in differentiation medium for 7 days with magnetic actuation at 1 Hz or 2 Hz showed a non-significant decrease in actin but a significant decrease in calponin ($p<0.01$) mRNA expression compared with control cells (no SPION, no actuation), as shown in Figure 4.15 (a, d).

No change in myosin heavy chain, caldesmon, vimentin and tropomyosin 4 mRNA expression was observed in SPION-loaded HRSMC incubated in differentiation medium for 7 days of actuation compared with control cells (no SPION, no actuation), as shown in Figure 4.15 (b, c, e, f).

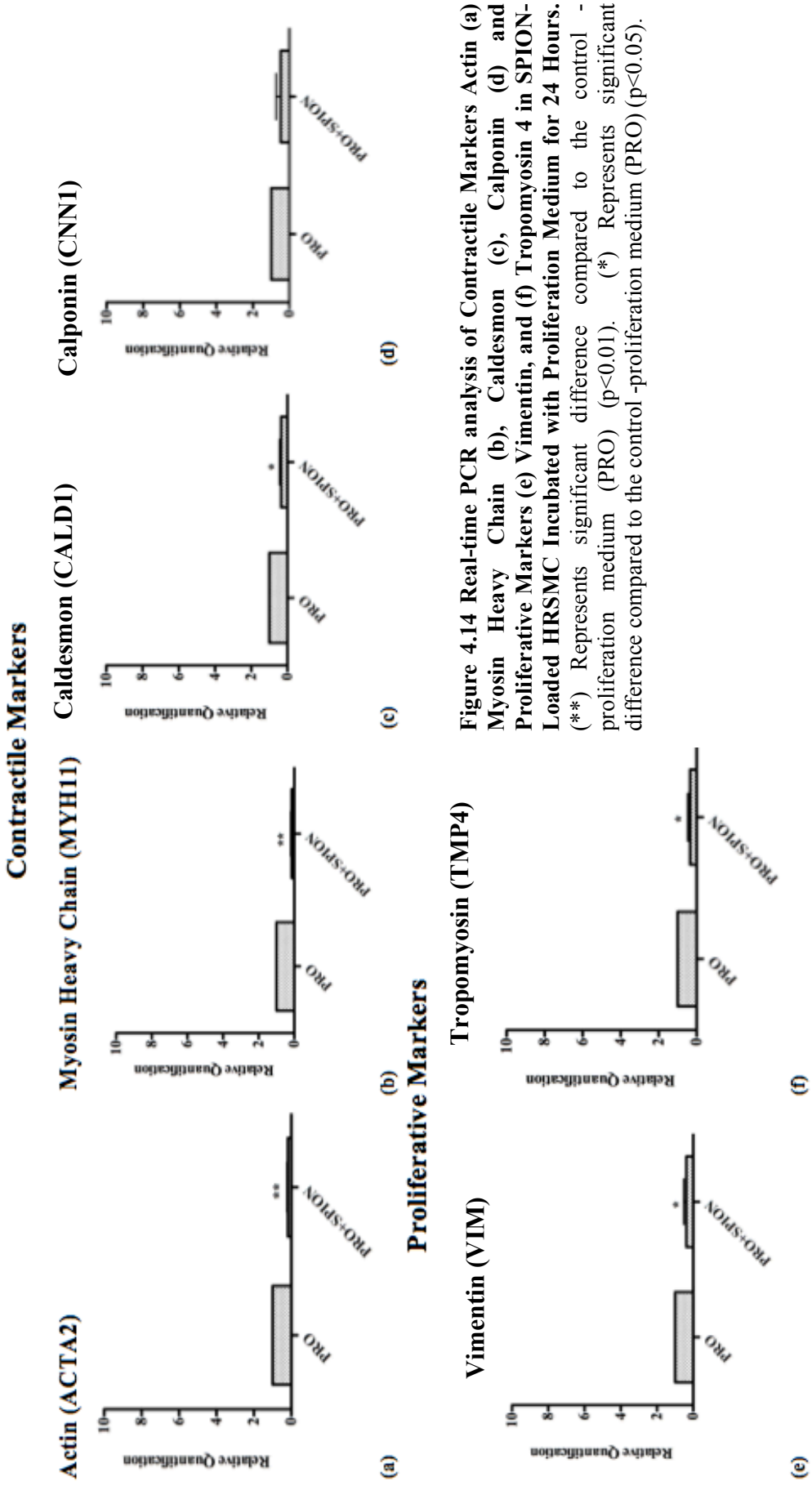

Figure 4.14 Real-time PCR analysis of Contractile Markers Actin (a) Myosin Heavy Chain (b), Caldesmon (c), Calponin (d) and Proliferative Markers (e) Vimentin, and (f) Tropomyosin 4 in SPION-Loaded HRSMC Incubated with Proliferation Medium for 24 Hours. (**) Represents significant difference compared to the control - proliferation medium (PRO) ($p<0.01$). (*) Represents significant difference compared to the control -proliferation medium (PRO) ($p<0.05$).

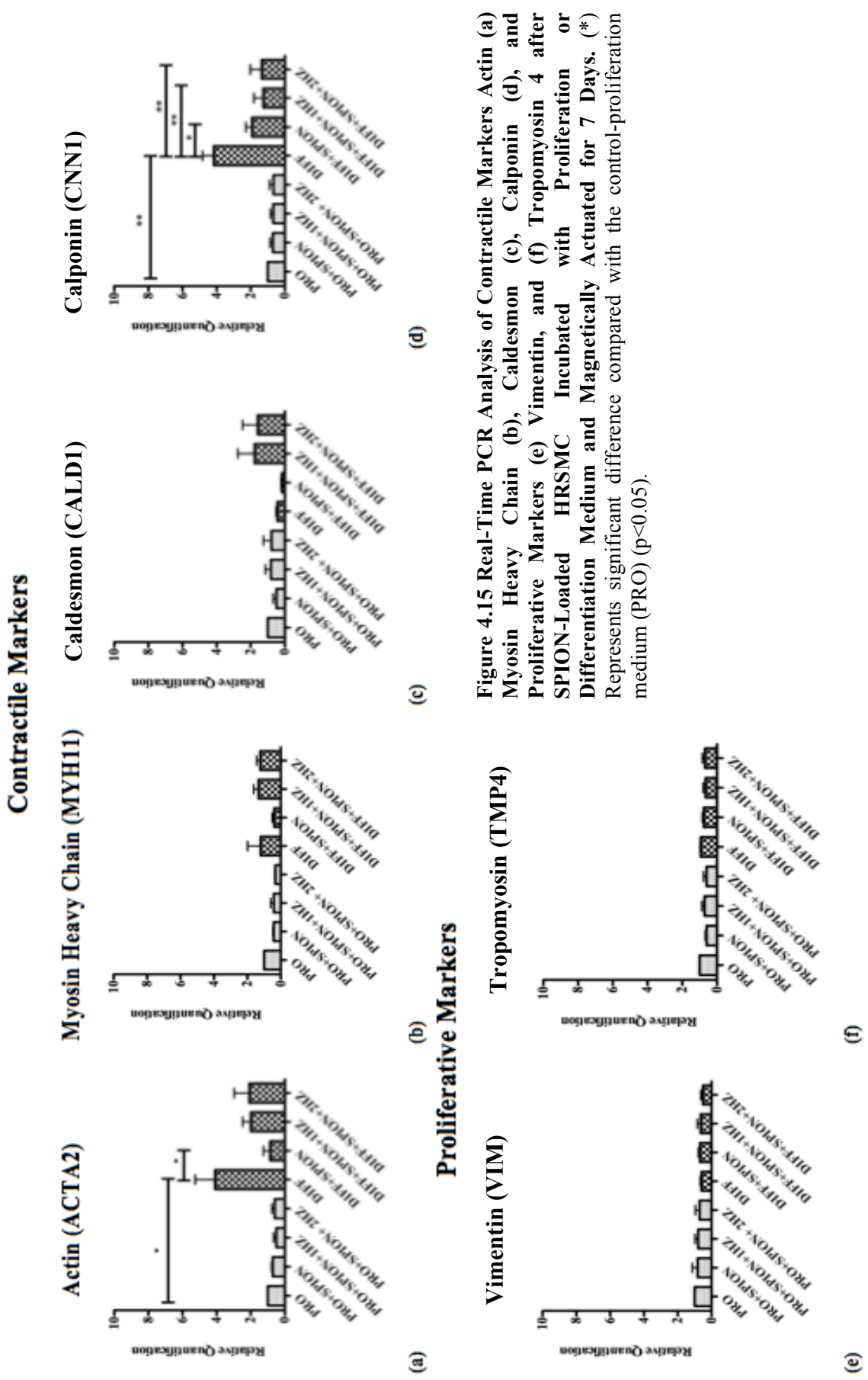

Figure 4.15 Real-Time PCR Analysis of Contractile Markers Actin (a) Myosin Heavy Chain (b), Caldesmon (c), Calponin (d), and Proliferative Markers (e) Vimentin, and (f) Tropomyosin 4 after SPION-Loaded HRSMC Incubated with Proliferation or Differentiation Medium and Magnetically Actuated for 7 Days. (*) Represents significant difference compared with the control-proliferation medium (PRO) ($p<0.05$).

4.3.5.3 Aspect Ratio of SPION-Loaded HRSMC Following Magnetic Actuation

The aspect ratio is the ratio of the width of a cell to its length. The aspect ratio of cells differentiated towards a contractile phenotype is typically greater than the aspect ratio of cells in a proliferative state and can be used as an indicator of the phenotypic status of cells in culture. The aspect ratio was therefore used to investigate whether proliferation or differentiation medium affected the morphology of SPION-loaded HRSMC.

No significant difference was observed in the aspect ratio of SPION-loaded HRSMC incubated for 24 hours in proliferation medium compared with control cells (Figure 4.16 a).

Non-loaded HRSMC incubated in differentiation medium for 7 days had a greater aspect ratio compared with non-loaded cells incubated in proliferation medium (control cells) ($p<0.001$) (Figure 4.16 b). SPION-loaded cells incubated in differentiation medium for 7 days showed a non-significant decrease in the aspect ratio compared with non-SPION loaded cells incubated in differentiation medium.

SPION-loaded cells incubated in proliferation medium and exposed to magnetic actuation at 2 Hz showed a significant increase in the aspect ratio compared with control cells (no SPION, no actuation; $p<0.05$) (Figure 4.16 b). SPION-loaded cells incubated in differentiation medium and exposed to magnetic actuation at 2 Hz showed a non-significant decrease in the aspect ratio compared with control cells (no SPION, no actuation) (Figure 4.16 b).

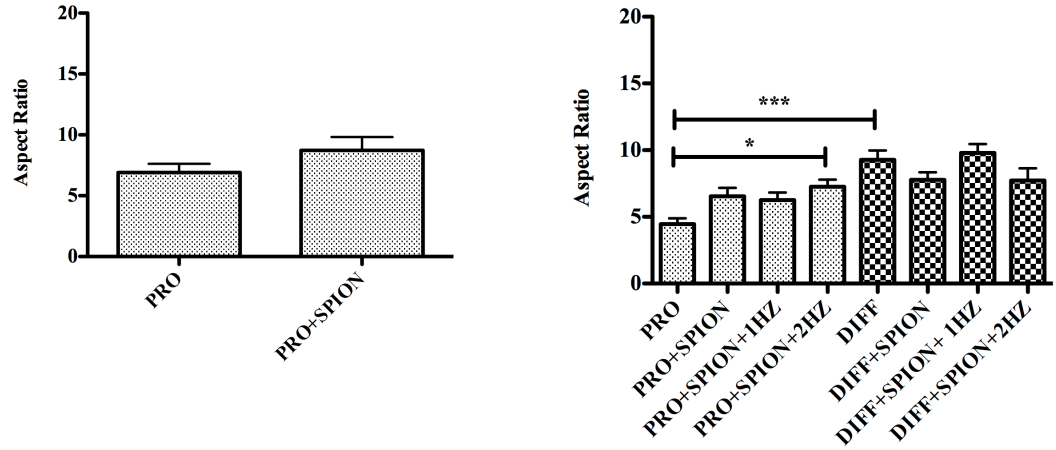

(a) **(b)**

Figure 4.16 Aspect Ratio of SPION-loaded HRSMC. (a) After 24 Hours in Proliferation Medium. (b) In Proliferation and Differentiation Medium after Magnetic Actuation. A non-significant decrease was observed in SPION-loaded cells incubated with differentiation medium compared with control cells (no SPION). A significant increase was observed in the aspect ratio of SPION-loaded HRSMC incubated in proliferation medium and exposed to magnetic actuation at 2 Hz ($p<0.05$) compared with control cells (no SPION, no actuation). A non-significant decrease was observed in SPION-loaded cells incubated with differentiation medium and actuated at 2 Hz compared with control cells (no SPION, no actuation).

4.3.5.4 Cell Proliferation of SPION-Loaded HRSMC Following Magnetic Actuation

Three methods were used to investigate the effect of magnetic actuation on the proliferation of SPION-loaded HRSMC.

4.3.5.4.1 BrdU ELISA Assay

A BrdU ELISA assay was performed in order to investigate the effect of magnetic actuation on the proliferation of SPION-loaded HRSMC incubated in proliferation or differentiation medium for 7 days. No difference was observed in the optical density values between SPION-loaded HRSMC incubated in proliferation medium for 24 hours compared with control cells (no SPION), as shown in Figure 4.17 a.

No difference was observed in the optical density values between SPION-loaded HRSMC in either proliferation or differentiation medium compared with control cells (no SPION) as shown in Figure 4.17 b.

Similarly no difference was observed in the optical density values between SPION-loaded HRSMC in proliferation or differentiation medium after 7 days of magnetic actuation at 1 Hz or 2 Hz compared with control cells (no SPION, no actuation), as shown in figure 4.17 b.

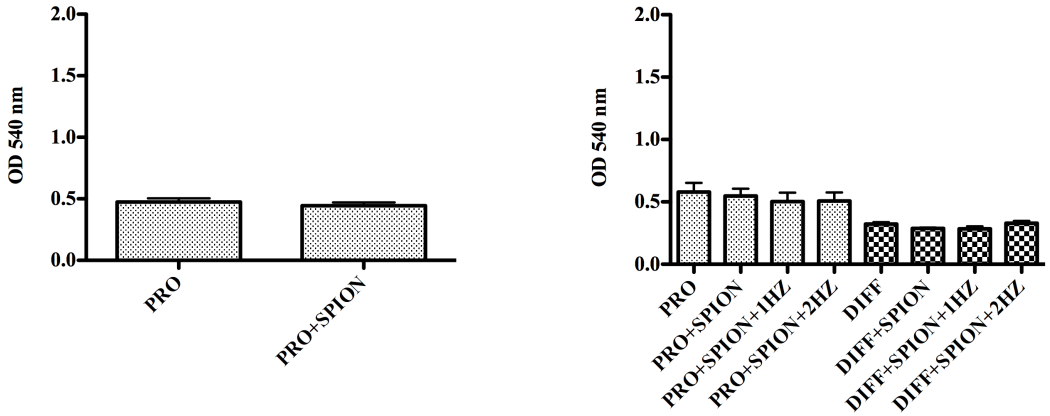

(a) **(b)**

Figure 4.17 Cell Proliferation of SPION-Loaded HRSMC Following Magnetic Actuation. (a) No difference was observed between SPION-loaded HRSMC after 24 hours compared with control cells (no SPION). (b) No change in the optical density values between HRSMC in differentiation medium after 7 days compared with HRSMC in proliferation medium (control cells-no SPION). (b) No difference was observed between SPION-loaded HRSMC in either proliferation or differentiation medium after 7 days of magnetic actuation compared with control cells (no SPION, no actuation).

4.3.5.4.2 Measurement of Cellular DNA Content Using the CyQUANT NF Assay

The CyQUANT NF assay was used to investigate the effect of magnetic actuation on the proliferation of SPION-loaded HRSMC incubated in proliferation or differentiation medium for 7 days. No difference in the fluorescence intensity values was observed between SPION-loaded HRSMC incubated in proliferation medium for 24 hours compared with control cells (no SPION), as shown in Figure 4.18 a.

No difference was observed in the fluorescence intensity values between SPION-loaded HRSMC incubated in proliferation or differentiation medium after 7 days compared with control cells (no SPION), as shown in Figure 4.18 b.

Similarly, no difference was observed in the fluorescence intensity values between SPION-loaded HRSMC incubated in proliferation or differentiation medium after 7 days of magnetic actuation at 1 Hz or 2 Hz compared with control cells (no SPION, no actuation), as shown in Figure 4.18 b.

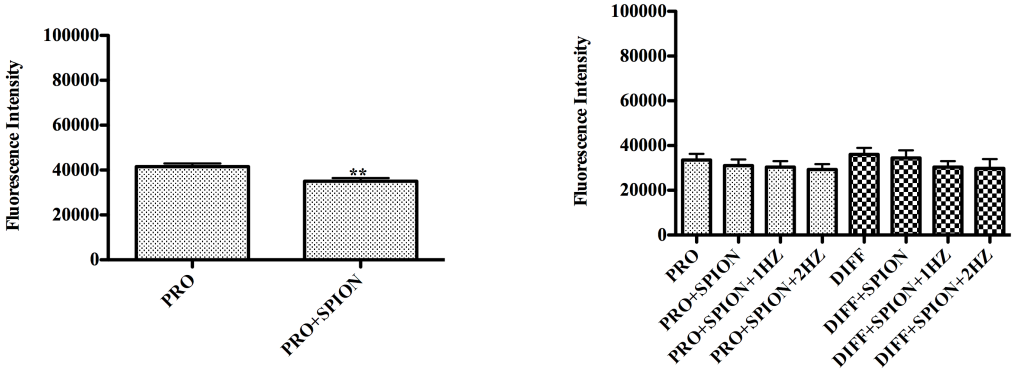

(a) **(b)**

Figure 4.18 Cell Proliferation of SPION-Loaded HRSMC Following Magnetic Actuation. (a) No difference was observed between SPION-loaded HRSMC after 24 hours compared with control cells (no SPION). (b) No difference was observed between SPION-loaded HRSMC in either proliferation or differentiation medium after 7 days compared with control cells (no SPION). (b) No difference was observed between SPION-loaded HRSMC in either proliferation or differentiation medium after 7 days of magnetic actuation compared with control cells (no SPION, no actuation).

4.3.5.4.3 Direct Cell Counts

Direct cell counting was performed to investigate the proliferative effect of magnetic actuation of SPION-loaded HRSMC after incubation in proliferation or differentiation medium for 7 days. No difference was observed between SPION-loaded HRSMC incubated in proliferation medium for 24 hours compared with control cells (no SPION), as shown in Figure 4.19 a.

No difference was observed between SPION-loaded HRSMC incubated in proliferation after 7 days compared with the control cells (no SPION). No difference in the number of cells between HRSMC in differentiation medium and control cells (HRSMC in proliferation medium) after 7 days of incubation. No difference was observed between SPION-loaded HRSMC in differentiation medium after 7 days compared with control cells (no SPION) as shown in Figure 4.19 b. Similarly, no difference was observed between SPION-loaded HRSMC incubated in proliferation or differentiation medium after 7 days of magnetic actuation at 1 Hz or 2 Hz compared with control cells (no SPION, no actuation), as shown in Figure 4.19 b.

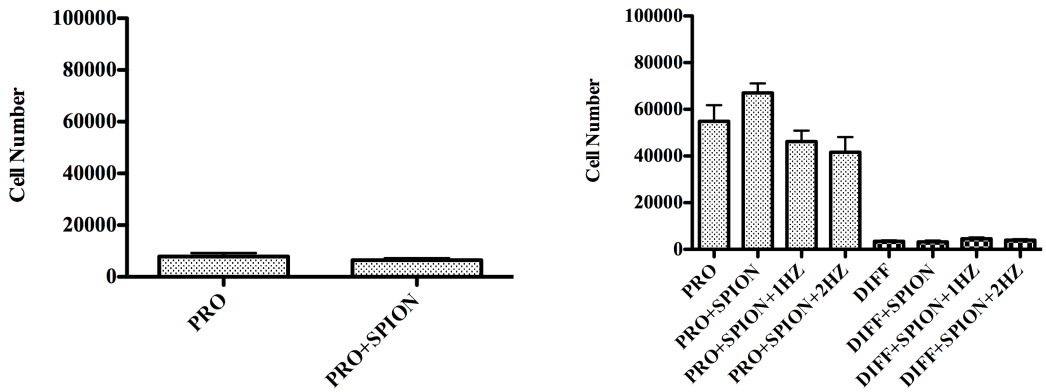

(a) (b)

Figure 4.19 The Effect of Magnetic Actuation on SPION-Loaded HRSMC Cell Counts Following Magnetic Actuation. (a) No difference was observed between SPION-loaded HRSMC after 24 hours compared with control cells. b) No difference was observed between SPION-loaded HRSMC in proliferation medium after 7 days of incubation compared with control cells (no SPION). No difference was observed between SPION-loaded HRSCM in differentiation medium after 7 days of incubation compared with control cells (no SPION). (b) No difference was observed between SPION-loaded HRSMC in either proliferation or differentiation medium after 7 days of magnetic actuation compared with control cells (no SPION, no actuation).

4.3.5.4.4 The Effect of Magnetic Actuation on the Metabolic Activity of SPION-Loaded HRSMC

4.3.5.4.4.1 Measurement of Metabolic Activity-MTS/PMS

To investigate the metabolic activity of SPION-loaded HRSMC after 7 days of magnetic actuation, an MTS/PMS assay was performed. No difference was observed between SPION-loaded HRSMC incubated in proliferation medium for 24 hours compared with control cells (no SPION), as shown in Figure 4.20 a.

No difference was observed between SPION-loaded HRSMC incubated in proliferation medium after 7 days compared with control cells (no SPION) (Figure 4.20 b). There was a decrease in the metabolic activity of HRSMC incubated in differentiation medium for 7 days ($p<0.05$) compared with cells in proliferation medium (no SPION-control cells).

No difference was observed between SPION-loaded HRSMC incubated in differentiation medium after 7 days of magnetic actuation at 1 Hz or 2 Hz compared with control cells (no SPION, no actuation), as shown in Figure 4.20 b.

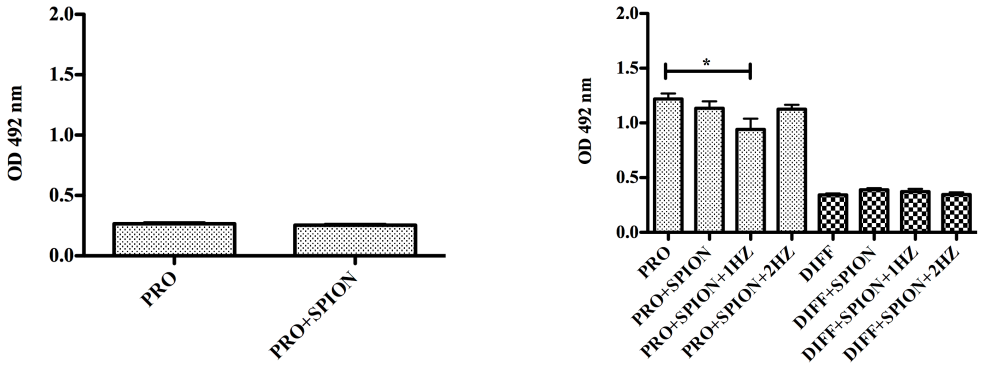

(a) (b)

Figure 4.20 The Effect of Magnetic Actuation on the Metabolic Activity of SPION-Loaded HRSMC Following Magnetic Actuation. (a) No difference in metabolic activity was observed between SPION-loaded HRSMC after 24 hours compared with control cells (no SPION, no actuation). (b) No difference was observed between SPION-loaded HRSMC incubated in proliferation medium after 7 days compared with control cells (no SPION). (b) A significant decrease in the metabolic activity of actuated SPION-loaded cells in proliferation medium after 7 days ($p<0.05$) compared with control cells (no SPION, no actuation). No change was observed between SPION-loaded HRSMC in differentiation medium after 7 days of magnetic actuation compared with control cells (no SPION, no actuation).

4.3.6 Biocompatibility of Magnetic Actuation on SPION-Loaded HRSMC

4.3.6.1 Reactive Oxygen Species in SPION-Loaded HRSMC Following Magnetic Actuation

The release of reactive oxygen species from cells incubated with SPION was investigated by measuring the production of a fluorogenic marker, 5-(and-6)-carboxy-2′,7′-dichlorodihydrofluorescen diacetate (carboxy-H2 DCFDA). The amount of green colour product produced by the assay is directly proportional to the production of reactive oxygen species within the cells. To induce cell apoptosis, tert-butyl hydroperoxide (TBHP) was used (Figure 4.21 c).

Fluorescence microscopy did not detect the release of reactive oxygen species in SPION-loaded HRSMC (Figure 4.21 b) incubated in proliferation medium for 24 hours. This was similar to control cells (no SPION), as shown in Figure 4.20 a.

SPION-loaded cells incubated in proliferation (Figure 4.22 b) or differentiation medium (Figure 4.22 f) for 7 days did not produce reactive oxygen species compared with control cells (no SPION), as shown in Figure 4.22 (a, e).

Similarly, SPION-loaded cells incubated in proliferation (Figure 4.22 c, d) or differentiation medium (Figure 4.22 g, h) with 7 days of magnetic actuation did not produce reactive oxygen species compared with control cells (no SPION, no actuation), as shown in Figure 4.22 (a, e).

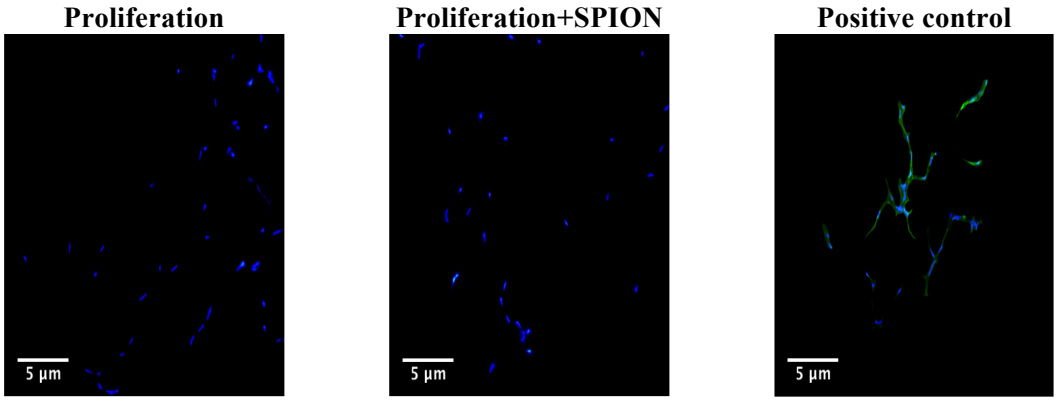

Figure 4.21 Fluorescence Microscopy Images from the Reactive Oxygen Species Assay in SPION-Loaded HRSMC after 24 Hours. (b) No change in staining was observed in SPION-loaded cells incubated with proliferation medium for 24 hours compared with control cells containing no SPION (a). (c) The positive control clearly showed detection of reactive oxygen species by the assay.

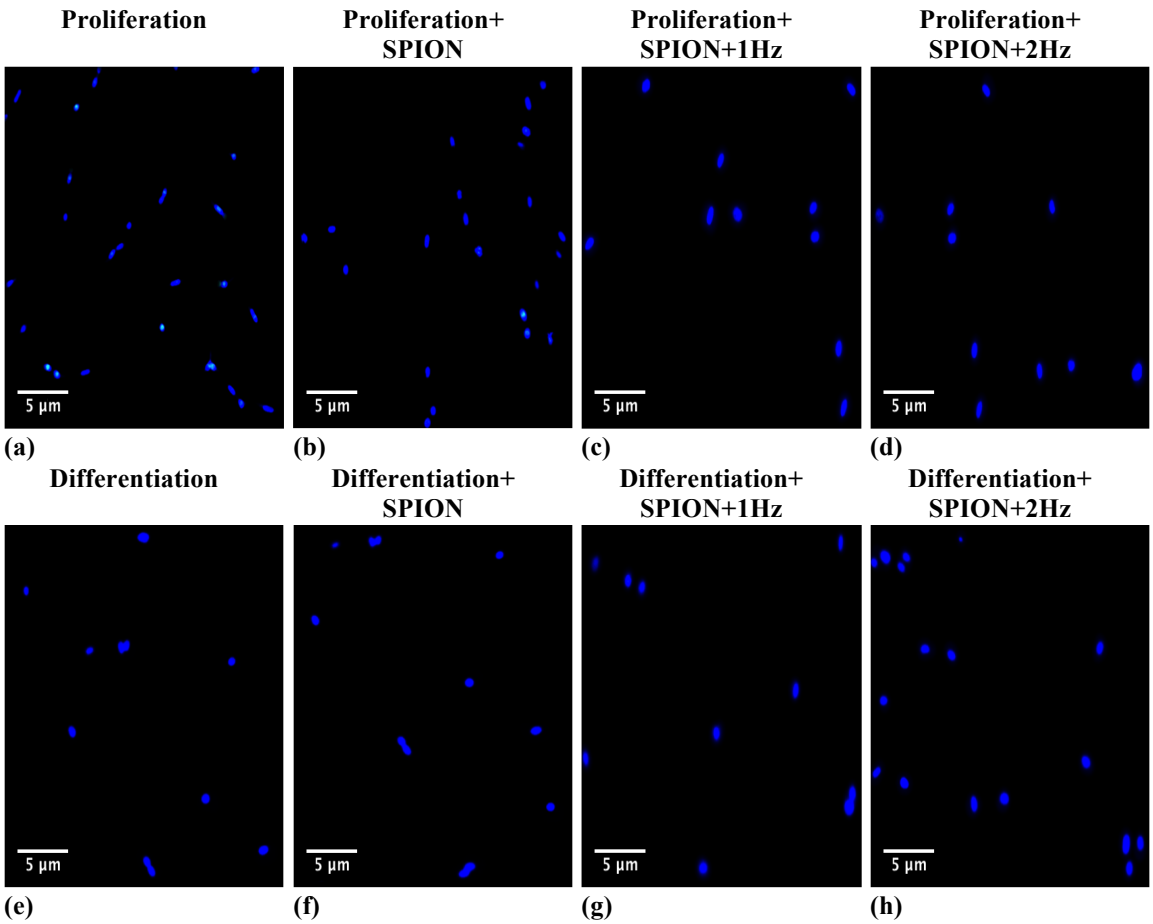

Figure 4.22 Fluorescence Microscopy Images Showing the Production of Reactive Oxygen Species in SPION-Loaded HRSMC Incubated in Proliferation and Differentiation Medium for 7 Days with Magnetic Actuation. No change was observed in SPION-loaded HRSMC incubated with proliferation (b) or differentiation medium (f) for 7 days compared with control cells (a+e) (no SPION). No change was observed in SPION-loaded HRSMC incubated with proliferation (c+d) or differentiation medium (g+h) and magnetic actuation for 7 days compared with control cells (a+e) (no SPION, no actuation).

4.3.6.2 Cell Toxicity of SPION-Loaded HRSMC Following Magnetic Actuation

The cytotoxic effect of SPION-loaded HRSMC incubated with proliferation or differentiation medium with exposure to magnetic actuation (1 Hz or 2 Hz) for 7 days was investigated by measuring cellular release of LDH. No difference was observed between SPION-loaded HRSMC incubated in proliferation medium for 24 hours compared with control cells (no SPION), as shown in Figure 4.23 (a).

A positive control (PC) was used in this study. HRSMC incubated with a lysis solution (provided with the kit). The lysis solution lyses the cell membrane resulting in the maximum production of LDH in the supernatant (100% toxic). The detailed process was described in sections 2.2.5.2.1 and 4.2.2.7.2.1.

No significant difference was observed between SPION-loaded HRSMC incubated in proliferation medium with or without 7 days of magnetic actuation at 1 Hz and 2 Hz compared with control cells (no SPION, no actuation). The positive control had increased 20% as shown in Figure 4.23 (b). No significant difference was observed between SPION-loaded HRSMC incubated in differentiation medium with or without 7 days of magnetic actuation at 1 Hz and 2 Hz compared with control cells (no SPION, no actuation), as shown in Figure 4.23 (b). The positive control (PC) had increased approximately 60% for the SPION-loaded HRSMC in proliferation medium and 20% for the SPION-loaded HRSMC in differentiation medium.

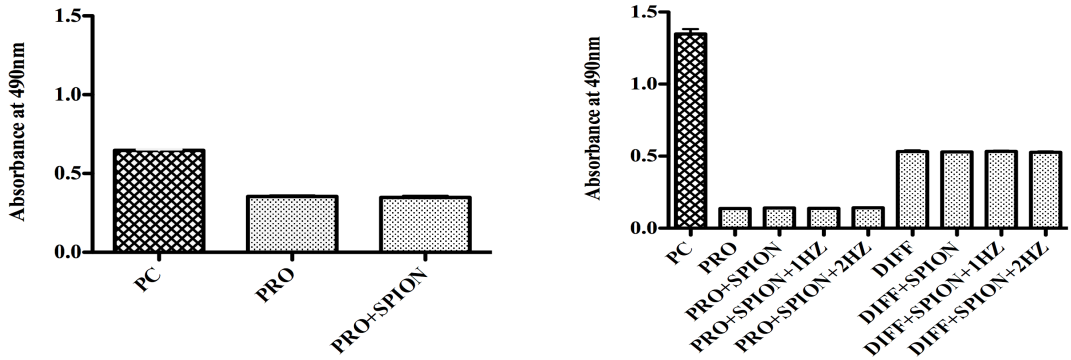

(a) **(b)**

Figure 4.23 LDH Release in the Supernatant from SPION-Loaded HRSMC Following Magnetic Actuation. (a) No change was observed between SPION-loaded HRSMC after 24 hours compared with control cells. There was an 20% increase in the release of LDH release (positive control) compared to control and SPION-loaded cells (b) No change was observed between SPION-loaded HRSMC in proliferation or differentiation medium with or without magnetic actuation for 7 days and control cells (no SPION). The was an apparent increase in the release of LDH in the supernatant in the positive control (PC)

4.3.6.3 Cell Apoptosis in SPION-Loaded HRSMC Following Magnetic Actuation

The effect of magnetic actuation apoptosis of SPION-loaded HRSMC incubated in proliferation or differentiation medium for 7 days with magnetic actuation was investigated by measuring the release of Caspase-3/7 in the tissue culture supernatant. No difference was observed between SPION-loaded HRSMC incubated in proliferation medium for 24 hours compared with control cells (no SPION), as shown in Figure 4.24 (a).

No difference was observed between SPION-loaded HRSMC incubated in proliferation or differentiation medium for 7 days compared with control cells (no SPION), as shown in Figure 4.24 (b). Similarly, no difference was observed between SPION-loaded HRSMC incubated in proliferation or differentiation medium with 7 days of magnetic actuation at 1 Hz and 2 Hz compared with control cells (no SPION, no actuation), as shown in Figure 4.24 (b).

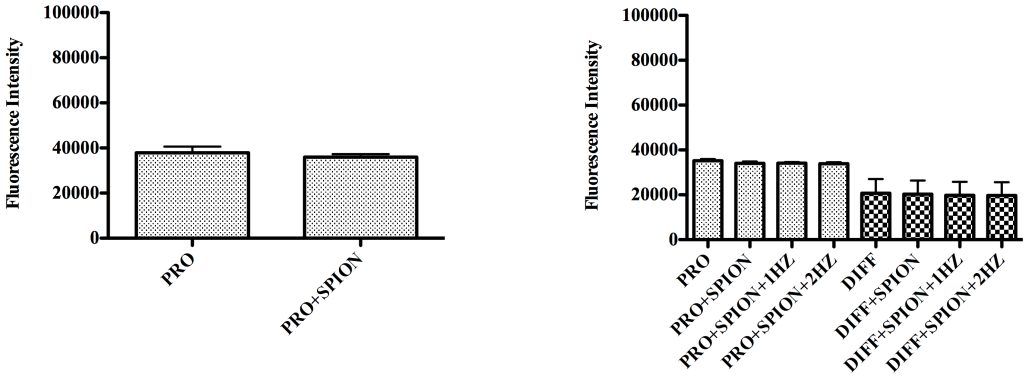

(a) (b)

Figure 4.24 Caspase 3/7 Release in the Supernatant from SPION-Loaded HRSMC Following Magnetic Actuation. (a) No change was observed between SPION-loaded HRSMC after 24 hours compared with control cells (no SPION). (b) No change was observed between SPION-loaded HRSMC incubated in either proliferation or differentiation medium for 7 days compared with control cells (no SPION). (b) No change was observed between SPION-loaded HRSMC incubated in either proliferation or differentiation medium after 7 days of magnetic actuation compared with control cells (no SPION, no actuation).

4.4 Discussion

4.4.1 Main Findings

- A magnetic actuator was devised to deliver magnetic force to HRSMC. The actuator was designed to deliver cyclic strain to HRSMC (continuous cycles of stretching-relaxation).
- SQUID measurements revealed that incubation of SPION-loaded HRSMC with differentiation medium for 7 days resulted in a similar average amount of iron per cell to that measured on day 1 (pre-actuation-control). However, the average amount of iron per cell for SPION-loaded HRSMC incubated in proliferation medium was reduced.
- TEM images of SPION-loaded HRSMC after magnetic actuation did not show any substantial movement of the SPION-loaded endosomes.
- Incubation of HRSMC with differentiation medium for 7 days caused up regulation of gene and re-localization of protein expression of different contractile proteins actin or calponin. No significant difference was observed with proliferation medium.
- The aspect ratio of HRSMC incubated in differentiation medium for 7 days was increased confirming the previous findings and suggesting that HRSMC were differentiated.
- Loading HRSMC with SPION inhibited the up regulation of actin and calponin genes caused by incubation in differentiation medium with control cells. No apparent change was observed in the protein expression of the same markers.

- Magnetic actuation did not change the inhibition of calponin up regulation caused by pre-loading cells with SPION before incubation in differentiation medium.
- Incubation of SPION-loaded HRSMC in proliferation or differentiation medium and with magnetic actuation did not affect the proliferation of HRSMC.
- Incubation of SPION-loaded HRSMC in proliferation or differentiation medium with magnetic actuation did not have any effect on the biocompatibility of HRSMC.

4.4.2 Magnetic Actuation of HRSMC

The effect of magnetic actuation on the phenotype and biocompatibility of SPION-loaded HRSMC was investigated using an *in vitro* model. HRSMC were incubated with 250 μg/ml of SPION in proliferation and differentiation medium and exposed to magnetic actuation for 1 hour per day at 1 Hz and 2 Hz for 7 days as described in more detail in section 4.2.2.3. The magnetic actuator designed for this study contained two-neodymium iron boron permanent magnets positioned in opposite directions with a steel block attached to the back in order to push the magnetic field forward as shown in Figure 4.1 a, b. The magnetic actuator was designed in such a way to give a cyclic strain to the cells by rotating 360 degrees with the help of a motor at different frequencies (1 Hz and 2 Hz). As the magnetic cylinder rotated the magnetic field changed from a high value to a lower value it was hypothesized this would create continuous cycles of cell stretching by moving the SPION-loaded endosomes or 'magnetosomes' (described in chapter 3). The physical movement of the SPION-loaded endosomes was proposed to stretch the cytoskeletal components such as actin filaments and microtubules and create a phenotypic change to the cells such as proliferation or

contraction. The type of cyclic mechanical stretching proposed in this study is different from the mechanical stretching caused by the Flexcell® unit. In this case the cells were seeded onto elastic membranes where continuous cycles of cyclic strain were applied to the cell. The external signal (cyclic strain) was received from different mechanoreceptors such as integrins located on the plasma membrane and translated into biochemical signal as described in section 1.7.2. This is summarized in the following diagram:

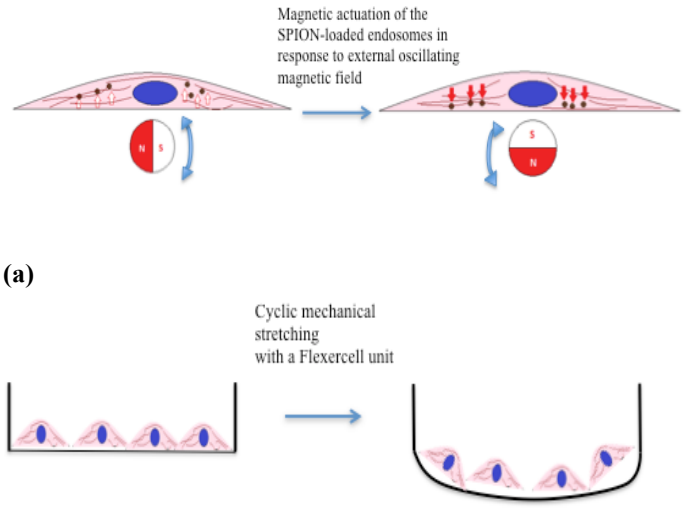

Figure 4.25 Different Types of Delivering Cyclic Strain to the Cells. (a) The cytoskeleton of cells is stretched in response to the movement after SPION-loaded endosomes after being magnetically actuated. **(b)** Continuous cyclic strain on cells using a Flexcell unit.

Having proposed a mode of action it was important to calculate the strength of the magnetic field produced by the actuator and also the theoretical amount of force per SPION inside the cells. The distance from the centre of the device to the bottom of the plate was 14 mm (which is approximately equivalent to the target anatomical distance in the anal canal as shown in Figure 1.1). The magnetic field and force plots showed that as the magnet rotated from 0 degrees to 180 degrees (farthest from the plate) the magnetic field and the magnetic force became weaker. At 0 degrees the magnetic field acting on the particles was 82 mT and the magnetic force 0.9 pN and at 180 degrees the

magnetic field dropped to 0 mT and the magnetic force was dropped to 0.1 pN as shown in Figure 4.5 and Figure 4.6.

The force per cell is influenced by the position of the magnet (0 degrees or 180 degrees), the amount of SPION internalised by the cells and also the position of the SPION-loaded HRSMC related to the magnetic actuators.

SQUID magnetometry was used to quantify the amount of SPION internalised. SPION-loaded HRSMC (250 μg/ml of SPION) were incubated with proliferation or differentiation medium for 7 days (SPION-loaded HRSMC-250 μg/ml of SPION in proliferation for 24 hours/pre-actuation was used as control). The results showed that each SPION-loaded HRSMC incubated for 7 days in proliferation medium had on average approximately 6 pg of SPION and in differentiation medium 16 pg of SPION, which was approximately the same amount of SPION measured in cells at day 1 pre actuation, as shown, in Figure 4.9 a. This is probably because SPION-loaded HRSMC in proliferation medium had divided and increased in number from 10,000 cells (day 1 pre actuation control) to 60,000 cells at day 7, whereas SPION-loaded HRSCM in differentiation medium had not proliferated, resulting in a similar number of cells to that on day 1 pre-actuation control, as shown, in Figure 4.9 b.

Based on the field plots the magnetic field had its highest value directly above of the magnets. To measure this directly, a visualization experiment was conducted using iron filings. The results showed the majority of the iron filings were positioned exactly above the magnet (0 degrees) where the magnetic field has its highest value as shown in Figure 4.7 a. Therefore in order for the cells to receive the maximum force they had to be located directly above the magnetic actuator. To achieve this, silicone moulds were designed as described in section 4.2.1.2 with a diameter of 17.5 mm to fit a 6 well

culture plate. Assuming that the HRSMC were seeded directly above the magnetic actuator with the help of the silicone moulds where the magnetic field had it highest value, the force per cell could be computed. The SQUID results indicated that the amount of SPION in the cells decreased over time when incubated with proliferation medium for 7 days. Therefore, the amount of force delivered per cell by the magnetic actuator was also likely to decrease over time. For example, on day 1 (pre-actuation control) the cells had 16 pg of SPION per cell. When the magnetic actuator was positioned at 0 degrees the force per cell was ~14.4 pN, but after 7 days of incubation with proliferation medium, the cells had 6 pg of SPION per cell. Therefore at the same position the force per cell was reduced to ~5.4 pN (0.9 pN x 6 pg of SPION/cell = 5.4 pN). However, when the HRSMC were cultured in differentiation medium for 7 days the amount of SPION inside the cells did not change. Therefore at 0 degrees the force per cell was ~14.4 pN which was the same as day 1. These results suggest that SPION-loaded HRSMC incubated with proliferation medium for 7 days did not receive the same magnetic force through out the incubation period. This is because the cells were continuously proliferating and the SPION became distributed amongst the progeny as the cells divided. On the other hand SPION-loaded HRSCM incubated in differentiation medium for 7 days maintained the amount of SPION and the force per cell also remained unchanged.

The non-uniform application of magnetic force per cell when SPION-loaded HRSMC were incubated with proliferation medium for 7 days could explain the results of fact no significant change in the phenotype of SPION-loaded HRSCM compared with cells incubated in differentiation medium, where a decrease in calponin mRNA expression was observed as will be described in more detail in section 4.4.4.

4.4.3 Cellular Localisation of SPION After Magnetic Actuation

In chapter 3 it was demonstrated by TEM that SPION were endocytosed by HRSMC and were located inside the endosomes or 'magnetosomes'. This chapter aimed to investigate whether movement of SPION (SPION-loaded endosomes) occurred in response to magnetic actuation. A different technique was used in this chapter to that described chapter 3. SPION-loaded-HRSMC monolayers were incubated with proliferation medium for 24 hours and then cells were exposed to magnetic actuation for 1 hour at 1 Hz at 37^0C, 5% CO_2. The monolayers processed for TEM were lifted with propylene oxide rather than detached with trypsin and pelleted, which allowed the visualisation of the attached cell morphology. The images revealed no significant change in the position of the SPION-loaded endosomes compared with non-actuated control cells as shown in Figure 4.10 a. The lack of movement of SPION-loaded endosomes might be explained due to the cytoskeleton being packed with organelles, making the movement of SPION-loaded endosomes difficult. Alternatively, and also the amount of SPION internalised may not have been enough to create a significant change in the movement of SPION-loaded endosomes. Thus, the movement of SPION-loaded endosomes may not have been significant enough to be captured with TEM. The limitations of this study were investigated in more detail in Chapter 5, where scanning electron microscopy (SEM) allowed the visualisation of the changes in the plasma membrane in response to an external magnetic field and also the movement of the SPION-loaded endosomes together with changes on the plasma membrane were captured with live cell imaging.

4.4.4 Effect of Magnetic Actuation on the Phenotype of SPION-Loaded HRSMC

Previous studies have used magnetic actuation to manipulate the phenotype of stem cells. In these studies no direct incubation of SPION with the cells were involved but a plasma membrane receptor of interest was magnetically tagged. An example is a study by Hu *et al* who examined the possibility of controlling the differentiation of stem cells by mechanically activate the PDFG receptor α and β of human bone marrow stromal cells (HBMSCs) with a lab based magnetic bioreactor. The objective of the study was to identify whether magnetic fields applied to nanoparticle bound PDGF receptors could promote smooth α-actin expression (SMA) up-regulation in HBMSC. Magnetic particles with a diameter of 250 nm (Micromod) were conjugated with anti-human PDGF-α and β antibodies (R&D Systems). The conjugated particles were incubated with cells and force was applied to them. The protein levels of SMA were estimated using immunocytochemistry. There was an increase in protein levels after 3 hours of continuous magnetic actuation and 24 hours further incubation of cells stimulated via PDGFRα compared with untreated cells. Additionally by performing real time PCR there was an up regulation of SMA mRNA levels after 3 hours of continuous magnetic actuation and 24 hours further incubation of cells stimulated via PDGFRα compared with untreated cells (93). Similarly Glossop *et al* investigated the differentiation of mesenchymal stem cells using magnetic actuation. Mechanical forces specifically uniaxial tensile strain versus magnetic particle forces were used to investigate the expression profile of mitogen-activated protein kinase kinase 8 (MAP3K8) and interleukin-1β (IL-1B). Human bone marrow-derived MSCs were seeded onto a pronectin coated uniflex flexible-bottomed six well plate (Flexcell International) and exposed to a 3% cyclic uniaxial tensile strain using a FX-4000T bioreactor (Flexcell International). Concurrently MSCs were incubated with 250 nm SPION (Nanomag-

silica; Micromod) and an oscillating magnetic field was applied of 90 mT with the use of a magnetic force bioreactor. Mechanical forces were applied for 1 hour at 1 Hz and cells treated with a static magnetic field used as control. The results showed no change in the mRNA expression of MAP3K8 and IL-1B both for mechanical stimulation and magnetic actuation. One of the limitations of the study highlighted by the authors was the short period of the study (24 hours) when the group concluded that there was a possibility that cells did not respond to mechanical or magnetic actuation as they have previously demonstrated that MSCs cells do respond to fluid shear stress with an up regulation of MAP3K8 and IL-1B (107).

In the current study, after determining the amount of force acting on HRSMC incubated with SPION as the magnetic actuator rotated and also the amount of SPION per cell (in either proliferation or differentiation medium), the effects of SPION-loaded HRSMC in response to magnetic actuation on the phenotype was investigated. This was conducted with real time PCR, where the expression of different contractile markers such as actin, myosin heavy chain, calponin and caldesmon and also proliferative markers such as vimentin and tropomyosin 4 were investigated. Immunocytochemistry and fluorescence microscopy, was used to examine the expression of different contractile markers such actin, myosin heavy chain, caldesmon and calponin were investigated. Measurement of the aspect ratio of SPION-loaded HRSCM in response to an external field and measuring the proliferation of SPION-loaded HRSMC after magnetic actuation using four different techniques (BrdU ELISA, cell CyQUANT, direct cell count and MTS/PMS) were also performed.

HRSMC were incubated with 250 μg/ml of SPION in proliferation medium for 24 hours and then switched to differentiation or proliferation medium for 7 days, whilst receiving exposure to magnetic actuation as described in section 4.2.2.3. Two types of

controls were used: i) HRSMC without SPION and no actuation, incubated with proliferation or differentiation medium for 7 days, and ii) SPION-loaded cells incubated with proliferation medium for 24 hours, included as a pre-actuation control.

HRSMC incubated in differentiation medium for 7 days, resulted in an increase in actin and calponin protein expression (Figure 4.13 a, e) suggesting a shift in the phenotype from a proliferative towards a contractile. The images revealed that the differentiated cells had a different more elongated shape compared with HRSMC in proliferation medium for 7 days as showed in Figure 4.12 a, e. Also there was an increase in the mRNA expression of actin and calponin when HRSMC incubated in differentiation medium for 7 days as shown in Figure 4.15 a, d. The changes in the morphology and the phenotype observed with fluorescent microscopy and real time PCR were confirmed with the aspect ratio experiment where the width of a cell was measured against its length. HRSMC incubated in differentiation medium for 7 days had a greater aspect ratio compared with HRSMC incubated in proliferation medium (control cells) ($p<0.001$) (Figure 4.16 b). The study has confirmed previous findings in the literature where TGF- β was used to differentiate smooth muscle cells (160).

SPION-loaded HRSCM in differentiation medium alone (Figure 4.13 b, c) and with magnetic actuation (1 Hz and 2 Hz) (Figures 13 c, g, d, h) showed no change in the protein expression or gene expression compared with their control cells. This might be accounted by the cells being insufficiently differentiated and required further incubation in differentiation medium before analysis. Previous studies have mentioned that caldesmon is considered an intermediate differentiation marker and myosin heavy chain is considered as a late differentiation marker in comparison actin and calponin which are early differentiation markers (85).

This finding partly corresponds with a previous mechanical study using a Flexcell unit which demonstrated that aortic smooth muscle cells when subjected to cyclic strain at a frequency of 30 cycles/minute and 15% elongations showed no expression of smooth muscle myosin and calponin but an increase in h-caldesmon was observed from immunostaining images, suggesting that mechanical strain induced the differentiation of smooth muscle cells (161). Similarly in another study, airway smooth muscle cells subjected to mechanical strain, pre-coated with collagen type I in six-well plates (Flexcell®, McKeesport, PA) were subjected to 10% membranes deformation for 2 seconds followed by 2 seconds of relaxation for 12 days. Myosin light chain kinase content was increased as shown by Western blotting (162).

The expression of the proliferative markers vimentin and tropomyosin 4 were not affected by either proliferation or differentiation medium, nor with magnetic actuation as shown in Figures 4.14. For these markers an increase in the mRNA expression was expected when HRSMC were incubated in proliferation medium. Further investigation is necessary to confirm these findings.

SPION-loaded HRSMC incubated in differentiation medium (Figure 4.13 b, f) for 7 days and with the addition of magnetic actuation (Figure 4.13 c, g, d, h) showed an increase in actin and calponin expression compared to SPION-loaded HRSCM in proliferation medium (Figure 4.12 b, f) for 7 days and with the addition of magnetic actuation (Figure 4.12 c, g, d, h) but no apparent differences were observed when compared with control HRSMC in differentiation medium for 7 days without SPION as shown in Figure 4.13 a, e. Additionally, a significant decrease in the mRNA expression of actin and calponin of SPION-loaded HRSMC in differentiation medium was observed compared with proliferation control cells as shown in Figure 4.12 a, d. A significant decrease in mRNA expression of calponin SPION-loaded HRSMC in

differentiation medium with magnetic actuation at 1 Hz was observed compared with proliferation control cells as shown in Figure 4.12. These results correspond with the aspect ratio findings where SPION-loaded HRSCM in differentiation medium and exposed to magnetic actuation at 2 Hz showed a decrease in the aspect ratio compared with control cells (no SPION, no actuation) (Figure 4.16 b). Finally, SPION-loaded cells incubated in proliferation medium and exposed to magnetic actuation at 2 Hz showed a significant increase in the aspect ratio compared with control cells (no SPION, no actuation; $p<0.05$) (Figure 4.16 b).

The decrease in the aspect ratio (Figure 4.16 b) and the mRNA expression observed in actin (Figure 4.15 a) for SPION-loaded HRSMC in differentiation medium and calponin (Figure 4.15 d) for SPION loaded in differentiation medium and with magnetic actuation suggested that maybe SPION are inhibiting the differentiation process of HRSMC and shifting them towards a more proliferative phenotype. Therefore the effect of magnetic actuation on proliferation on SPION-HRSMC was investigated with four different techniques (BrdU ELISA, CyQUANT cell proliferation, direct cell counts and MTS/PMS assay) as shown in Figures 4.17, 4.18, 4.19, 4.20.

The results showed no change in the proliferation of SPION-loaded HRSMC in differentiation medium after 7 days of magnetic actuation with none of the four different cell proliferation assays.

The decrease in the mRNA expression of actin and calponin of SPION-loaded HRSMC observed could be caused by SPION interference of the SMAD genes in the TGF-β signalling pathway. A previous study suggested that when HeLa cells were loaded with 2 mg ml^{-1} magnetite (Fe3O4) nanocrystals (MNC) 26 nm in diameter for 12 hours there

was a 4 fold down regulation of the mRNA of ID1, ID2 and SMAD6 compared to ID3 and SMAD7 as shown with real time PCR (163).

The oscillating magnetic field used in this study did not induce a change in cell proliferation when cells were incubated with proliferation or differentiation medium. However, different studies have demonstrated an increase in cell proliferation using static magnetic field (SMF). In a previous study where a SMF was used, human keratinocytes (HaCaT) were incubated with 15 mg/ml of SPION and exposed to SMF of 0.5 mT and 30 mT (cells were 4 mm above the magnet surface) for 24 hours. Control samples with no SPION and with/without SMF were investigated. The results showed an increase in cell proliferation (10-15%) in the SMF samples loaded with SPION suggesting that SMF affect the proliferation of SPION-loaded cells. The combination of SPION-loading and SMF increased the cell proliferation 60-fold in both 0.5 mT and 30 mT (164). However, the previous finding contradicts with another study, where mouse liver cell line (NCTC 1469) was incubated with 0.5 mM of SPION ferucarbotran (SHU 555A, Resovist) and the cells were exposed to a SMF of 0.4 T using permanent neodymium magnets. A cell viability/proliferation assay was used which measured the intracellular ATP concentration. The results showed a reduction of cell viability/cell proliferation after concomitant treatment with SPION and SMF exposure (75%) after 1 hour of exposure. The reduction in the viability/cell proliferation was proportional to the time of treatment and SPION concentration and duration of SMF exposure (142).

Other studies using a Flexcell unit have demonstrated a change in cell proliferation when the cells were subjected to cyclic strain. Aortic smooth muscle cells from embryonic rats (A10 cell line) were seeded on type I collagen pre-coated membranes and subjected to 5% elongation with the Bioflex membrane and 24% elongation with

the Flexercell membrane for 1 second followed by a 1 second relaxation of the membrane at 0.5 Hz frequency for 48 hours. The results showed that cell proliferation was reduced, with both techniques suggesting that cyclic strain affected the proliferation of cells and was independent of the cellular matrix (165). This finding contradicts the findings of another study where bovine airway smooth muscle cells were seeded onto pre-coated surface of laminin or type I collagen Flexcell plates (Flexcell, McKeesport, PA, USA) and subjected to a 4% cyclical deformation (this stretch amplitude is similar to that encountered by smooth muscle cells during quiet tidal breathing in a healthy individual). An increase in cell proliferation was observed in cells grown on a collagen surface under static conditions compared with cells grown on a laminin surface with the addition of 4% cyclic deformation. This study suggested that type I collagen encouraged the proliferation of cells regardless of mechanical activation (89). Additionally, vascular smooth muscle cells (VSM) were stretched with two different devices that delivered stretch along one axis (uniaxial) or along all axes (equiaxial). The Flexercell Strain Unit (FX-3000, Flexcell) and Bioflex were used to expose VSMC to an equiaxial or uniaxial cyclic stretch of 10% magnitude and a frequency of 1 Hz. The VSMC were quiescent for 48 hours in serum-free media (FCS replaced by 0.1% BSA) before exposure to the experimental treatments. The cell proliferation was investigated with direct cell counts. The results showed that a physiological level of cyclic stretch inhibits vascular SMC proliferation (166)

Based on the previous findings, it is evident that SMF or mechanical activation can affect the proliferation of cells. In this study the oscillating magnetic field used did not affect the proliferation of cells or their differentiation. Further investigation is necessary in order to understand what was responsible for this. Stronger magnetic fields or perhaps SMF could be investigated in a future study. Additionally, the amount

of magnetic material per cell could be increased by incubating the cells with higher concentration of SPION or using a larger diameter of SPION (above 200 nm). One disadvantage is that SPION-loaded HRSMC in proliferation medium did not maintain the same amount of SPION per cell throughout the 7 days incubation period and that affected the force acting on the cells as well. One way to overcome this limitation is to would be to deliver a sufficient amount of magnetic material in the area of interest that is going to be biocompatible but not biodegradable and will not be distributed with cell division. In this study, HRSMC were seeded on a rigid surface that does not provide a good simulation of the mechanical properties of tissue *in vivo*. Based on previous studies seeding cells on elastic membranes with the Flexcell unit that affected the cell proliferation and differentiation. Future studies could use HRSMC seeded on elastic membranes before subjecting them to the same oscillating magnetic field used in this study.

4.4.5 Biocompatibility of Magnetic Actuation on SPION-Loaded HRSMC

After investigating the effects of magnetic actuation on the phenotype of SPION-loaded HRSMC the biocompatibility of magnetic actuation on SPION-loaded HRSMC was investigated.

Fluorescence microscopy did not detect the release of reactive oxygen species in SPION-loaded HRSMC incubated in proliferation or differentiation medium after 7 days of incubation and with magnetic actuation as shown in Figure 4.22 b, c, d, f, g, h compared with control cells (Figure 4.22 a, e).

The toxic effect of SPION and magnetic actuation was investigated with an LDH assay. No difference was observed between SPION-loaded HRSMC incubated in proliferation medium for 24 hours compared with control cells (no SPION), as shown in Figure 4.23

(a). Also No significant difference was observed between SPION-loaded HRSMC incubated in proliferation medium with or without 7 days of magnetic actuation at 1 Hz and 2 Hz compared with control cells (no SPION, no actuation). The positive control had increased 20% as shown in Figure 4.23 (b). No significant difference was observed between SPION-loaded HRSMC incubated in differentiation medium with or without 7 days of magnetic actuation at 1 Hz and 2 Hz compared with control cells (no SPION, no actuation), as shown in Figure 4.23 (b). The positive control (PC) had increased approximately 60% for the SPION-loaded HRSMC in proliferation medium and 20% for the SPION-loaded HRSMC in differentiation medium.

Apoptosis of HRSMC was investigated using a Caspase 3-7 assay. No difference was observed in the fluorescence intensity values between SPION-loaded HRSMC in proliferation or differentiation medium after 7 days and with magnetic actuation compared with control cells (no SPION, no actuation), as shown in Figure 4.24 b.

Incubation of SPION-loaded HRSMC in differentiation medium alone did not affect the apoptosis of cells. Previously it has been described that SPION loading interfered with SMAD genes responsible in the TGF-β signalling pathway. The effect of apoptosis was investigated by quantifying the expression of CASP9 (a gene responsible for apoptosis) on HeLa cells loaded with 2 mg ml^{-1} magnetite (Fe3O4) nanocrystals (MNC) 26 nm in diameter for 12 hours. The results showed a down regulation of CASP9 activity suggesting that SPION-loading caused cell apoptosis (163).

Results from the current study suggest that the oscillating magnetic field used did not affect the viability of SPION-loaded HRSMC. This differs to other studies investigating the effect of SMF on the biocompatibility of different types of cells. In a previous study where SMF was used, human keratinocytes (HaCaT) were incubated with 15 mg/ml of SPION and exposed to SMF of 0.5 mT and 30 mT (cells were 4 mm

above the magnet surface) for 24 hours. The ROS were investigated in response to SMF with a ROS-fluorescent probe dichlorofluorescin diacetate. The results showed an increase in the production of ROS compared with control cells by approximately 15–20%. ROS production was measured 24 h after the introduction of combinations of SPION and SMF. Additionally, the apoptosis was investigated by looking at the gene expression of the profile of different genes such as CASP10 and TNFSF10 that are responsible for the apoptosis of cells. The results revealed no change for the no SPION no SMF treated cells but SPION-loaded HaCaT with SMF showed a 2 fold and 3 fold increase in the mRNA expression of these genes suggesting that SPION-loading and SMF caused apoptosis to the cells (164).

Similar findings were observed in another study where the cytotoxicity, apoptosis and ROS were investigated in response to a SMF. Mouse liver cell line cells (NCTC 1469) were incubated with 0.5 mM of SPION ferucarbotran (SHU 555A, Resovist) and were exposed to a SMF of 0.4 T using permanent neodymium magnets. The apoptosis was measured based on the Caspase 3-7 release using a Caspase-3/7 Glo assay and the necrosis/cytotoxicity by measuring the activity of LDH released from membrane damaged cells using the CytoTox-ONE Homogeneous Membrane Integrity assay and the ROS was evaluated by spectrofluorometry and fluorescence microscopy using the ROS-detectable cell-permeable reagent 5-(and-6)-carboxy-20, 70-dichlorodihydrofluorescin diacetate (carboxy-H2 DCFDA). The results showed an increase in apoptotic activity relative to the concentration of SPION whereas necrotic activity was only marginally changed by SMF exposure. An increase in the formation of reactive oxygen species was observed (142).

Other studies using a Flexcell unit have demonstrated a change in the biocompatibility when the cells were subjected to cyclic strain. Aortic smooth muscle cells from

embryonic rats (A10 cell line) were stretched and cell damage/cytotoxicity and apoptosis measured. No significant change in cell damage or necrosis was observed and also the apoptosis rate was similar between stretched cells and control cells (165). In the previous study the apoptosis or toxicity was not affected but in another study, vascular smooth muscle cells were exposed to an equiaxial or uniaxial cyclic stretch of 10% magnitude and a frequency of 1 Hz resulting in a change in caspase-3 activity with stretch vs static controls (166).

4.4.6 Conclusion

A magnetic actuator was devised in an attempt to deliver force to HRSMC in a cyclic manner. SQUID measurements revealed that SPION-loaded HRSMC in proliferation medium after 7 days of incubation had approximately 3 times less SPION compared with control cells. SPION-loaded HRSMC in differentiation medium maintained the amount of SPION throughout the incubation period. An increase in the mRNA expression and protein localization of HRSMC in differentiation medium was observed suggesting that cells had shifted towards a differentiated phenotype. The aspect ratio findings confirmed the previous results.

SPION-loaded HRSMC alone and with magnetic actuation in differentiation medium showed a decrease in the mRNA expression for actin and calponin expression suggesting that the cells were maintained towards a proliferative phenotype. However, this finding was not confirmed with cell proliferation assays. Magnetic actuation of SPION-loaded HRSMC did not affect the biocompatibility of cells.

The magnetic actuation results from the study need further investigation because they might not have been optimal for achieving magnetic actuation of cells. For example, the strength of the magnets used, their orientation, and the frequency of the oscillating

magnets are all parameters that need further investigation. Based on the current results, the amount of SPION was reduced after 7 days, therefore the force per cell was not constant. This issue could be overcome by using a different type of magnetic material to achieve long-term actuation, such as different SPION that are not lost from the cells.

Chapter 5

Membrane Deformation of SPION-Loaded HRSMC in Response to an Externally Applied Magnetic Field

5.1 Introduction

There are several ways to induce mechanical stretching in cells. One way to achieve this is with a FlexCell system, where the cells are seeded onto an elastic membrane and stretched using an applied vacuum (161). Magnetic actuation has been achieved by tagging magnetically specific mechanoreceptors of interest on the plasma membrane and then applying magnetic force to them, resulting in a biochemical effect by stretching the specific receptor (167-170). In Chapter 4 a novel technique was described for delivering strain to cells previously loaded with SPION using a magnetic actuator. It was hypothesized that the cells loaded with SPION inside the endosomes would be actuated towards an externally applied magnetic field, causing a stretching effect to the cytoskeleton of cells. However, TEM analysis suggested that SPION internalized by HRSMC located inside the endosomes did not undergo any observable movement to the externally applied magnetic field. In this chapter, deformation of the plasma membrane of SPION-loaded HRSMC by an externally applied magnetic field was investigated using scanning electron microscopy (SEM) and live-cell imaging.

5.2 Materials and Methods

5.2.1 Materials

5.2.1.1 Magnets

Permanent magnets were used to investigate the effect of delivering a magnetic field to cells loaded with SPION. Four circular neodymium-iron-boron magnets (NdFeB; N42; MagnetSales, UK) with dimensions 16 mm x 5 mm (Figure 5.1 a) and magnetized through their thickness were stacked with opposing poles facing each other and mounted on top of a rectangular plastic box with dimensions 60 mm x 30 mm. The

distance between the top of the magnets to the bottom of the plate was 5 mm (Figure 5.1 b).

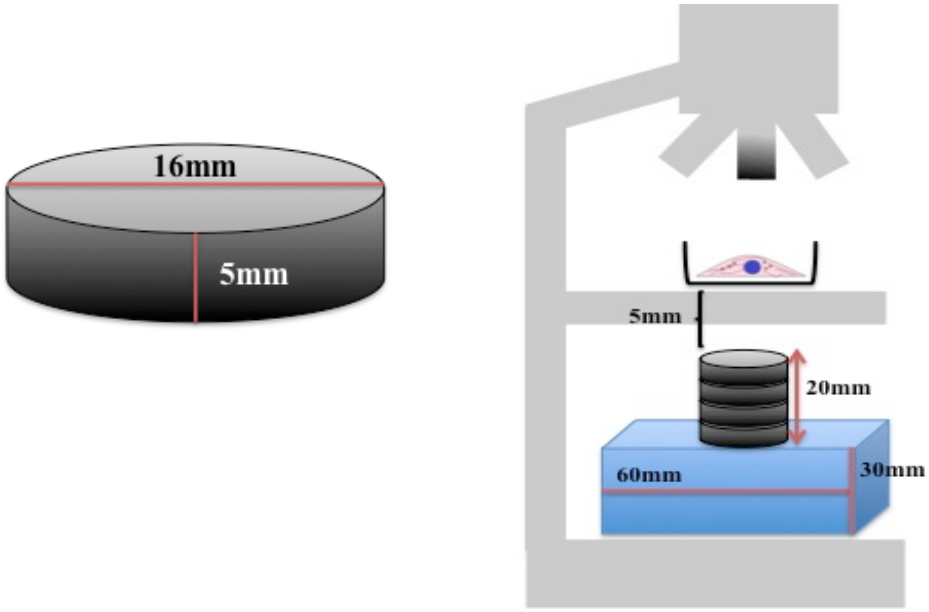

(a) **(b)**

Figure 5.1 Dimensions of the Magnets and the Rectangular Mounting Box Used to Apply the External Magnetic Field to Cells.

5.2.1.2 SPION

Two types of SPION were investigated in these experiments:

- SPION (fluidMAG-UC/A anionic charged SPION; 50 nm particles with a magnetite core suspended in water with a stock concentration of 25 mg/ml and particle density of ~$1.3x10^{16}$ particles/g; Chemicell GmbH, Berlin, Germany).
- SPION (fluidMAG-UC/A anionic charged SPION; 200 nm particles with a magnetite core suspended in water with a stock concentration of 25 mg/ml and particle density of ~ 2.2×10^{14} particles/g; Chemicell GmbH, Berlin, Germany).

5.2.1.3 Confocal Microscope

A Leica SP2 AOBS laser scanning confocal microscope (Leica Microsystems Ltd, UK) was used to image membrane deformation in response to the external magnetic field.

The condenser beneath the stage of the microscope was removed to create space for the magnets to be introduced manually, as shown in Figure 5.2.

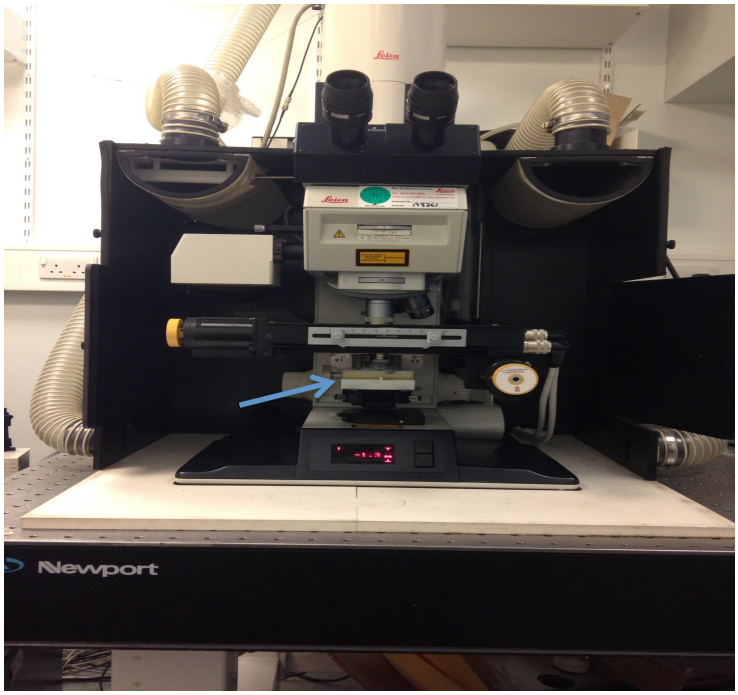

Figure 5.2 Leica SP2 AOBS Laser Scanning Confocal Microscope. The condenser was removed so the magnets could be manually inserted under the microscope as indicated by the arrow.

5.2.2 Methods

5.2.2.1 Computer Modelling of Magnetic Fields Produced by the Magnets

Finite element modelling was used to model the magnetic field and magnetic force produced by the oscillating magnetic actuator described in this chapter. The modelling was performed by Mr George Frodsham (Department of Biochemical Engineering, University College London, London and Institute of Biomedical Engineering, University College London).

Finite element modelling with Opera-3D (Version 12; Vector Fields, UK) was used to calculate the strength of the magnetic field produced by the magnets. The distance from

the centre of the magnets (with assigned co-ordinates x=0, y=0, z=0) to the base of the tissue culture plate was 5 mm. (Figure 5.1 b).

The force produced by the magnets on each SPION particle in the cells was calculated using mathematical software (MATLAB, MathWorks, Natick, MA, U.S.A), from which the net magnetic force per cell was calculated. For all calculations, the direction of the force was assumed to be downward.

The force acting on each particle was between 1.8 - 2.0 pN 0.9 pico Newton (pN). The calculations were made assuming each SPION was 200 nm diameter, had a density 1.25 g/cm^3 and mass of 6.545x10^{-4} pg. Therefore, if the HRSMC were loaded with 100 pico grams of magnetic material the force acting on a cell was:

$$1.8 \times 10^{-10}\text{N (180-200 pN)}$$

5.2.2.2 Live Cell Imaging of SPION-Loaded HRSMC Exposed to a Magnetic Field

Live cell imaging was used to investigate membrane deformation of SPION-loaded HRSMC in response to the externally applied magnetic field.

(i) 2x10^4 HRSMC were seeded in a 25 cm^2 cell culture flask (Nunclon^{TM} Delta surface, Denmark) and incubated for 24 hours at 37^{0}C, 5% CO_2.

(ii) The medium was removed and experimental (proliferation) medium containing 250 μg/ml of SPION (50 nm or 200 nm) was added and incubated at 37^{0}C, 5% CO_2 for 24 hours.

(iii) After the incubation period, the medium was removed and the cells were washed 5x with 5 ml of PBS.

(iv) 1 ml of trypsin-EDTA was added to each flask and incubated at 37^{0}C, 5% CO_2 for 1 minute.

(v) 5 ml of fresh media was added in each flask and the detached cells were collected in a 30 ml container.

(vi) Samples were centrifuged at 1000 rpm for 5 minutes, the supernatant was removed and the pellets were re-suspended in 1ml of fresh media.

(vii) A cell count was performed and 100,000 cells were extracted and transferred into a 35 mm FluoroDish cell culture dish (World precision Instruments, USA) and incubated at 37^0C, 5% CO_2 for 24 hours.

(viii) The medium was removed and the cells were incubated with 1 µl of CellMask™ Deep Red Plasma membrane Stain (1:2000 in culture medium) (Life Technologies, USA) for 1 hour at 37^0C, 5% CO_2 in order to visualise the plasma membrane of the cells.

(ix) The solution was removed and the cells were washed 3x with 1 ml of PBS.

(x) The cells were placed in an upright confocal microscope Leica SP2 AOBS Laser Scanning Confocal (Leica Microsystems Ltd, UK) where the condenser was removed previously to create space for the stack of magnets to be introduced manually.

(xi) Phase contrast microscopy was used to capture the movement of SPION particles inside the cells and the fluorescently labelled plasma membrane was imaged at 649 nm excitation and 666 nm emission.

(xii) 185 individual images overall were acquired (1 image every 1.62 seconds) over a period of 300 seconds. At t=30 seconds, the magnets were manually introduced beneath the microscope stage at distance of 40 mm below the base of the cell culture dish. The magnets were steadily raised over a period of 20 seconds until they were at a distance of 5 mm below the base of the cell culture dish. The magnets were held in a steady position for a total of 220 seconds

underneath the cell culture dish then lowered initially to 40 mm below the base of the cell culture dish for 20 seconds before being finally removed. Images were acquired for a further 40 seconds after the magnet was removed.

5.2.2.3 Quantification of Membrane Deformation and SPION Movement

Image J (Image Processing and Analysis in Java, National Institute of Health, USA) was used to quantify changes to the position of the membrane and SPION movement in response to the applied external magnetic field. For HRSMC loaded with 200 nm SPION, the movement of the magnetic particles and the plasma membrane was recorded in a 5-minute movie clip, which resulted in 185 images (1 image every 1.62 seconds). For HRSMC loaded with 50 nm SPION, the movement of the magnetic particles and the plasma membrane was recorded in a 5-minute movie clip, which resulted in 89 images (1 image every 3.37 seconds).

For the analysis, the movement of the plasma membrane and SPION were analysed separately. Each of the acquired images in the movie clip was converted to black and white. This led to the appearance of clusters of SPION particles within each image, which were used to quantify bulk movement. Each cluster in the frame was assigned a number that was kept the same for each image. The central point of each numbered cluster was assigned an x and y location coordinate within the image.

To calculate the overall distance moved by the cluster of SPION particles and the plasma membrane in each image after magnetic actuation relative to their starting location (x, y coordinate), a set reference point at the base (B) of the cell in the image (Bx, By) was subtracted from each cluster (C) coordinate (Cx, Cy). It was observed from the video clips that there was also movement of the SPION and plasma membrane clusters in both axis X and Y. Therefore the displacement of the SPION and plasma

membrane clusters relative to the cell base was calculated for X and Y axes separately, as summarized in Figure 5.3. Limitations with the software used meant it was not possible to follow individual clusters of SPION during the movie clip. Therefore, the average movement of all the clusters relative to a set reference point per image was calculated for all images acquired in the movie clips. The average movement of SPION clusters per image was then plotted against time and changes caused by magnetic actuation compared with SPION-loaded cells exposed to no magnetic actuation.

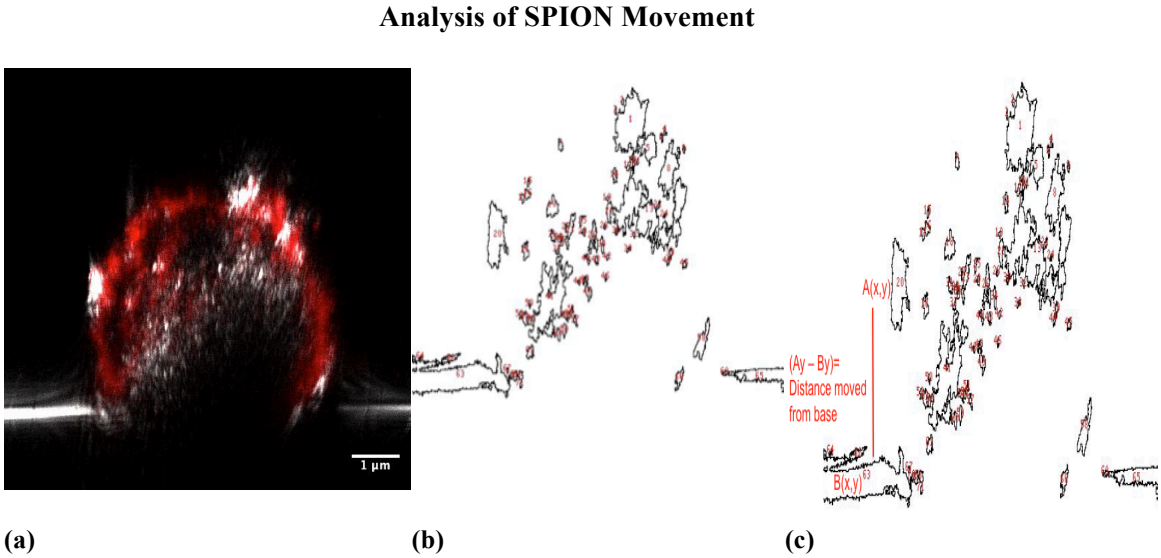

Figure 5.3 Analysis of SPION and Plasma Membrane Movement. (a and c) A single HRSMC with the plasma membrane stained red using the Cell Mask dye. The white specks in the cell are caused by refractance of the SPION particles. Movement of the plasma membrane and SPION clusters were analyzed separately. (b, d) Each image underwent thresholding to

create a black and white image with the cluster of particles and plasma membrane outlined. Each cluster was numbered and the x, y coordinate of the center of the cluster recorded. (c and e) The distance moved by the plasma membrane or cluster from a set base position was calculated for each image.

5.2.2.4 Scanning Electron Microscopy of SPION-Loaded HRSMC after Magnetic Actuation

Scanning electron microscopy (SEM) was used to investigate morphological changes to the membrane of SPION-loaded HRSMC in response to an external magnetic field.

(i) Steps i- vi from section 5.2.2.2 were followed for this experiment.

(ii) A cell count was performed and 50,000 cells were extracted and transferred in a 24 well plate (Nunclon^{TM} Delta treated, Denmark).

(iii) Cells were incubated for 24 hours at 37^0C 5% CO_2.

(iv) After the incubation period the stack of 4 magnets was placed under the plate for 1 hour.

(v) After 1 hour of static exposure the supernatant was removed and 1 ml of 2% paraformaldehyde + 2.5% gluteraldehyde in 0.1M cacodylate buffer, pH 7.2 was added to fix the cells inside a fume cupboard for 10 minutes.

(vi) The fixative was removed and the samples were washed 2x with 1 ml of PBS.

(vii) The samples were post fixed with 2% osmium tetroxide (OsO_4) (Ceimig Limited, UK) for 1 hour inside a fume cupboard.

(viii) The samples were dehydrated in a progressive series in water/ethanol mixtures:

a. 25% v/v ethanol 4 minutes
b. 50% v/v ethanol 4 minutes
c. 75% v/v ethanol 4 minutes
d. 95% v/v ethanol 4 minutes

e. 100% v/v ethanol 4 minutes (the last step was repeated 5 times).

(ix) The samples are carefully mounted on an aluminium stub using silver paint and then introduced into the chamber of the sputter coater and coated with a very thin film of gold\palladium for its examination under a JSM-7500F Scanning Electron Microscope (JEOL, USA).

5.2.2.5 Quantification of Cellular Loading with SPION

5.2.2.5.1 Superconducting Quantum Interference Device (SQUID)

SQUID magnetometry was used to measure the amount of SPION in each cell as described in 4.2.2.

(i) Steps i- vi from section 5.2.2.2 were followed for this experiment.

(ii) Steps vii-xi from section 2.2.2.1 were followed for this experiment.

5.2.2.6 Cell Viability Assays

5.2.2.6.1 Cytotoxicity Assay - LDH Assay

(i) 2 x 10^4 HRSMC were seeded in a 25 cm^2 cell culture flask (Nunclon^{TM} Delta surface, Denmark) and incubated for 24 hours at 37^0C, 5% CO_2.

(ii) The medium was removed and experimental (proliferation) medium containing 250 μg/ml of SPION (50 nm or 200 nm) was added and incubated at 37^0C, 5% CO_2 for 24 hours.

(iii) After the incubation period the medium was removed and the cells were washed 5x with 5 ml of PBS.

(iv) 1 ml of trypsin was added to each flask and incubated at 37^0C, 5% CO_2 for 1

minute.

(v) 5 ml of fresh media was added in each flask and the detached cells were collected in a 30ml container.

(vi) Samples were centrifuged at 1000 rpm for 5 minutes, the supernatant was removed and the pellets were re-suspended in 1 ml of fresh media.

(vii) A cell count was performed and 10,000 cells were extracted and seeded in a 24 well plate (Thermo Scientific, Nunc, Fisher Scientific, UK).

(viii) The plate was incubated at 37^0C %, 5% CO_2 for 24 hours.

(ix) The stack of magnets described in section 6.2.1.1 were placed under the plate exerting a static field to the cells at 37^0C, 5% CO_2 for 1 hour.

(x) Supernatants of cells incubated with SPION (50 nm or 200 nm) for 24 hours were collected and transferred to a fresh 96 well plate (Thermo Scientific, Nunc, Fisher Scientific, UK) accordingly.

(xi) 50 µl of medium was removed and placed in a new well and 50 µl of the LDH assay reagents was added to each well and the plate was incubated in the dark at room temperature for 30 minutes.

(xii) 50 µl of stop solution was added to each well and the optical density of the reaction produced in the well was read with a plate reader Multiskan FC (Thermoscientific, UK) at 490 nm.

5.2.2.6.2 Cytotoxicity Assay (Positive Control)

(i) Steps i-ix from section 5.2.2.6.1 were followed for this experiment.

(ii) 10 µl of cell lysis solution (provided with the assay) per 100 µl was added to all the wells.

(iii) The cells were incubated for 45 minutes at 37^0C, 5% CO_2.

(iv) The plate was centrifuged at 250 x g for 4 minutes.

(v) Supernatants of cells incubated with SPION (50nm or 200nm) for 24 hours were collected and transferred to a fresh 96 well plate (Thermo Scientific, Nunc, Fisher Scientific, UK) accordingly.

(vi) 50 µl of medium was removed and placed in a new well and 50 µl of the LDH solution was added to each well and the plate was incubated in the dark for 30 minutes.

(vii) 50 µl of stop solution was added to each well and the optical density of the reaction product in the well was read with a plate reader Multiskan FC (Thermoscientific, UK) at 490 nm.

5.3. Results

5.3.1 Modelling of the Magnetic Field and Forces on SPION Loaded HRSMC

The field plots in Figure 5.4 show the magnetic field produced at the base of the tissue culture plate 5 mm from the centre of the device. At the edges of the magnet the magnetic field became weaker. In the centre of the magnet (red region) the magnetic field acting on the particles was 180 mT and at the edges the magnetic field dropped to 110 mT. The areas of the plot coloured red indicated the magnetic field had its highest value and those coloured blue had the lowest value.

The force plot shown in Figure 5.5 indicates that at the edges of the magnet the magnetic force also became weaker. In the centre of the magnet (red region) the magnetic force acting on the particles was 1.9 pN and at the edges the magnetic force dropped to 0.4 pN.

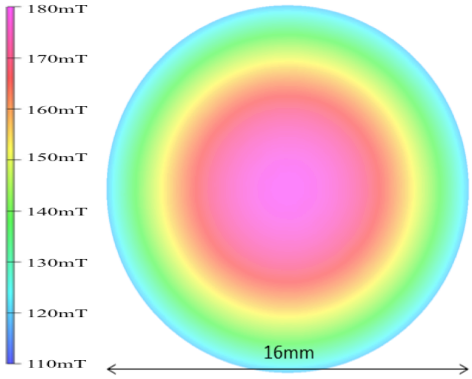

Figure 5.4 Magnetic Field Plots from the Magnets Used to Investigate HRSMC Deformation. In the centre of the magnet the magnetic field had its highest value of 180 mT. At the edges of the magnet the magnetic field had each weakest value of 110 mT.

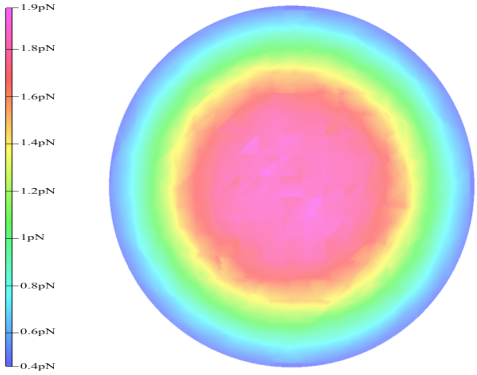

Figure 5.5 Magnetic Force Plots from the Magnets Used to Investigate HRSMC Deformation. In the centre of the magnet the magnetic force had its highest value of 1.9 pN. At the edges of the magnet the magnetic force had each weakest value of 0.4 pN.

5.3.2 Quantification of Cellular Loading with SPION

SQUID magnetometry was used to quantify the amount of SPION in HRSMC in proliferation medium. HRSMC loaded with 200 nm SPION, incubated in proliferation medium for a period of 24 hours contained approximately 100 pg of SPION. Previous SQUID measurements (Chapter 4) showed that HRSMC loaded with 50 nm SPION in in proliferation medium for 24 hours had approximately 16 pg of SPION.

5.3.3 Membrane Disruption to SPION-Loaded HRSMC Following Exposure to Magnets

5.3.3.1 Measurement of Lactate Dehydrogenase

Membrane damage to SPION-loaded HRSMC exposed to the magnets was investigated by measuring cellular release of LDH. HRSMC were incubated with SPION (50 nm or 200 nm) as described in section 5.2.2.2. A positive control (PC) was obtained by incubating HRSMC in lysis solution (provided with the kit). The lysis solution lyses the cell membrane resulting in the maximum production of LDH in the supernatant (100% toxic). The detailed process was described in sections 2.2.5.2.1 and 5.2.2.6.2. No significant change was observed between SPION-loaded HRSMC (200 nm) and control cells (no magnet) in Figure 5.6 a. Similar results were observed between SPION-loaded HRSMC (50 nm) and control cells (no magnet). The optical density of the positive control (PC) had approximately 30% increased for both experiments (200 nm and 50 nm) Figure 5.6 a+b.

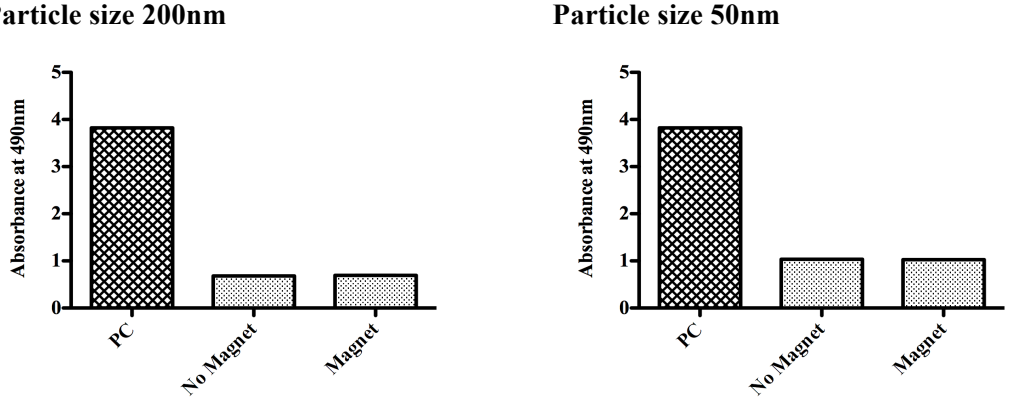

Figure 5.6 LDH Release in the Supernatant from SPION-Loaded HRSMC Following Magnetic Actuation. (a) No significant change was observed between the SPION-loaded HRSMC (200 nm) after exposure to a magnetic field compared with control cells (no magnet). (b) No significant change was observed between the SPION-loaded HRSMC (50 nm) after exposure to a magnetic field compared with control cells (no magnet). The was an apparent

increase in the release of LDH in the supernatant in the positive control (PC) for both experiments (a+b)

5.3.4 Morphological Changes to SPION-Loaded HRSMC in Response to an Externally Applied Magnetic Field

SEM was used to investigate deformation of SPION-loaded HRSMC membranes after exposure to the permanent magnets for 1 hour. HRSMC were incubated with SPION (50 nm in diameter) as described in section 5.2.2.2. Electron micrographs show the membranes of the SPION-loaded cells not exposed to the magnets had a similar appearance to non-loaded control cells. The membranes of SPION-loaded cells exposed to the magnets had many protrusions rising from the membrane surface.

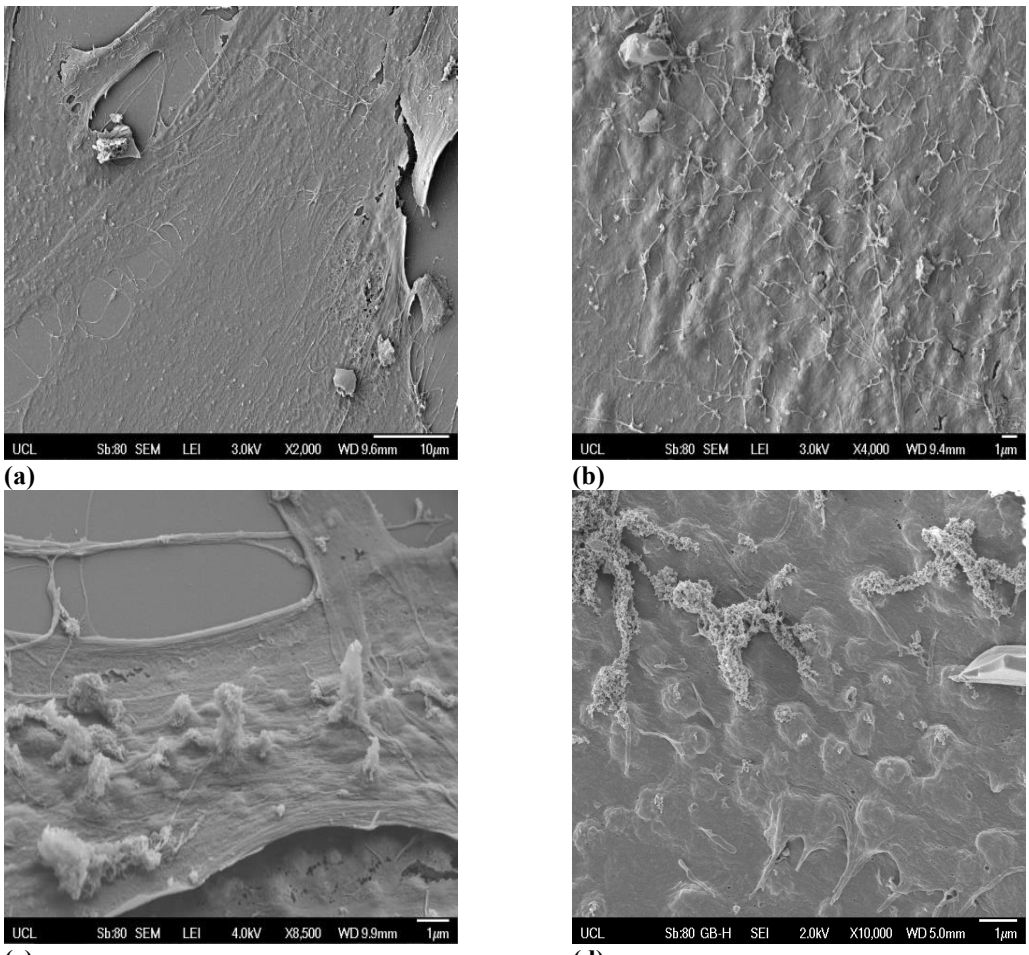

Figure 5.7 Scanning Electron Microscopy of SPION-Loaded HRSMC after Exposure to a Magnetic Fields for 1 Hour. (a) Control cells. (b) SPION-loaded cells without magnet

exposure. (c) SPION-loaded cells exposed to a magnet for 1 hour. (d) The protrusions observed on membrane of SPION-loaded cells exposed to a magnet were not uniformly distributed.

5.3.5 Quantification of Membrane Deformation and SPION Movement

Deformation of the cell membrane of SPION-loaded HRSMC and the clusters of internalized SPION following exposure to an externally applied magnetic field were investigated for both types of SPION (50 nm and 200 nm). HRSMC monolayers were incubated with 250 μg/ml of SPION (50 nm and 200 nm) as described in section 5.2.2.2.

Analysis of the acquired images rendered into movie clips revealed significant movement of the clusters of 200 nm SPION in the Y axis after the magnetic field was applied compared with control cells (no magnetic field; $p<0.001$; Figure 5.8 a and 5.9 a). The movement that occurred with the clusters of 50 nm SPION in the Y axis after the magnetic field was applied compared with control cells was smaller but also significant (Figure 5.8 c and 5.9 c; $p<0.001$).

There was significant movement of the plasma membrane in the Y axis for cells loaded with 200 nm SPION after the magnetic field was applied compared with control cells (no magnetic field; $p<0.001$; Figure 5.8 b and 5.9 b). Similarly, there was significant movement of the plasma membrane in the Y axis for cells loaded with 50 nm SPION after the magnetic field was applied compared with control cells (no magnetic field; $p<0.001$; Figure 5.8 d and Figure 5.9 d).

Analysis of the acquired images rendered into movie clips revealed significant movement of the clusters of 200 nm SPION in the X axis after the magnetic field was applied compared with control cells (no magnetic field; $p<0.00$; Figure 5.10 a and 5.11 a). The movement that occurred with the clusters of 50 nm SPION in the X axis after

the magnetic field was applied compared with control cells was smaller but also significant (Figure 5.10 c and 5.11 c; $p<0.001$).

There was significant movement of the plasma membrane in the X axis for cells loaded with 200 nm SPION after the magnetic field was applied compared with control cells (no magnetic field; $p<0.001$; Figure 5.10 b and 5.11 b). There was no significant movement of the plasma membrane in the X axis for cells loaded with 50 nm SPION after the magnetic field was applied compared with control (Figure 5.10 d and Figure 5.11 d).

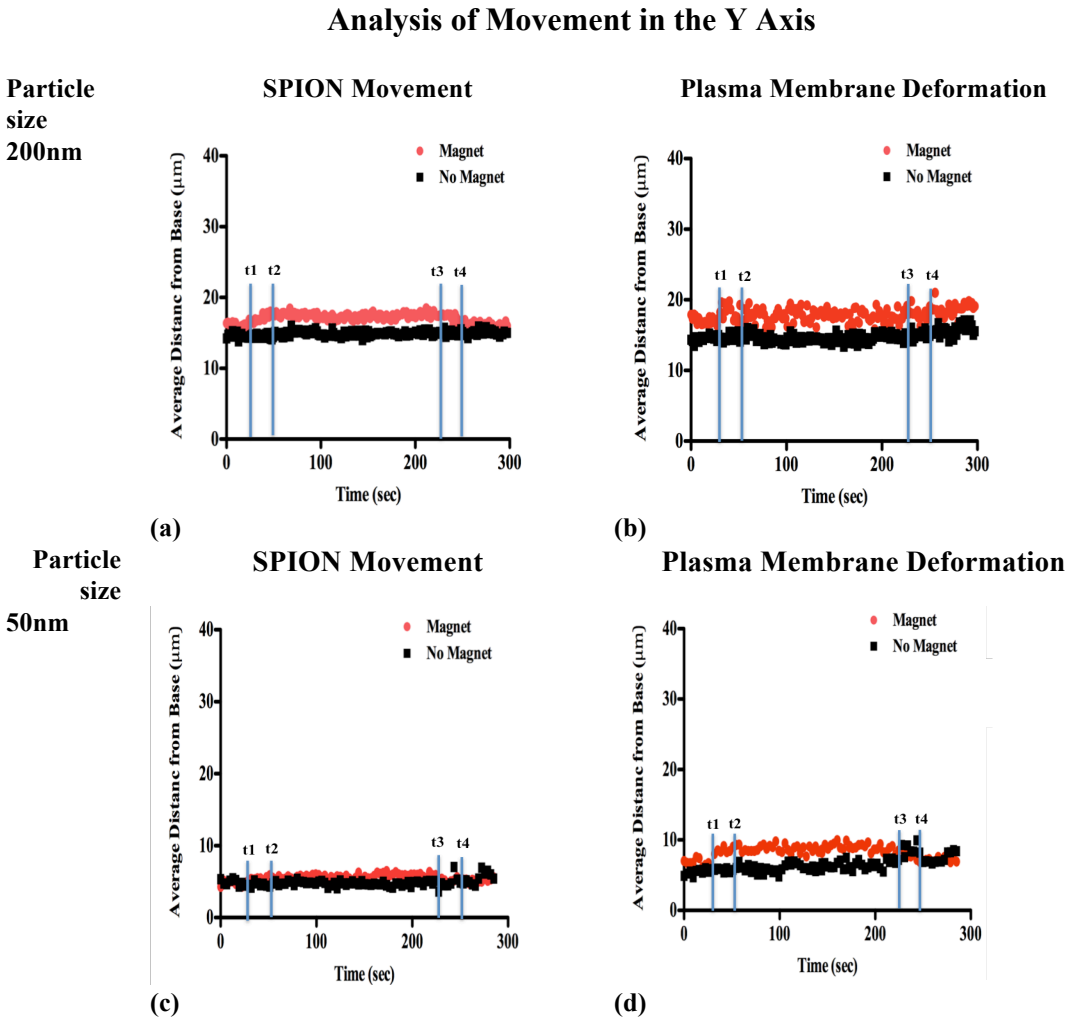

Figure 5.8 SPION (50 nm and 200 nm) and Plasma Membrane Movement in the Y-axis. t1 = 30 seconds-the time point at which magnets were manually introduced beneath the microscope stage at a distance of 40 mm below the base of the cell culture dish. t2 = The magnets were steadily raised over a period of 20 seconds until they were at a distance of 5 mm

below the base of the cell culture dish. t3 = The magnets were held in a steady position for a total of 230 seconds underneath the cell culture dish. t4 = The magnets were lowered initially to 40mm below the base of the cell culture dish for 20 seconds before being finally removed.

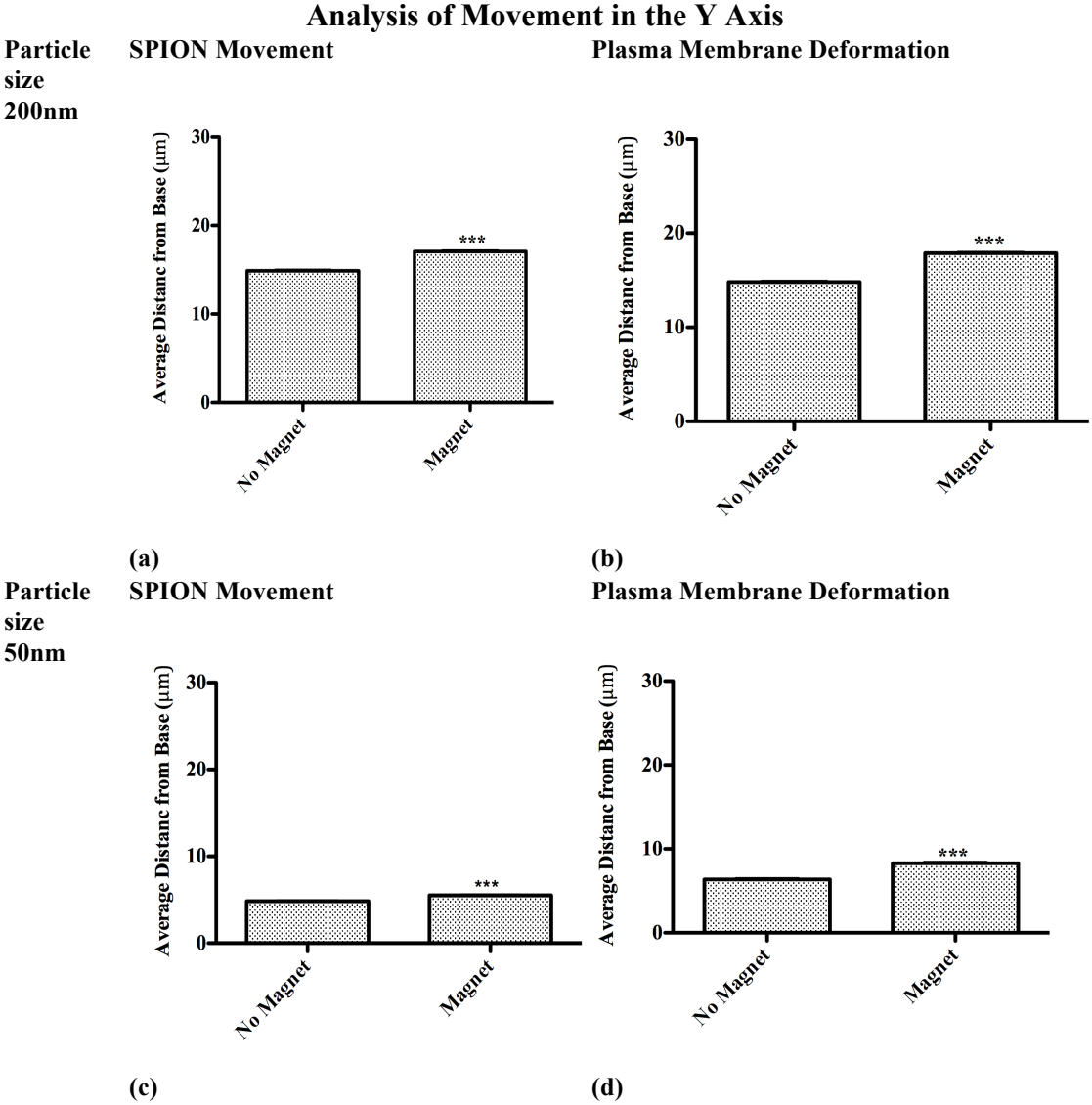

Figure 5.9 Statistical Analysis of SPION (50 nm and 200 nm) and Plasma Membrane Migration on the Y-Axis.

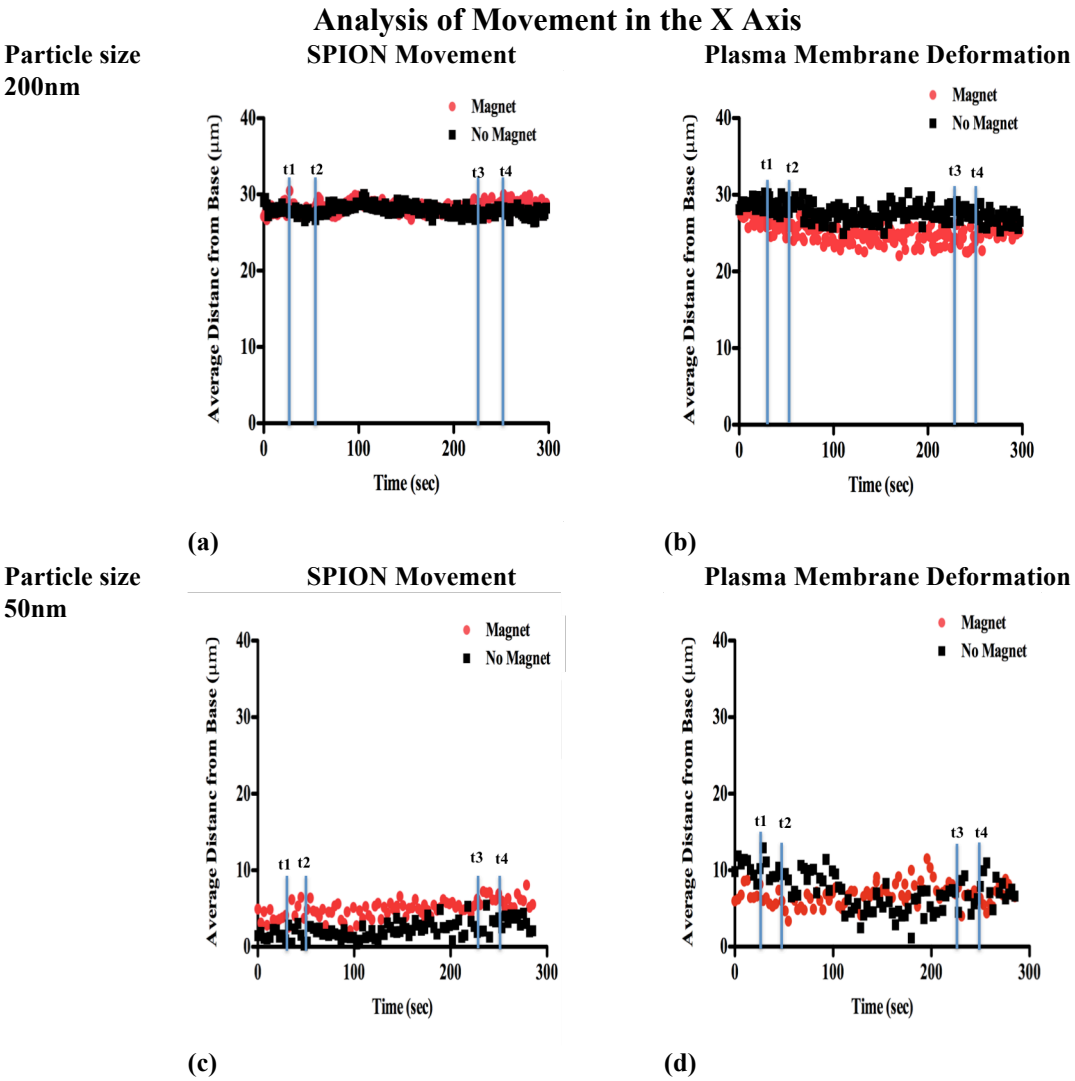

Figure 5.10 SPION (50 nm and 200 nm) and Plasma Membrane Migration on the X-Axis. t1 = 30 seconds, the magnets were manually introduced beneath the microscope stage at a distance of 40 mm below the base of the cell culture dish. t2 = The magnets were steadily raised over a period of 20 seconds until they were at a distance of 5 mm below the base of the cell culture dish. t3 = The magnets were held in a steady position for a total of 230 seconds underneath the cell culture dish. t4= The magnets were lowered initially to 40 mm below the base of the cell culture dish for 20 seconds before being finally removed.

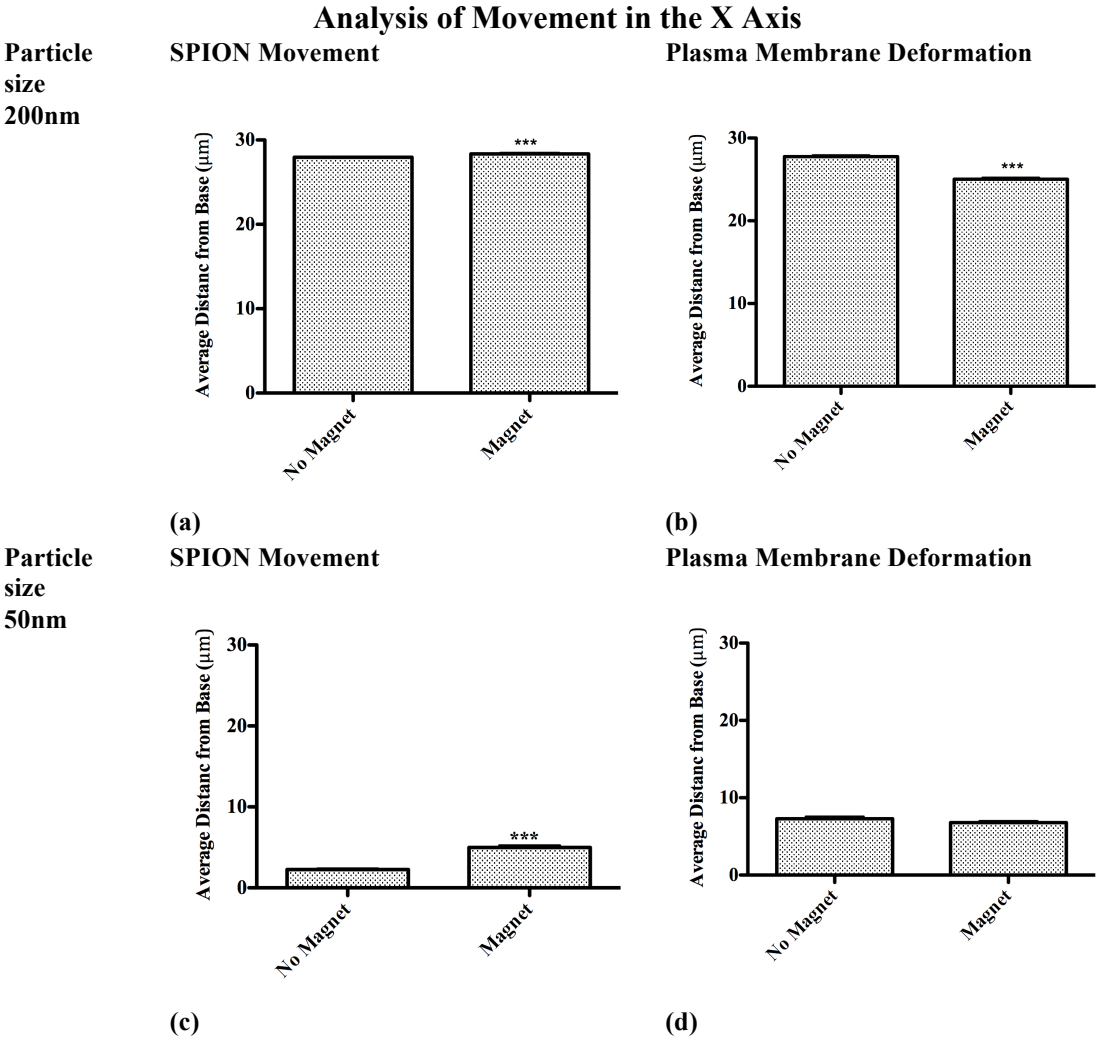

Figure 5.11 Statistical Analysis of SPION (50 nm and 200 nm) and Plasma Membrane Migration on the X-Axis.

5.4 Discussion

5.4.1 Main findings:

- HRSMC incubated with 200 nm SPION had approximately 100 pg of SPION internalized whereas HRSMC incubated with 50 nm SPION had approximately 16 pg after 24 hours of incubation.
- SEM images of HRSMC incubated with 50 nm SPION showed evidence of membrane deformation in response to an externally applied magnetic field.
- Live cell imaging analysis revealed that SPION movement and plasma membrane deformation were more prominent on the Y-axis (movement upwards) for 50 nm and 200 nm particles confirming the SEM results.
- Movement was observed the X-axis (movement sideways) by the plasma membrane for 200 nm particles. This suggests that the plasma membrane not only moved upwards but also sideways.

5.4.2 Magnetic Actuation of SPION-loaded HRSM and Membrane Deformation

In chapter 4, TEM was used to determine movement of the SPION-loaded endosomes. No movement was observed compared to non-actuated control cells. To explore this further, this chapter used SEM and live cell imaging.

Some important differences existed between the experiment in this chapter and those described in Chapter 4. HRSMC were incubated with 200 nm particles, resulting in a higher concentration of iron per cell. The amount of SPION per cell was 100 pg compared with 16 pg of SPION when HRSMC incubated with 50 nm diameter particles. The magnets used in this chapter also had a stronger magnetic field. Four neodymium-iron-boron (NdFeB) permanent disc magnets with dimensions 16 mm x 5 mm (Figure 5.1 b) were stacked together in order to increase the strength of the

magnetic field. Additionally the distance between the tissue culture plate was 5 mm compared to 14 mm with the magnetic actuator used in Chapter 4. Therefore the magnetic force applied per cell was significantly increased.

SEM was used to investigate the deformation of the cell membrane of SPION-loaded HRSMC (50 nm in diameter) and the clusters of internalized SPION following exposure to an externally applied magnetic field. The results showed that the membranes of SPION-loaded cells exposed to the magnets had many protrusions rising from the membrane surface for HRSCM incubated with 50 nm suggesting that SPION had pushed the plasma membrane resulting in a deformation.

Live cell imaging was used to observe changes in SPION movement or plasma membrane deformation. From the movie clips captured it was observed that SPION and the plasma membrane not only move in the Y-axis but also on the X-axis.

For the plasma membrane deformation there was a significant movement for both 50 nm and 200 nm in the Y-axis. Interestingly there was no change in the membrane movement on the X-axis for 50 nm but for 200 nm there was movement. This result showed that the deformation of the plasma membrane occurred in a negative quadrant and possibly the SPION-loaded endosomes pushed the plasma membrane in the opposite direction. Overall, for the 200 nm SPION movement occurred only in the Y-axis but plasma membrane movement occurred in both the Y-axis and X-axis. These findings suggest that the SPION not only pushed the membrane upward but also shifted it sideways, possibly causing a stretching effect. For 50 nm SPION, movement was observed on the X-axis suggesting that the SPION clusters moved sideways and not upwards, which is the opposite from what was observed with 200 nm SPION. Significant movement in the plasma membrane in the Y-axis was observed, suggesting

that even if the SPION move sideways and not upwards like the 200 nm, this movement was sufficient to cause a membrane deformation. The live cell imaging results confirmed the SEM findings, where the membranes of SPION-loaded cells exposed to the magnets had many protrusions appearing to rise from the membrane surface.

The SPION movement and the membrane deformation did not affect the viability of HRSMC. LDH data suggested that no membrane damage occurred in the SPION-loaded cells exposed to magnets for either both 50 nm and 200 nm of SPION.

A previous study described the deformation of SPION-loaded endosomes. Hela cells were incubated with 10 nM of cobalt ferrite nanoparticles ($CoFe_2O_4$) with a diameter of 10 nm. The particles were coated with negatively charged citrate ligands to ensure colloidal stability in aqueous suspension through electrostatic repulsions. Hela cells were incubated for 1 hour at 37^0C and the cell magnetophoresis assay revealed that the number of magnetic particles per cell was $1.1x10^7$ nanoparticles per cell. To observe endosome deformation TEM was used. The cells were exposed to a uniform magnetic field of 660 mT for 15 seconds. The results showed the magnetic endosomes were elongated and aligned in the direction of the magnetic field (171).

In another study similar findings were observed for SPION-loaded endosomes that were attracted to each other via dipole-dipole magnetic interactions and formed chains inside the cytoplasm along with the direction of the magnetic field, but this did not affect the architecture of actin filaments and microtubules (172). Magnetic tweezers have been used for manipulating small magnetic beads inside the cell cytoplasm in order to gain insight into the structural and mechanical properties of the cytoskeleton (173, 174). This allowed investigation of the intracellular dynamics, such as the

viscoelasticity of the cell interior. Granulocytes were incubated with magnetic beads (0.35 mm 1.05 mm) for 30 minutes. Each granulocyte phagocytosed a single bead which was moved between the 3 different poles of the magnetic tweezers in a cyclic manner. The granulocytes incubated with 1.05-mm beads experienced forces of 120 pN and granulocytes incubated with 0.35-mm beads experienced forces of 12 pN. Live cell-imaging experiments showed that beads could be manipulated through the interior of a cell. Magnetic beads with a diameter of 0.35 mm showed reduced elasticity and a 10-fold reduction in viscosity (3 Pa) compared with the 1.05 mm. The measured viscosity was 3 times greater than the viscosity of water. This was thought to have resulted because of the breaking of the cross-links within the cytoplasmic region (175).

In this study Image J analysis was used to analyse the SPION movement and membrane deformation. A limitation of using this technique was that SPION or plasma membrane had to be measured separately, which made the combined assessment more difficult. There are previous studies that have tried to manipulate cells with magnetic actuation (167) and mechanical studies using the Flexcell unit (170). These are likely to have created a cytoskeletal change but the studies did not describe how mechanical stimuli were transmitted into biochemical signals and if it was possible to visualize or quantify this.

To quantify intracellular changes in response to an external magnetic field, fluorescence energy transfer technology (FRET) imaging has been used. FRET is a popular imaging technique in order to label specific intracellular components (176, 177). Many studies have investigated mechanical or magnetic stimulation of cells using FRET and a Src reporter that allows the imaging and quantification of spatio-temporal changes upon activation of Src in living cells. It is known that Src regulate integrin-cytoskeleton interactions following mechanical stimuli. When integrins are

activated with a mechanical or magnetic signal, Src is associated with integrin via the SH3 domain and cause dissolution of actin stress fibres and the release of mechanical tensile stress.

Based on the FRET technology and the limitations encountered with the use of Image J in this chapter, a different approach to study the movement of could be used to study the effect of SPION movement and membrane deformation could be used. Microtubules are connected with endosomes with Rab5 protein (178, 179). A FRET green fluorescent protein (GFP)-Rab 5 could be developed for the visualisation of endosome and microtubule movement in response to an external magnetic field.

5.4.3 Conclusion

The findings from this chapter suggest that magnetic actuation of SPION-loaded HRSMC causes the plasma membrane to move upwards and sideways. This is likely to cause deformation of the cytoskeleton. Future studies will involve the use of FRET imaging and magnetic tweezers in order to explore the cytoskeletal changes in response to an external magnetic field.

Chapter 6

Thesis Conclusion and Future Work

6.1 Conclusion

Faecal incontinence is a debilitating condition that affects a big percentage of the population (6-9). Is defined as an alteration of the faecal passage where the patient experiences involuntary loss of flatus, liquid or solid faecal contents(1, 2). People who suffer from faecal incontinence have a consequence in their quality of life by avoiding activities such as shopping, go to the cinema, dinning with friends or family are some examples. Furthermore they hesitate to disclose their conditions to friends or to a health professional, which scales up the severity of their problem.

There are a number of treatment options for people who suffer from faecal incontinence. Depends on the severity of their situation, treatments can be classified as non-invasive such as biofeedback, minimally invasive such as bulking agents and finally invasive procedures such as surgery, sacral nerve stimulation and artificial anal sphincter.

Biofeedback as conservative treatment is a reliable treatment, which could improve the quality of life but only in the short term. In addition to people who suffer from severe faecal incontinence are not benefiting from this treatment (55) (56) (44).

In patients with faecal incontinence in whom conservative treatment fails different options are incorporated such as bulking agent. Bulking agents have been used to narrow the anal canal and consequently to help retain stool (4, 48). The use of these agents is considered a minimally invasive treatment for incontinence (46). Several injectable materials have been tried such as carbon-based, silicone particles, collagen agents, autologous fat, none have been shown to provide long-term efficacy. If the condition of the patient has not been improved at this stage, further invasive procedures will be incorporated. (48).

When conservative or minimally invasive procedures fails then invasive procedures need to be incorporated such as dynamic graciloplasty, an artificial anal sphincter, and sacral nerve stimulation. Sacral nerve stimulation greatly improves continence and quality of life does not have long-term functional improvement. (61) (62) (65). Similar result shave been observed with dynamic gracioplasty (71) (72). Patients subjected to ASS implantation showed Early infection and rectal erosion, together with difficulty in evacuating and mechanical failure (67) (68). If none of the previous treatments have been successful, aggressive surgery such as colostomy needs to be incorporated. Colostomy does not restore sphincter function but permits bowel evacuation and allows the patient to return to a normal life (6) (73) (74).

New regenerative medicine therapies are still at very early stage. They involve regenerating the sphincter tissue with the injection of stem cells(76) (77) or the complete replacement of a 3D bioengineered sphincter (78). Regenerative medicine approaches hold a great promise, however the studies conducted require further investigation. More research is necessary to be conducted in order to be safe for clinical applications.

The current magnetic stimulation therapies involve a Magnetic Anal Sphincter (MAS), it is a promising new technique, however, the results are not very conclusive and the number of patients is very low. Also there is no study investigating the long-term effects (79) (80).

Therefore, there is still a need for developing new technologies or interventions to improve faecal incontinence. This will help incontinent people to reach a normal level of faecal continence. Ideally new interventions should use minimal or non-invasive and cost effective methods that people can easily access.

Previously human cardiac stem cells have been regulated mechanically with a Flexcell system. Mechanical strain was applied with 60 cycles per minute and 120% elongation (stretching conditions that mimic the heart rate and 20% fractional shortening). Non-stretched cells were used as controls. The release of different growth factors after 12 hours of stretching was investigated to determine how mechanical strain affected the release of different growth factors. Results showed there was a 1.9-fold and 29.5-fold increase in the concentration of VEGF and bFGF in the stretched group compared with the non-stretched group (90). Similarly bovine airway smooth muscle cells (ASM) were enhanced their proliferation proliferation after mechanical strain applied to the cells (89).

Also different studies have controlled remotely with magnetic fields and magnetic particles the phenotype of cells by tagging specific receptors responsible for the differentiation of cells. Hu *et al* examined the possibility of controlling differentiation by mechanically activating the PDFG receptor α and β of HBMSCs. The results have shown an increase in α-actin (SMA) gene and protein expression (106).

Therefore combining the cyclic mechanical strain with the magnetic force. The overall aim of the work described in this thesis was to investigate magnetic actuation of the SPION-loaded HRSMC. In this study HRSMC were used as a model of sphincter smooth muscle cells. The phenotypic continuum of smooth muscle cells has been controlled mechanically with Flexcell units as shown in previous studies. However, in this study HRSMC were incubated with SPION and seeded in culture plates with a rigid bottom. The different mode of action allowed the oscillating magnetic field to stretch the plasma membrane of HRSMC creating a stretching effect similar to a Flexcell unit.

The nanoparticles used in this study were negatively charged uncoated iron oxide crystals, manufactured by chemical precipitation. In chapter 3, the effects of SPION on HRSMC were explored. The particles retain the hydrodynamic diameter in water but in culture medium they form big clusters due to the corona effect where particles, surrounded by biological fluids such as the culture medium and form clusters of various sizes. Also SPION were endocytosed by HRSMC and located inside the endosomes as showed by TEM and also concentrations above 250 μg/ml loading saturation occurred according to SQUID measurements. The exact endocytic process was not investigated in this study. It is likely that caveolae-mediated or caveolae-independent endocytosis occurs. This type of endocytosis creates 50 nm diameter vesicles to endocytose nanoparticles, similar in size to the magnetic nanoparticles used in this study. Caveolae-mediated or independent endocytosis fall into a broad category of endocytosis called pinocytosis, together with clathrin-mediated and independent endocytosis and macropinocytosis (148)

In Chapter 4 a magnetic actuator devise was devised to deliver magnetic force to HRSMC. As the magnetic cylinder rotated the magnetic field changed from a high value to a lower value it was hypothesized this would create continuous cycles of cell stretching by moving the SPION-loaded endosomes or 'magnetosomes'. The physical movement of the SPION-loaded endosomes was proposed to stretch the cytoskeletal components such as actin filaments and microtubules and create a phenotypic change to the cells such as proliferation or contraction. The type of cyclic mechanical stretching proposed in this study is different from the mechanical stretching caused by the Flexcell® unit. In this case the cells were seeded onto elastic membranes where continuous cycles of cyclic strain were applied to the cell. The concentration of 250 μg/ml of SPION was chosen as the optimum concentration for magnetic actuation.

HRSMC were subjected to magnetic actuation for 1 hour per day at 1 Hz and 2 Hz for 7 days. SQUID measurement have shown that SPION-loaded HRSMC in proliferation medium had 6 pg of SPION and in differentiation medium 16 pg of SPION. This is because SPION-loaded HRSMC have proliferated and increased the number of cells compared to SPION-loaded HRSMC in differentiation medium. The force per cell is influenced by the position of the magnet (0 degrees or 180 degrees) and the amount of SPION internalised by the cells. The SQUID results showed that SPION-loaded HRSMC in proliferation medium for 7 days had a reduced number of SPION therefore the force per cell is likely to have been decreased over time. For example, SPION-loaded HRSCM in proliferation medium; from 14.4 pN (pre-actuation) to 5.4 pN after 7 days of actuation. On the other hand SPION-loaded HRSMC in differentiation preserved the same force (14.4 pN) for 7 days.

The effect of magnetic actuation of SPION-loaded HRSMC on the phenotype and biocompatibility was investigated. The expression of the proliferative markers vimentin and tropomyosin 4 were not affected by either proliferation or differentiation medium, nor with magnetic actuation. For these markers an increase in the mRNA expression was expected when HRSMC were incubated in proliferation medium. Further investigation is necessary to confirm these findings.

SPION-loaded HRSMC in differentiation medium alone or with magnetic actuation did not show any increase in caldesmon or myosin heavy chain expression. This is because caldesmon and myosin heavy chain are intermediate or late differentiation markers (85). Therefore a longer incubation period (more than 7 days) perhaps was required. Previous mechanical study using the Flexcell system has found similar findings. The results showed that airway smooth muscle cells subjected to mechanical strain for 12 days express myosin heavy chain protein as shown by western blot. (162)

SPION-loaded HRSMC in differentiation medium and with magnetic actuation inhibited the expression of actin and calponin genes but no apparent differences were observed in the protein level. This finding may suggest that cells were maintained towards a proliferative phenotype. However this finding was not confirmed with cell proliferation assays.

The oscillating magnetic field used in this study did not induce a change in cell proliferation when cells were incubated with proliferation or differentiation medium. However, different studies have demonstrated an increase in cell proliferation using static magnetic field (SMF) (164). Also mechanical studies using a Flexcell system have demonstrated that cyclic strain could enhance cell proliferation(89). Or reduce cell proliferation (165, 166)

Based on the current findings, it is evident that the oscillating magnetic field produced by the magnetic actuator did affect the proliferation of cells or their differentiation. Incubation of SPION-loaded HRSMC in proliferation or differentiation medium with magnetic actuation did not have any effect on the biocompatibility of HRSMC.

The main disadvantage in this study is the SPION-loaded HRSMC in proliferation medium did not maintain the same amount of SPION per cell throughout the 7 days incubation period and that affected the force acting on the cells as well. That could explain also the fact that magnetic actuation did not cause any change in the phenotype of HRSMC. One way to overcome this limitation is to would be to deliver a sufficient amount of magnetic material in the area of interest that is going to be biocompatible but not biodegradable and will not be distributed with cell division. In this study, HRSMC were seeded on a rigid surface that does not provide a good simulation of the mechanical properties of tissue *in vivo*. Based on previous studies seeding cells on elastic membranes with the Flexcell unit that affected the cell proliferation and

differentiation. Future studies could use HRSMC seeded on elastic membranes before subjecting them to the same oscillating magnetic field used in this study.

The effects of magnetic actuation on the biocompatibility of SPION-loaded HRSMC was investigated. No change was observed with LDH-toxicity assay or Caspase 3-7 apoptosis assay and reactive oxygen species.

Different studies have demonstrated that incubation of magnetite (Fe3O4) nanocrystals (MNC) 26 nm with HeLa cells induce cell apotptosis (163). In a different study the effect of static magnetic fields (0.5mT) on human keratinocytes (HaCaT) incubated with 15 mg/ml of SPION showed an increase in ROS production compared to control cells. (164). Also, mouse liver cell line cells (NCTC 1469) were incubated with 0.5 mM of SPION ferucarbotran (SHU 555A, Resovist) and were exposed to a SMF of 0.4 T. The results showed an increase in apoptotic activity relative to the concentration of SPION whereas necrotic activity was only marginally changed by SMF exposure. An increase in the formation of reactive oxygen species was observed (142).

From the previous findings can be concluded that the oscillating field is safe compared to a static magnetic field. Also the conditions used in this study such as the frequency are optimum for the magnetic actuation of cells.

In Chapter 5 the movement of the SPION-loaded ‘’magnetosomes’’ was investigated with scanning electron microscopy and live cell imaging. Different type of SPION (200 nm) and also stronger magnetic field was used therefore the amount of SPION per cells had significantly increased (100 pg of SPION). Therefore the magnetic force applied per cell was significantly increased compared to the magnetic actuator set-up in Chapter 4. This becuase no signifcant movement of the SPION-loaded magnetosomes was observed with the magnetic actuator therefore the change was necessary.

SEM images of SPION-loaded HRSMC showed evidence of membrane deformation in response to an externally applied magnetic field. Live cell imaging analysis revealed that SPION movement and plasma membrane deformation were more prominent on the Y-axis (movement upwards) confirming the SEM results. Movement was observed the X-axis (movement sideways) by the plasma membrane for 200 nm particles. This suggests that the plasma membrane not only moved upwards but also sideways. The findings from this chapter suggest that magnetic actuation of SPION-loaded HRSMC causes the plasma membrane to move upwards and sideways. This is likely to cause deformation of the cytoskeleton.

In a previous study the deformation of SPION-loaded endosomes were described. HeLa cells were incubated with 10 nM of cobalt ferrite nanoparticles ($CoFe_2O_4$) and exposed to of 660 mT magnetic field. The results showed the magnetic endosomes were elongated and aligned in the direction of the magnetic field (171).

The limitation of this study was the use of Image J analysis to analyse the SPION movement and membrane deformation. A limitation of using this technique was that SPION or plasma membrane had to be measured separately, which made the combined assessment more difficult.

Fluorescence energy transfer technology (FRET) has been used previously in order to quantify spatio-temporal changes in the cytoskeleton with the use of reporters, which label specific intracellular receptors. Many mechanical or magnetic stimulation studies have incorporated FRET and a Src reporter which regulates the integrin activation followed by a mechanical stimuli (176, 177). Based on the FRET technology and the limitations encountered with the use of Image J in this chapter, a different approach to study the movement of could be used to study the effect of SPION movement and membrane deformation could be used. Microtubules are connected with endosomes

with Rab5 protein (178, 179). A FRET green fluorescent protein (GFP)-Rab 5 could be developed for the visualisation of endosome and microtubule movement in response to an external magnetic field.

6.2 Future work

The magnetic actuation results from this study need further investigation because they might not have been optimal for achieving magnetic actuation of cells. For example, the strength of the magnets used, their orientation, and the frequency of the oscillating magnets together with the fact that the cells were seeded on a rigid bottom culture plates are all parameters that need further investigation. Based on the current results, the amount of internalized SPION was reduced after 7 days incubation; therefore the force per cell was not constant over the period of actuation. This issue could be overcome by using a different type of magnetic material to achieve long-term actuation, such as different SPION that are not ejected from the cells.

Stronger magnetic fields and/or static magnetic fields could be incorporated for a future study. Also the amount of magnetic material endocytosed by the cells could be increased with larger diameter particles such as 200 nm instead of 50 nm. As demonstrated in chapter 5, SPION-loaded HRSCM with 200 nm had a greater effect and the deformation of the plasma membrane was more pronounced.

It was observed that it was possible to achieve magnetic actuation of the cell membrane with stronger magnetic fields. Also future studies could involve the use of FRET imaging and magnetic twizzers in order to explore the cytoskeletal changes in response to an external magnetic field.

Long-term cell studies (more than 7 days) will be necessary, as some of the markers such as myosin heavy chain or caldesmon require prolong incubation periods.

Animal studies were not conducted in this study. These will eventually be necessary to investigate the in vivo effects of magnetic actuation.

Although in this study magnetic actuation of SPION-Loaded HRSMC did not demonstrate any significant change in the phenotype, the inhibition of actin and calponin gene expression in SPION-loaded HRSMC without magnetic actuation is an interesting finding that could be used as part of a novel therapeutic approach for controlling muscle regeneration in conditions such as incontinence. The magnetic regulation of the smooth muscle phenotypic continuum is a very promising concept. The work presented within this thesis provides useful insights into novel approaches for muscle conditioning that could be utilized for human application.

References

1. Chatoor DR, Taylor SJ, Cohen CR, Emmanuel AV. Faecal incontinence. The British journal of surgery. 2007;94(2):134-44.

2. Dudding TC, Vaizey CJ, Kamm MA. Obstetric anal sphincter injury: incidence, risk factors, and management. Annals of surgery. 2008;247(2):224-37.

3. Tan JJY, Chan M, Tjandra JJ. Evolving therapy for fecal incontinence. Disease of Colon and Rectum. 2007;50:1950-67.

4. National Collaborating Centre for Acute Care. Faecal incontinence: the management of faecal incontinence in adults. NICE, 2007.

5. Stern JM. Psychological aspects of fecal incontinence. In: Ratto C, Doglietto GB, editors. Fecal incontinence: diagnosis and treatment. Milan: Springer; 2007. p. 43-66.

6. Madoff RD, Parker SC, Varma MG, Lowry AC. Faecal incontinence in adults. Lancet. 2004;364(9434):621-32.

7. Bharucha AE. Management of fecal incontinence. Gastroenterology & hepatology. 2008;4(11):807-17.

8. Wang JY, Abbas MA. Current management of fecal incontinence. The Permanente journal. 2013;17(3):65-73.

9. Rao SS. Diagnosis and management of fecal incontinence. American College of Gastroenterology Practice Parameters Committee. The American journal of gastroenterology. 2004;99(8):1585-604.

10. Tan JJ, Chan M, Tjandra JJ. Evolving therapy for fecal incontinence. Diseases of the colon and rectum. 2007;50(11):1950-67.

11. Nelson R, Norton N, Cautley E, Furner S. Community-based prevalence of anal incontinence. Jama. 1995;274(7):559-61.

12. Johanson JF, Lafferty J. Epidemiology of fecal incontinence: the silent affliction. The American journal of gastroenterology. 1996;91(1):33-6.

13. Melville JL, Fan MY, Newton K, Fenner D. Fecal incontinence in US women: a population-based study. American journal of obstetrics and gynecology. 2005;193(6):2071-6.

14. Bharucha AE, Zinsmeister AR, Locke GR, Seide BM, McKeon K, Schleck CD, et al. Prevalence and burden of fecal incontinence: a population-based study in women. Gastroenterology. 2005;129(1):42-9.

15. Quander CR, Morris MC, Melson J, Bienias JL, Evans DA. Prevalence of and factors associated with fecal incontinence in a large community study of older individuals. The American journal of gastroenterology. 2005;100(4):905-9.

16. Chassagne P, Landrin I, Neveu C, Czernichow P, Bouaniche M, Doucet J, et al. Fecal incontinence in the institutionalized elderly: incidence, risk factors, and prognosis. The American journal of medicine. 1999;106(2):185-90.

17. Siproudhis L, Pigot F, Godeberge P, Damon H, Soudan D, Bigard MA. Defecation disorders: a French population survey. Diseases of the colon and rectum. 2006;49(2):219-27.

18. Kalantar JS, Howell S, Talley NJ. Prevalence of faecal incontinence and associated risk factors; an underdiagnosed problem in the Australian community? The Medical journal of Australia. 2002;176(2):54-7.

19. Ho YH, Muller R, Veitch C, Rane A, Durrheim D. Faecal incontinence: an unrecognised epidemic in rural North Queensland? Results of a hospital-based outpatient study. The Australian journal of rural health. 2005;13(1):28-34.

20. Mellgren A, Jensen LL, Zetterstrom JP, Wong WD, Hofmeister JH, Lowry AC. Long-term cost of fecal incontinence secondary to obstetric injuries. Diseases of the colon and rectum. 1999;42(7):857-65; discussion 65-7.

21. Borrie MJ, Davidson HA. Incontinence in institutions: costs and contributing factors. CMAJ : Canadian Medical Association journal = journal de l'Association medicale canadienne. 1992;147(3):322-8.

22. National Collaborating Centre for Acute Care. Faecal incontinence. Costing report. NICE, 2007.

23. Standring S. Grays Anatomy: the anatomical basis of clinical practise. 14th edition ed: elsevier; 2008.

24. Keightey MR, Williams NS. Surgery of the anus, rectum and colon. 3rd edition ed: Editorial Saunders Elsevier; 2008.

25. Feki A, Faltin DL, Lei T, Dubuisson JB, Jacob S, Irion O. Sphincter incontinence: is regenerative medicine the best alternative to restore urinary or anal sphincter function? The international journal of biochemistry & cell biology. 2007;39(4):678-84.

26. Read MG, Read NW, Haynes WG, Donnelly TC, Johnson AG. A prospective study of the effect of haemorrhoidectomy on sphincter function and faecal continence. The British journal of surgery. 1982;69(7):396-8.

27. McHugh SM, Diamant NE. Effect of age, gender, and parity on anal canal pressures. Contribution of impaired anal sphincter function to fecal incontinence. Digestive diseases and sciences. 1987;32(7):726-36.

28. Otto IC, Ito K, Ye C, Hibi K, Kasai Y, Akiyama S, et al. Causes of rectal incontinence after sphincter-preserving operations for rectal cancer. Diseases of the colon and rectum. 1996;39(12):1423-7.

29. Lupattelli M, Mascioni F, Bellavita R, Draghini L, Tarducci R, Castagnoli P, et al. Long-term anorectal function after postoperative chemoradiotherapy in high-risk rectal cancer patients. Tumori. 2010;96(1):34-41.

30. Nyam DC, Pemberton JH. Long-term results of lateral internal sphincterotomy for chronic anal fissure with particular reference to incidence of fecal incontinence. Diseases of the colon and rectum. 1999;42(10):1306-10.

31. Casillas S, Hull TL, Zutshi M, Trzcinski R, Bast JF, Xu M. Incontinence after a lateral internal sphincterotomy: are we underestimating it? Diseases of the colon and rectum. 2005;48(6):1193-9.

32. Donnelly V, Fynes M, Campbell D, Johnson H, O'Connell PR, O'Herlihy C. Obstetric events leading to anal sphincter damage. Obstetrics and gynecology. 1998;92(6):955-61.

33. Varma A, Gunn J, Gardiner A, Lindow SW, Duthie GS. Obstetric anal sphincter injury: prospective evaluation of incidence. Diseases of the colon and rectum. 1999;42(12):1537-43.

34. Zetterstrom J, Mellgren A, Jensen LL, Wong WD, Kim DG, Lowry AC, et al. Effect of delivery on anal sphincter morphology and function. Diseases of the colon and rectum. 1999;42(10):1253-60.

35. Faltin DL, Sangalli MR, Roche B, Floris L, Boulvain M, Weil A. Does a second delivery increase the risk of anal incontinence? BJOG : an international journal of obstetrics and gynaecology. 2001;108(7):684-8.

36. Vaizey CJ, Carapeti E, Cahill JA, Kamm MA. Prospective comparison of faecal incontinence grading systems. Gut. 1999;44(1):77-80.

37. Felt-Bersma RJ, Klinkenberg-Knol EC, Meuwissen SG. Anorectal function investigations in incontinent and continent patients. Differences and discriminatory value. Diseases of the colon and rectum. 1990;33(6):479-85; discussion 85-6.

38. Mundy L, Merlin TL, Maddern GJ, Hiller JE. Systematic review of safety and effectiveness of an artificial bowel sphincter for faecal incontinence. The British journal of surgery. 2004;91(6):665-72.

39. Cheetham M, Brazzelli M, Norton C, Glazener C. Drug treatment for faecal incontinence in adults. Cochrane Database Syst Rev. 2003;3:CD002116.

40. Burch J, Collins B. Using biofeedback to treat constipation, faecal incontinence and other bowel disorders. Nursing Times. 2010;106(37):20-1.

41. Chiarioni G, Ferri B, Morelli A, Iantorno G, Bassotti G. Bio-feedback treatment of fecal incontinence: where are we, and where are we going? World J Gastroenterol. 2005;11(31):4771-5.

42. Heymen S, Jones K, Ringel Y, Scarlett Y, Whitehead W. Biofeedback treatment of fecal incontinence: a critical review. Diseases of the colon and rectum. 2001;44(5):5728-736.

43. Norton C, Kamm MA. Anal sphincter biofeedback and pelvic floor exercises for faecal incontinence in adults--a systematic review. Alimentary pharmacology & therapeutics. 2001;15(8):1147-54.

44. Norton C, Chelvanayagam S, Wilson-Barnett J, Redfern S, Kamm MA. Randomized controlled trial of biofeedback for fecal incontinence. Gastroenterology. 2003;125(5):1320-9.

45. Hansen J, Bliss D, Peden-McAlpine C. Diet strategies used by women to manage fecal incontinence. J Wound Ostomy Continence Nurs. 2006;33(1):52-61.

46. Davis K, Kumar D, Poloniecki J. Preliminary evaluation of an injectable anal sphincter bulking agent (Durasphere) in the management of faecal incontinence. Alimentary Pharmacology & Theraputics. 2003;18:237–43.

47. Malouf AJ, Vaizey CJ, Norton CS, MA. K. Internal anal sphincter augmentation for fecal incontinence using injectable silicone biomaterial. Diseases of the colon and rectum. 2001;44(4):595-600.

48. Vaizey CJ, Kamm MA. Injectable bulking agents for treating faecal incontinence. The British journal of surgery. 2005;92(5):521-7.

49. Conaghan P, Farouk R. Sacral nerve stimulation can be successful in patients with ultrasound evidence of external anal sphincter disruption. Diseases of the colon and rectum. 2005;48(8):1610-4.

50. Jarrett ME, Mowatt G, Glazener CM, Fraser C, Nicholls RJ, Grant AM, et al. Systematic review of sacral nerve stimulation for faecal incontinence and constipation. The British journal of surgery. 2004;91(12):1559-69.

51. Rongen MJ, Uludag O, El Naggar K, Geerdes BP, Konsten J, Baeten CG. Long-term follow-up of dynamic graciloplasty for fecal incontinence. Diseases of the colon and rectum. 2003;46(6):716-21.

52. Baeten CG, Geerdes BP, Adang EM, Heineman E, Konsten J, Engel GL, et al. Anal dynamic graciloplasty in the treatment of intractable fecal incontinence. The New England journal of medicine. 1995;332(24):1600-5.

53. Christiansen J, Rasmussen O, Lindorff-Larsen K. Long-term results of artificial anal sphincter implantation for severe anal incontinence. Annals of surgery. 1999;230(1):45-8.

54. Norton CS, Burch J, Kamm MA. Patients' views of a colostomy for fecal incontinence. Diseases of the colon and rectum. 2005;48(5):1062-9.

55. Fynes MM, Marshall K, Cassidy M, Behan M, Walsh D, O'Connell PR, et al. A prospective, randomized study comparing the effect of augmented biofeedback with sensory biofeedback alone on fecal incontinence after obstetric trauma. Diseases of the colon and rectum. 1999;42(6):753-8; discussion 8-61.

56. Whitehead WE, Burgio KL, Engel BT. Biofeedback treatment of fecal incontinence in geriatric patients. Journal of the American Geriatrics Society. 1985;33(5):320-4.

57. Kenefick NJ, Vaizey CJ, Malouf AJ, Norton CS, Marshall M, Kamm MA. Injectable silicone biomaterial for faecal incontinence due to internal anal sphincter dysfunction. Gut. 2002;51(2):225-8.

58. Feretis C, Benakis P, Dailianas A, Dimopoulos C, Mavrantonis C, Stamou KM, et al. Implantation of microballoons in the management of fecal incontinence. Diseases of the colon and rectum. 2001;44(11):1605-9.

59. Shafik A. Perianal injection of autologous fat for treatment of sphincteric incontinence. Diseases of the colon and rectum. 1995;38(6):583-7.

60. Kumar D, Benson MJ, Bland JE. Glutaraldehyde cross-linked collagen in the treatment of faecal incontinence. The British journal of surgery. 1998;85(7):978-9.

61. Matzel KE, Stadelmaier U, Hohenfellner M, Hohenberger W. Chronic sacral spinal nerve stimulation for fecal incontinence: long-term results with foramen and cuff electrodes. Diseases of the colon and rectum. 2001;44(1):59-66.

62. Vaizey CJ, Kamm MA, Turner IC, Nicholls RJ, Woloszko J. Effects of short term sacral nerve stimulation on anal and rectal function in patients with anal incontinence. Gut. 1999;44(3):407-12.

63. Ganio E, Ratto C, Masin A, Luc AR, Doglietto GB, Dodi G, et al. Neuromodulation for fecal incontinence: outcome in 16 patients with definitive implant. The initial Italian Sacral Neurostimulation Group (GINS) experience. Diseases of the colon and rectum. 2001;44(7):965-70.

64. Matzel KE, Kamm MA, Stosser M, Baeten CG, Christiansen J, Madoff R, et al. Sacral spinal nerve stimulation for faecal incontinence: multicentre study. Lancet. 2004;363(9417):1270-6.

65. Hull T, Giese C, Wexner SD, Mellgren A, Devroede G, Madoff RD, et al. Long-term durability of sacral nerve stimulation therapy for chronic fecal incontinence. Diseases of the colon and rectum. 2013;56(2):234-45.

66. Altomare DF, Dodi G, La Torre F, Romano G, Melega E, Rinaldi M. Multicentre retrospective analysis of the outcome of artificial anal sphincter implantation for severe faecal incontinence. The British journal of surgery. 2001;88(11):1481-6.

67. O'Brien PE, Skinner S. Restoring control: the Acticon Neosphincter artificial bowel sphincter in the treatment of anal incontinence. Diseases of the colon and rectum. 2000;43(9):1213-6.

68. Lehur PA, Roig JV, Duinslaeger M. Artificial anal sphincter: prospective clinical and manometric evaluation. Diseases of the colon and rectum. 2000;43(8):1100-6.

69. Wong WD, Congliosi SM, Spencer MP, Corman ML, Tan P, Opelka FG, et al. The safety and efficacy of the artificial bowel sphincter for fecal incontinence: results from a multicenter cohort study. Diseases of the colon and rectum. 2002;45(9):1139-53.

70. Christiansen J, Rasmussen OO, Lindorff-Larsen K. Long-term results of artificial anal sphincter implantation for severe anal incontinence. Annals of surgery. 1999;230(1):45-8.

71. Madoff RD, Rosen HR, Baeten CG, LaFontaine LJ, Cavina E, Devesa M, et al. Safety and efficacy of dynamic muscle plasty for anal incontinence: lessons from a prospective, multicenter trial. Gastroenterology. 1999;116(3):549-56.

72. Baeten CG, Bailey HR, Bakka A, Belliveau P, Berg E, Buie WD, et al. Safety and efficacy of dynamic graciloplasty for fecal incontinence: report of a prospective, multicenter trial. Dynamic Graciloplasty Therapy Study Group. Diseases of the colon and rectum. 2000;43(6):743-51.

73. Hasegawa H, Yoshioka K, Keighley MR. Randomized trial of fecal diversion for sphincter repair. Diseases of the colon and rectum. 2000;43(7):961-4; discussion 4-5.

74. Young CJ, Mathur MN, Eyers AA, Solomon MJ. Successful overlapping anal sphincter repair: relationship to patient age, neuropathy, and colostomy formation. Diseases of the colon and rectum. 1998;41(3):344-9.

75. Bitar KN. Aging and Gi smooth muscle fecal incontinence: Is bioengineering an option. Experimental gerontology. 2005;40(8-9):643-9.

76. Kang SB, Lee HN, Lee JY, Park JS, Lee HS, Lee JY. Sphincter contractility after muscle-derived stem cells autograft into the cryoinjured anal sphincters of rats. Diseases of the colon and rectum. 2008;51(9):1367-73.

77. Aghaee-Afshar M, Rezazadehkermani M, Asadi A, Malekpour-Afshar R, Shahesmaeili A, Nematollahi-mahani SN. Potential of human umbilical cord matrix and rabbit bone marrow-derived mesenchymal stem cells in repair of surgically incised rabbit external anal sphincter. Diseases of the colon and rectum. 2009;52(10):1753-61.

78. Hecker L, Baar K, Dennis RG, Bitar KN. Development of a three-dimensional physiological model of the internal anal sphincter bioengineered in vitro from isolated smooth muscle cells. American journal of physiology Gastrointestinal and liver physiology. 2005;289(2):G188-96.

79. Lehur PA, McNevin S, Buntzen S, Mellgren AF, Laurberg S, Madoff RD. Magnetic anal sphincter augmentation for the treatment of fecal incontinence: a preliminary report from a feasibility study. Diseases of the colon and rectum. 2010;53(12):1604-10.

80. Wong MT, Meurette G, Wyart V, Lehur PA. Does the magnetic anal sphincter device compare favourably with sacral nerve stimulation in the management of faecal incontinence? Colorectal disease : the official journal of the Association of Coloproctology of Great Britain and Ireland. 2012;14(6):e323-9.

81. Sanders KM. regulation of smooth muscle excitation and contraction. neurogastroenterology motil. 2008:39-53.

82. Bitar KN. Function of gastrointestinal smooth muscle: from signalling to contractile proteins. The American journal of medicine. 2003;115(S3A):15s-23s.

83. Webb R. Smooth muscle contraction and relaxation. Adv Physiol Educ. 2003;27(1):201-6.

84. Hodgkinson JL, el-Mezgueldi M, Craig R, Vibert P, Marston SB, Lehman W. 3-D image reconstruction of reconstituted smooth muscle thin filaments containing calponin : visulaization of interactions between F-actin and calponin. Journal of molecular biology. 1997; 273(1):150-9.

85. Beamish JA, He P, Kottke-Marchant K, Marchant RE. Molecular regulation of contractile smooth muscle cell phenotype: implications for vascular tissue engineering. Tissue Eng Part B Rev. 2010;16(5):467-91.

86. Riehl BD, Jae-Hong Park, Keun Kwon, Jung Yul Lim. Mechanical streching for tissue engineering: two-dimensional and three-dimensional constructs. Tissue engineering Part B. 2012;18(4):288-300.

87. Ethier CR, Simmons CA. Indroductory Biomechanics From cells to organisms: University of Cambridge; 2007.

88. Williams B. Mechanical influences on vascular smooth muscle cell function: J Hypertens. 1998 Dec;16(12 Pt 2):1921-9.

89. Bonacci JV, Harris T, Stewart AG. Impact of extracellular matrix and strain on proliferation of bovine airway smooth muscle. Clinical and experimental pharmacology & physiology. 2003;30(5-6):324-8.

90. Kurazumi H, Kubo M, Ohshima M, Yamamoto Y, Takemoto Y, Suzuki R, et al. The effects of mechanical stress on the growth, differentiation, and paracrine factor production of cardiac stem cells. PloS one. 2011;6(12):e28890.

91. Crick FHC, Hughes AFW. The physical properties of cytoplasm: a study by means of the magnetic particle method. Exp Cell Res. 1950(1): 37–80.

92. Kyrtatos PG, Lehtolainen P, Junemann-Ramirez M, Garcia-Prieto A, Price AN, Martin JF, et al. Magnetic tagging increases delivery of circulating progenitors in vascular injury. JACC Cardiovascular interventions. 2009;2(8):794-802.

93. Riegler J, Wells JA, Kyrtatos PG, Price AN, Pankhurst QA, Lythgoe MF. Targeted magnetic delivery and tracking of cells using a magnetic resonance imaging system. Biomaterials. 2010;31(20):5366-71.

94. Vigor KL, Kyrtatos PG, Minogue S, Al-Jamal KT, Kogelberg H, Tolner B, et al. Nanoparticles functionalized with recombinant single chain Fv antibody fragments

(scFv) for the magnetic resonance imaging of cancer cells. Biomaterials. 2010;31(6):1307-15.

95. Gonzalez-Molina J, Riegler J, Southern P, Ortega D, Frangos CC, Angelopoulos Y, et al. Rapid magnetic cell delivery for large tubular bioengineered constructs. Journal of the Royal Society, Interface / the Royal Society. 2012;9(76):3008-16.

96. Perea H, Aigner J, Heverhagen JT, Hopfner U, Wintermantel E. Vascular tissue engineering with magnetic nanoparticles: seeing deeper. Journal of tissue engineering and regenerative medicine. 2007;1(4):318-21.

97. Perea H, Aigner J, Hopfner U, Wintermantel E. Direct magnetic tubular cell seeding: a novel approach for vascular tissue engineering. Cells, tissues, organs. 2006;183(3):156-65.

98. Dobson J. Remote control of cellular behaviour with magnetic nanoparticles. nature nanotechnology 2008;3.

99. Sniadecki NJ. Minireview: A Tiny Touch: Activation of Cell Signaling Pathways with Magnetic Nanoparticles. Endocrinology 2010;151(2):451–7.

100. Wang N, Butler JP, Ingber DE. Mechanotransduction across the cell surface and through the cytoskeleton. Science. 1993;260:1124-7.

101. Dobson J, Keramane A, El Haj AJ. Theory and aplications of a magnetic force bioreactor. European Cells and Materials. 2002;4(2):42-4.

102. Janos M. Kanczler, Harpul S. Sura, Julia Magnay, David Green, Richard O.C. Oreffo, Jon P. Dobson, et al. Controlled Differentiation of Human Bone Marrow Stromal Cells Using Magnetic Nanoparticle Technology. TISSUE ENGINEERING: Part A. 2010;16(10):3241-50.

103. Glogauer M, Ferrier J. A new method for application of force to cells via ferric oxide beads. Eur J Physiol. 1998(435):320–7.

104. Hughes S, McBain S, Dobson J, El Haj AJ. Selective activation of mechanosensitive ion channels using magnetic particles. J R Soc Interface. 2008(5):855–63.

105. Kirkham GR, Elliot KJ, Keramane A, Salter DM, Dobson J, El Haj AJ, et al. Hyperpolarization of Human Mesenchymal Stem Cells in Response to Magnetic Force. IEEE transactions on Nanobioscience. 2010;9(1):71-4.

106. Hu B, Yang Y, Dobson JP, Haj A. Mechanical Conditioning Using Magnetic Nanoparticles Bound to PDGF Receptors on HBMSCs Promotes the Smooth Muscle

Alpha Actin (SMA) Expression. In: Haj A, Bader D, editors. 8th International Conference on Cell & Stem Cell Engineering (ICCE). IFMBE Proceedings. 30: Springer Berlin Heidelberg; 2011. p. 23-5.

107. Glossp JR, Cartmell SH. Tesile strain and magnetic particle force application do not induce MAP3K8 and IL-1B differential gene expression in a similar manner to fluid shear stress in human mesenchymal stem cells. Journal of tissue engineering and regenerative medicine. 2010(4):577-9.

108. Chikazumi S, Charap SH. Physics of Magnetism Krieger Pub Co 1978.

109. Pankhurst QA, Connolly J, Jones SK, Dobson J. Applications of magnetic nanoparticles in biomedicine. Journal of Physics D: Applied Physics. 2003;36(13):R167.

110. Hatch GP, Stelter RE. Magnetic design considerations for devices and particles used for biological high-gradient magnetic separation (HGMS) systems. Journal of Magnetism and Magnetic Materials. 2001;225(1–2):262-76.

111. Ortega D. Structure and magnetism in magnetic nanoparticles. magnetic nanoparticles from fabrication to clinical applications: CRC press Taylor and Francis group, LLC; 2012.

112. Laurent S, Forge D, Port MR, Alain; Robic C, Vander Elst, Luce; Muller, et al. Magnetic Iron Oxide Nanoparticles: Synthesis, Stabilization, Vectorization, Physicochemical Characterizations, and Biological Applications. Chemical Reviews. 2008;108 (6):2064–110.

113. Jeon ES, Moon HJ, Lee MJ, Song HY, Kim YM, Bae YC, et al. Sphingosylphosphorylcholine induces differentiation of human mesenchymal stem cells into smoothmuscle- like cells through a TGF-B dependent mechanism. Journal of Cell Science 2006;119:4994-5005.

114. Harris LJ, Abdollahi H, Zhang P, McIlhenny S, Tulenko T, DiMuzio PJ. Differentiation of Adult Stem Cells into Smooth Muscle for Vascular Tissue Engineering. J Surg Res. 2011 168(2):306-14.

115. Yongzhong Wu, Xueping Zhang, Morgan Salmon, Xia Lin, Zehner ZE. TGFβ1 regulation of vimentin gene expression during differentiation of the C2C12 skeletal myogenic cell line requires Smads, AP-1 and Sp1 family members. Biochim Biophys Acta. 2007 March 1773(3):427–39.

116. McElfresh M, Li S, Sager R. Effects of magnetic field uniformity on the measurement of superconducting samples. Quantum Design.

117. Richards WO, Garrard CL, Allos SH, Bradshaw LA, Staton DJ, Wikswo JP, Jr. Noninvasive diagnosis of mesenteric ischemia using a SQUID magnetometer. Annals of surgery. 1995;221(6):696-704; discussion -5.

118. Hautot D, Pankhurst QA, Dobson J. Superconducting quantum interference device measurements of dilute magnetic materials in biological samples. Review of Scientific Instruments. 2005;76(4):045101--4.

119. Sawicki M, Stefanowicz W, Ney A. Sensitive SQUID magnetometry for studying nanomagnetism. Semiconductor Science and Technology. 2011;26(6):064006.

120. Lauzon AM, Tyska MJ, Rovner AS, Freyzon Y, Warshaw DM, Trybus KM. A 7-amino-acid insert in the heavy chain nucleotide binding loop alters the kinetics of smooth muscle myosin in the laser trap. Journal of muscle research and cell motility. 1998;19(8):825-37.

121. Wells L, Edwards KA, Bernstein SI. Myosin heavy chain isoforms regulate muscle function but not myofibril assembly. The EMBO journal. 1996;15(17):4454-9.

122. Babu GJ, Pyne GJ, Zhou Y, Okwuchukuasanya C, Brayden JE, Osol G, et al. Isoform switching from SM-B to SM-A myosin results in decreased contractility and altered expression of thin filament regulatory proteins. American journal of physiology Cell physiology. 2004;287(3):C723-9.

123. Morgan KG, Gangopadhyay SS. Invited review: cross-bridge regulation by thin filament-associated proteins. Journal of applied physiology (Bethesda, Md : 1985). 2001;91(2):953-62.

124. Sobue K, Sellers JR. Caldesmon, a novel regulatory protein in smooth muscle and nonmuscle actomyosin systems. The Journal of biological chemistry. 1991;266(19):12115-8.

125. Li S, Sims S, Jiao Y, Chow LH, Pickering JG. Evidence from a novel human cell clone that adult vascular smooth muscle cells can convert reversibly between noncontractile and contractile phenotypes. Circulation research. 1999;85(4):338-48.

126. Sobue K, Hayashi K, Nishida W. Expressional regulation of smooth muscle cell-specific genes in association with phenotypic modulation. Molecular and cellular biochemistry. 1999;190(1-2):105-18.

127. Hayashi K, Saga H, Chimori Y, Kimura K, Yamanaka Y, Sobue K. Differentiated phenotype of smooth muscle cells depends on signaling pathways through insulin-like growth factors and phosphatidylinositol 3-kinase. The Journal of biological chemistry. 1998;273(44):28860-7.

128. Gerthoffer WT, Pohl J. Caldesmon and calponin phosphorylation in regulation of smooth muscle contraction. Canadian journal of physiology and pharmacology. 1994;72(11):1410-4.

129. Winder SJ, Walsh MP. Smooth muscle calponin. Inhibition of actomyosin MgATPase and regulation by phosphorylation. The Journal of biological chemistry. 1990;265(17):10148-55.

130. Lazarides E. Intermediate filaments as mechanical integrators of cellular space. Nature. 1980;283(5744):249-56.

131. Osborn M. Intermediate filaments as histologic markers: an overview. The Journal of investigative dermatology. 1983;81(1 Suppl):104s-9s.

132. Skalli O, Bloom WS, Ropraz P, Azzarone B, Gabbiani G. Cytoskeletal remodeling of rat aortic smooth muscle cells in vitro: relationships to culture conditions and analogies to in vivo situations. Journal of submicroscopic cytology. 1986;18(3):481-93.

133. Asada H, Paszkowiak J, Teso D, Alvi K, Thorisson A, Frattini JC, et al. Sustained orbital shear stress stimulates smooth muscle cell proliferation via the extracellular signal-regulated protein kinase 1/2 pathway. Journal of vascular surgery. 2005;42(4):772-80.

134. Zhou W, Dasgupta C, Negash S, Raj JU. Modulation of pulmonary vascular smooth muscle cell phenotype in hypoxia: role of cGMP-dependent protein kinase. American journal of physiology Lung cellular and molecular physiology. 2007;292(6):L1459-66.

135. Goldman RD, Khuon S, Chou YH, Opal P, Steinert PM. The function of intermediate filaments in cell shape and cytoskeletal integrity. The Journal of cell biology. 1996;134(4):971-83.

136. Abouhamed M, Reichenberg S, Robenek H, Plenz G. Tropomyosin 4 expression is enhanced in dedifferentiating smooth muscle cells in vitro and during atherogenesis. European journal of cell biology. 2003;82(9):473-82.

137. Vlahovich N, Schevzov G, Nair-Shaliker V, Ilkovski B, Artap ST, Joya JE, et al. Tropomyosin 4 defines novel filaments in skeletal muscle associated with muscle remodelling/regeneration in normal and diseased muscle. Cell motility and the cytoskeleton. 2008;65(1):73-85.

138. Gunning P, Gordon M, Wade R, Gahlmann R, Lin CS, Hardeman E. Differential control of tropomyosin mRNA levels during myogenesis suggests the

existence of an isoform competition-autoregulatory compensation control mechanism. Developmental biology. 1990;138(2):443-53.

139. Vigora KL, Kyrtatos PG, Minoguec S, Al-Jamald KT, Kogelberga H, Tolnera B, et al. Nanoparticles functionalised with recombinant single chain Fv antibody fragments (scFv) for the magnetic resonance imaging of cancer cells. Biomaterials. 2009;31(6):1307–15.

140. Tang M, Russell PJ, Khatri A. Magnetic Nanoparticles: Prospects in Cancer Imaging and Therapy. Discovery Medicine. 2009;7(38):68-74.

141. Pankhurst Q, Connolly J, Jones S, Dobson J. Applications of magnetic nanoparticles in biomedicine. J Phys D: Appl Phys. 2003; 36(03): R167-R81.

142. Bae JE, Huh MI, Ryu BK, Do JY, Jin SU, Moon MJ, et al. The effect of static magnetic fields on the aggregation and cytotoxicity of magnetic nanoparticles. Biomaterials. 2011;32(35):9401-14.

143. Walczyk D, Bombelli FB, Monopoli MP, Lynch I, Dawson KA. What the cell "sees" in bionanoscience. Journal of the American Chemical Society. 2010;132(16):5761-8.

144. Casals E, Pfaller T, Duschl A, Oostingh GJ, Puntes V. Time evolution of the nanoparticle protein corona. ACS nano. 2010;4(7):3623-32.

145. Safi M, Courtois J, Seigneuret M, Conjeaud H, Berret JF. The effects of aggregation and protein corona on the cellular internalization of iron oxide nanoparticles. Biomaterials. 2011;32(35):9353-63.

146. Frank JA, Miller BR, Arbab AS, Zywicke HA, Jordan EK, Lewis BK, et al. Clinically applicable labeling of mammalian and stem cells by combining superparamagnetic iron oxides and transfection agents. Radiology. 2003;228(2):480-7.

147. Zhang S, Chen X, Gu C, Zhang Y, Xu J, Bian Z, et al. The Effect of Iron Oxide Magnetic Nanoparticles on Smooth Muscle Cells. Nanoscale Res Lett. 2009;4(1):70-7.

148. Conner SD, Schmid SL. Regulated portals of entry into the cell. Nature. 2003;422(6927):37-44.

149. Gu J, Xu H, Han Y, Dai W, Hao W, Wang C, et al. The internalization pathway, metabolic fate and biological effect of superparamagnetic iron oxide nanoparticles in the macrophage-like RAW264.7 cell. Science China Life sciences. 2011;54(9):793-805.

150. Diana V, Bossolasco P, Moscatelli D, Silani V, Cova L. Dose dependent side effect of superparamagnetic iron oxide nanoparticle labeling on cell motility in two fetal stem cell populations. PloS one. 2013;8(11):e78435.

151. Albukhaty S, Naderi-Manesh H, Tiraihi T. In vitro labeling of neural stem cells with poly-L-lysine coated super paramagnetic nanoparticles for green fluorescent protein transfection. Iranian biomedical journal. 2013;17(2):71-6.

152. Miyoshi S, Flexman JA, Cross DJ, Maravilla KR, Kim Y, Anzai Y, et al. Transfection of neuroprogenitor cells with iron nanoparticles for magnetic resonance imaging tracking: cell viability, differentiation, and intracellular localization. Molecular imaging and biology : MIB : the official publication of the Academy of Molecular Imaging. 2005;7(4):286-95.

153. Arbab AS, Bashaw LA, Miller BR, Jordan EK, Bulte JW, Frank JA. Intracytoplasmic tagging of cells with ferumoxides and transfection agent for cellular magnetic resonance imaging after cell transplantation: methods and techniques. Transplantation. 2003;76(7):1123-30.

154. Kyrtatos PG. Cell Targeting and Imaging using Magnetic Nanoparticles: University College London; 2009.

155. Chen CC, Ku MC, D MJ, Lai JS, Hueng DY, Chang C. Simple SPION incubation as an efficient intracellular labeling method for tracking neural progenitor cells using MRI. PloS one. 2013;8(2):e56125.

156. Gupta AK, Gupta M. Cytotoxicity suppression and cellular uptake enhancement of surface modified magnetic nanoparticles. Biomaterials. 2005;26(13):1565-73.

157. Mahmoudi M, Simchi A, Milani AS, Stroeve P. Cell toxicity of superparamagnetic iron oxide nanoparticles. Journal of colloid and interface science. 2009;336(2):510-8.

158. Farrell E, Wielopolski P, Pavljasevic P, Kops N, Weinans H, Bernsen MR, et al. Cell labelling with superparamagnetic iron oxide has no effect on chondrocyte behaviour. Osteoarthritis and cartilage / OARS, Osteoarthritis Research Society. 2009;17(7):961-7.

159. Saha S, Yang XB, Tanner S, Curran S, Wood D, Kirkham J. The effects of iron oxide incorporation on the chondrogenic potential of three human cell types. Journal of tissue engineering and regenerative medicine. 2013;7(6):461-9.

160. Gawaziuk JP, Sheikh F, Cheng ZQ, Cattini PA, Stephens NL. Transforming growth factor-beta as a differentiating factor for cultured smooth muscle cells. The European respiratory journal. 2007;30(4):643-52.

161. Birukov KG, Shirinsky VP, Stepanova OV, Tkachuk VA, Hahn AW, Resink TJ, et al. Stretch affects phenotype and proliferation of vascular smooth muscle cells. Molecular and cellular biochemistry. 1995;144(2):131-9.

162. Smith PG, Roy C, Dreger J, Brozovich F. Mechanical strain increases velocity and extent of shortening in cultured airway smooth muscle cells. The American journal of physiology. 1999;277(2 Pt 1):L343-8.

163. Khan JA, Mandal TK, Das TK, Singh Y, Pillai B, Maiti S. Magnetite (Fe3O4) nanocrystals affect the expression of genes involved in the TGF-beta signalling pathway. Molecular bioSystems. 2011;7(5):1481-6.

164. Comfort KK, Maurer EI, Hussain SM. The biological impact of concurrent exposure to metallic nanoparticles and a static magnetic field. Bioelectromagnetics. 2013;34(7):500-11.

165. Hipper A, Isenberg G. Cyclic mechanical strain decreases the DNA synthesis of vascular smooth muscle cells. Pflugers Archiv : European journal of physiology. 2000;440(1):19-27.

166. Chapman GB, Durante W, Hellums JD, Schafer AI. Physiological cyclic stretch causes cell cycle arrest in cultured vascular smooth muscle cells. American journal of physiology Heart and circulatory physiology. 2000;278(3):H748-54.

167. Hughes S, El Haj AJ, Dobson J. Magnetic micro- and nanoparticle mediated activation of mechanosensitive ion channels. Medical engineering & physics. 2005;27(9):754-62.

168. Hughes S, Magnay J, Foreman M, Publicover SJ, Dobson JP, El Haj AJ. Expression of the mechanosensitive 2PK+ channel TREK-1 in human osteoblasts. Journal of cellular physiology. 2006;206(3):738-48.

169. Dobson J, Cartmell SH, Keramane A, El Haj AJ. Principles and design of a novel magnetic force mechanical conditioning bioreactor for tissue engineering, stem cell conditioning, and dynamic in vitro screening. IEEE Trans Nanobioscience. 2006;5(3):173-7.

170. Kanczler JM, Sura HS, Magnay J, Green D, Oreffo RO, Dobson JP, et al. Controlled differentiation of human bone marrow stromal cells using magnetic nanoparticle technology. Tissue engineering Part A. 2010;16(10):3241-50.

171. Wilhelm C, Cebers A, Bacri JC, Gazeau F. Deformation of intracellular endosomes under a magnetic field. European biophysics journal : EBJ. 2003;32(7):655-60.

172. Wilhelm C, Gazeau F, Bacri JC. Rotational magnetic endosome microrheology: viscoelastic architecture inside living cells. Physical review E, Statistical, nonlinear, and soft matter physics. 2003;67(6 Pt 1):061908.

173. Kanger JS, Subramaniam V, van Driel R. Intracellular manipulation of chromatin using magnetic nanoparticles. Chromosome research : an international journal on the molecular, supramolecular and evolutionary aspects of chromosome biology. 2008;16(3):511-22.

174. Tanase M, Biais N, Sheetz M. Magnetic tweezers in cell biology. Methods in cell biology. 2007;83:473-93.

175. de Vries AH, Krenn BE, van Driel R, Kanger JS. Micro magnetic tweezers for nanomanipulation inside live cells. Biophysical journal. 2005;88(3):2137-44.

176. Wang Y, Wang N. FRET and mechanobiology. Integrative biology : quantitative biosciences from nano to macro. 2009;1(10):565-73.

177. Liu B, Kim TJ, Wang Y. Live cell imaging of mechanotransduction. Journal of the Royal Society, Interface / the Royal Society. 2010;7 Suppl 3:S365-75.

178. Pfeffer SR. Motivating endosome motility. Nature cell biology. 1999;1(6):E145-7.

179. Fischer JA, Eun SH, Doolan BT. Endocytosis, endosome trafficking, and the regulation of Drosophila development. Annual review of cell and developmental biology. 2006;22:181-206.